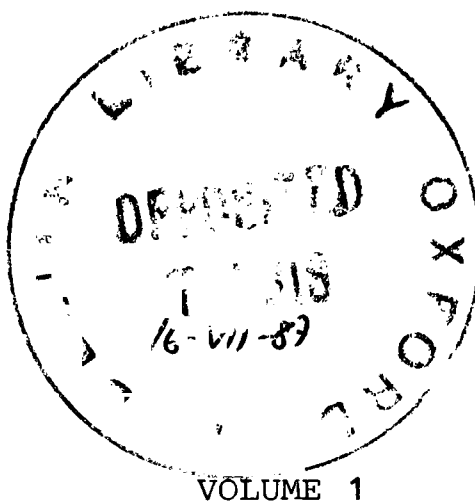


Thesis presented to the University of Oxford
for the Degree of Doctor of Philosophy.

PALAEOCLIMATIC SIGNIFICANCE OF OPEN-MARINE CYCLIC SEQUENCES.



GRAHAM PETER WEEDON B.Sc., A.R.S.M.

Linacre College
and Department of Earth Sciences,
Hilary Term, 1987.

'Analysis of Pleistocene climate records inferred from deep-sea sediments has established relations between orbital parameters and glaciation by identifying astronomical cycles of 19,000yr, 23,000yr, 41,000yr and perhaps 100,000yr within the geological record. A search for these cycles in older rocks and for other cycles is now possible; they may be present in Mesozoic, Palaeozoic and perhaps even Precambrian sequences. The task is to find long, continuous stratal sequences recording a signal (e.g. thickness variations in limestone-shale couplets) that permit frequency analysis.'

from Berger et al. 1982 p14.

PALAEOCLIMATIC SIGNIFICANCE OF OPEN-MARINE CYCLIC SEQUENCES

GRAHAM P. WEEDON

LINACRE COLLEGE, OXFORD

D.Phil. Thesis

Hilary Term 1987

ABSTRACT

The offshore facies of the basal Lias of S. Britain was studied as a typical example of an open-marine cyclic sequence. The sedimentology, geochemistry and power-spectral analysis were investigated in order to understand the cause of the interbedded rock types. Three sediment types were deposited on the sea-floor: light marl, dark marl and laminated carbonate-rich shale. Calcite microspar, the dominant carbonate component, appears to have been formed from the neomorphic aggradation of coccoliths supplied in zooplankton faecal pellets. During sulphate reduction, the most carbonate-rich horizons in the light marl and laminated shale beds were cemented by carbonate, producing early diagenetic limestone and laminated limestone beds and nodules.

Walsh power-spectral analysis of several measured sections in the basal Lias indicate that two regular sedimentary cycles, with periods of tens of thousands of years, are present. The regularity, stability and periods of the cycles invokes the Milankovitch Theory of orbital forcing of sedimentation; the cycles thus probably represent periods of 41,000 and 21,000 years. The sedimentation appears to have been linked to climatic variation by the levels of runoff and the formation and destruction of wedges of brackish water. During dry periods relatively little runoff and low clay input allowed turbulent, oxygenated bottom-waters and the deposition of burrowed, organic-poor marl. During wet periods, brackish wedges caused widespread density stratification, bottom-water anoxia and high clay inputs that resulted in laminated shale beds.

Walsh power spectra were generated for one Silurian, five Upper Lower Jurassic, one Kimmeridgian and one Oligocene formation. Unexpectedly the Early Jurassic appears to have been dominated by the Milankovitch cycles related to obliquity and precession rather than eccentricity. Of the thirteen spectra produced, including five from the basal Lias, ten (or about 80%) contain evidence for regular sedimentary cycles consistent with orbital forcing of sedimentation. Therefore the Milankovitch Theory should be considered whilst investigating open-marine 'cyclic' sequences.

LONG ABSTRACT.

There are many examples of open-marine, interbedded or 'cyclic' sequences documented from the Phanerozoic. When the Milankovitch or Orbital Theory of palaeoclimates explains the cyclicity of these rocks, regular sedimentary cycles with periods of tens of thousands of years should be recognizable from power-spectral analysis. However, even when regular cyclicity has been demonstrated, it is not possible to infer the precise climatic and depositional mechanisms involved; instead an understanding of the sedimentology is required. The offshore facies of the basal Lias of South Britain (uppermost Triassic-Lower Sinemurian, Jurassic) was selected as a typical example of a cyclic open-marine sequence. The field aspects, petrography, and geochemistry were investigated and Walsh power-spectral analysis was applied to five stratigraphic logs. The suitability of the relatively new Walsh technique was tested by applying it to the Upper Birkhill Shales of Scotland (Llandovery, Silurian), Upper Lower ^{Jurassic} rocks in Britain and Switzerland, the Kimmeridge Clay of England (Kimmeridgian, Jurassic), and the Boom Clay of Belgium (Rupelian, Oligocene).

In the field, the offshore facies of the basal Lias (including the Blue Lias Member) consists of five rock types: limestone, light marl, dark marl, laminated shale and laminated limestone. The limestone is associated with light marl beds and forms continuous beds and elliptical nodules. Laminated limestone forms beds and nodules enclosed by laminated shale. The limestone appears to have formed by early diagenetic cementation of light marl and the laminated limestone by cementation of laminated shale. Light marl and limestone is homogeneous, probably due to bioturbation, whereas the dark marl and laminated rocks preserve organic and clay laminae about 30µm thick. On a carbonate-free

basis, organic-carbon contents are the same in the limestone and light marl and in the laminated shale and laminated limestone. The sequence light marl, dark marl, laminated shale involves an increase in the proportion of clay relative to carbonate and an increase in the amount of organic matter. The petrography, organic-carbon contents, benthonic fossils and heavy metal contents (Le Riche 1959) of the laminated shale suggest almost permanent bottom-water anoxia. Conversely, the bottom-water was probably oxygenated during deposition of the light marl, although the organic-carbon contents are much higher than would be expected for normal oxygenation. Dark marl appears to represent an intermediate environment to those of the light marl and laminated shale.

Cathodoluminescence indicates that ostracods dominate the carbonate fraction of the laminated shale. In the marls and limestones microspar forms the bulk of the carbonate. Dark marls contain microspar in small (250 by 75 μ m) elliptical 'blebs'. The blebs appear to represent neomorphically-aggraded coccolith aggregates that are visible using the SEM. The coccolith aggregates and blebs are also present, although less commonly, in the laminated shale. In light marl, the homogeneous mixture of microspar and clay was probably produced by burrowers and coccoliths are very rare and poorly preserved. It is argued that clay encouraged the neomorphism of coccoliths, especially in the light marl. Coccolith aggregates preserved in the dark marl and laminated shale may have been protected from neomorphism by organic membranes. It is assumed that the coccolith aggregates and microspar blebs represent zooplankton faecal pellets. It is believed that most carbonate mud which formed the precursor to the microspar in the light marl was coccolithic in origin. Most microspar in the limestones probably represents pore-space occluded

by early diagenetic cement that was nucleated on coccoliths.

The formation of pyrite was investigated using the methods of Berner & Raiswell (1985) and involved the determination of %Fe, %S, %TOC and the 'degree of pyritization' (DOP). The results indicate that the deposition of iron was coupled to the deposition of organic matter and that pyrite formation was iron-limited for all rock types. The high values of DOP and the iron-limited mode of pyrite formation implies that bottom-waters were poorly oxygenated (light marl and dark marl deposition) or anoxic (laminated shale deposition).

The petrography and cathodoluminescence of Gryphaea arcuata specimens suggest that the carbonate in these fossils is unaltered. Oxygen isotopes for thirty five specimens indicate an average palaeotemperature of 15°C ($\delta^{18}\text{O} = -0.85$ per mil). The oxygen isotope values for bulk samples of all rock types are lighter than most Gryphaea results. Additionally, many oxygen and carbon results are correlated so all the bulk sample results probably involve substantial diagenetic components.

As pyrite is found inside limestone beds and nodules, early diagenetic cementation post-dated the start of sulphate reduction. Yet, the lack of compactional features and the stable isotopes of the limestone beds indicate cementation during the very early stages of sulphate reduction. On the other hand carbonate contents decrease towards the edges of limestone nodules indicating cementation during compaction. Further, the oxygen isotopes become lighter and the carbon isotopes heavier towards the outside of limestone nodules. Therefore, limestone nodules probably formed during the later phases of sulphate reduction. The location of cementation within light marl and laminated shale beds appears to have been determined by primary carbonate

contents. The common trend in oxygen- and carbon-isotope ratios in the limestone beds, light marl, dark marl and laminated shale, might reflect a common phase of neomorphism of coccoliths and micrite. The microspar that was produced is non-ferroan implying that neomorphism occurred during sulphate reduction. Beef calcite, perhaps related to over-pressuring, formed at the end of sulphate reduction and the start of fermentation. Compaction continued during fermentation.

After digitizing the rock types of the measured sections for the basal Lias, Walsh power-spectral analysis was performed. Dating used the assumption that each ammonite zone in the Jurassic represents about one million years. The thickness of ammonite zones was used to estimate the sedimentation rate at the tens-of-thousands-of-years scale for each location. Field evidence suggests that many small hiatuses are present in the sections, so the method employed has probably underestimated the appropriate sedimentation rate. Nevertheless, the dating is good enough to constrain the maximum period of any regular cycles identified. In three cases, two regular sedimentary cycles representing tens of thousands of years were identified. In one case only one regular cycle was identified, but this might be because the spectrum involved lacked the resolution to distinguish two cycles. In the last case, exceptional sedimentology and problems with section measuring might have destroyed any regular signal.

The regular sedimentary cycles may represent the theoretical Milankovitch cycles possessing periods of 41,000 (41kyr) and 21kyr. Alternatively, the wavelength ratio of the regular cycles might indicate that cycles with durations of 30kyr and 21kyr are involved. The dating, regularity and stability of the cycles is consistent with their generation by indirect orbital forcing of sedimentation. This hypothesis

implies that particular beds in the offshore facies of the basal Lias should have formed synchronously over large areas. The literature reveals a large number of correlations of limestone beds previously made and individual laminated shale beds are correlated here over 8000km². The wavelengths of the regular cycles are related to the average thickness of ammonite zones at particular locations. It is inferred that the average thickness of ammonite zones was partly determined by local sedimentation rates.

The mechanism that is suggested to have linked climatic changes and sedimentation concerns variations in runoff and the formation of density stratification. Times of dry climates are thought to have involved relatively minor runoff with little clay input so that the sediment was dominated by carbonate mud supplied in coccolithic zooplankton faecal pellets. The water column would have been turbulent so that the bottom-waters remained oxygenated. Thus organic matter would have been oxidized on the sea-floor and infauna would have thoroughly mixed the sediment, so producing light marl. Conversely, during wet climates, it is hypothesized that higher runoff produced a brackish-water wedge across the shelf which led to density stratification. The stagnant bottom-water would have become anoxic so that large quantities of organic matter remained unoxidized, infauna were excluded and clay and organic laminae were preserved. The increased runoff might have supplied more clay than usual so that laminated shale rather than laminated marl accumulated. There is some evidence that the hypothetical wet/dry climatic cycles affected large areas. Thus there are published accounts of coastal Hettangian sequences that consist of ^{interbedded} sandstone and shale and sandstone and limestone in Poland, Sweden and Scotland. There is also evidence for lake-level oscillations in north eastern U.S.A.

Times of relatively high sea-level appear to have caused basin-wide increases in the average proportion of dark marl and laminated shale. Thus, increased water depths might have promoted anoxia. 'Expanded' sequences contain higher proportions of dark marl and laminated shale than 'condensed' sequences. This can be explained by areas of relatively high sedimentation rates which were associated with relatively rapid subsidence and depressions on the sea-floor. Thus the locally deep water might have encouraged anoxia. It is suggested that mixing by wind and waves was only able to affect the top few tens of metres of the water column. When and where the water was deep enough, the bottom-water is thought to have become stagnant and then anoxic as a result. The association of anoxia and high clay contents might be explained in terms of the relative settling rates of clay and coccolithic zooplankton faecal pellets. In turbulent water the clay was more likely to have remained suspended so that carbonate-rich sediment was deposited. Where the bottom-water was stagnant, and thus anoxic, clay would have been able to settle more easily so that more clay-rich sediments accumulated. The interbedding of the basal Lias appears to represent regular cyclicity controlled climatically with the average proportions of different sediment types controlled by local and regional water depths. Minor hiatuses, which appear to be present in all the sections analysed, were perhaps associated with the turbulence produced by exceptional storms and hurricanes.

As well as the five basal Lias sections, eight other formations were analysed with Walsh power spectra. The technique used for time series generation, digitization of measured sections, proved to be readily applicable in most cases. However, this method requires the presence of few rock types that have sharp contacts and which can be demonstrated

to be related to the primary sediment composition. In three examples of the thirteen analyses, no regular cycles with periods of tens of thousands of years were detected. A large number of geological processes are able to destroy regular climatic signals which would otherwise be recorded by the sequence. Therefore, the absence of regular cyclicity according to power spectra does not necessarily indicate that orbital forcing of sedimentation can be ruled out. Indeed, regular and stable sedimentary cycles detected on power spectra which have periods of tens of thousands of years are most easily explained by orbital forcing of sedimentation via climatic processes. Nevertheless, hitherto unknown, perhaps tectonic, processes might mimic Milankovitch cycles in terms of their regularity and periods.

Seven power spectra for Lower ^{Jurassic} strata revealed regular sedimentary cycles consistent with orbital forcing. These spectra indicate that in the Early Jurassic the precession and/or the obliquity cycles were more important than the eccentricity cycles. This is the reverse of the situation previously documented for the later Mesozoic and the Cenozoic. There is no evidence for ice on the globe during the Jurassic so models designed to explain the regular cycles detected must invoke regional climatic changes rather than sedimentation governed by glacio-eustatic fluctuations. In five of the Lower ^{Jurassic} spectra, including three for the basal Lias of Britain, the wavelength ratios are consistent with an orbital cycle possessing a period of 30kyr. However, at present there is only minor independent evidence for such a cycle in Pleistocene and Triassic strata. Overall the power spectra indicate regular cycles explicable in terms of the Milankovitch Theory in about 80% of the sequences studied. Therefore the Milankovitch Theory represents an explanation which should be considered for most examples of open-marine 'cyclic' sequences.

CONTENTS OF VOLUME 1 - TEXT

PAGE

Acknowledgements.

Chapter 1 - Introduction.

1.1 Aim and context.	1
1.2 Milankovitch Theory, power spectra and cyclic rocks.	3
1.3 The basal Lias of Britain; selection for a case study and introduction.	7

Chapter 2 - Field observations and petrography for the basal Lias of South Britain.

2.1 Field description of rock types and exposures.	13
2.1.1 Rock type descriptions.	14
2.1.2 Locality descriptions.	18
2.2 Petrography.	23
2.2.1 'Marginal facies' limestones.	24
2.2.2 'Offshore' or 'Blue Lias facies'.	25
2.3 X-ray diffractometer results.	31
2.4 Scanning electron microscopy.	32
2.5 Hiatuses.	35
2.6 Origin of the microspar.	40
2.7 Primary and secondary considerations in the offshore facies.	44
2.7.1 Evidence for diagenetic limestone formation.	44
2.7.2 Evidence for limestone nucleation related to sediment composition.	46
2.7.3 Evidence for a primary distinction of light marl, dark marl and laminated shale.	47
2.8 Correlation.	49
2.8.1 Large-scale correlation.	50
2.8.2 Correlation bed by bed.	52

Chapter 3 - Geochemical Study of the basal Lias of South Britain.

3.1 Introduction.	55
3.2 Composition according to rock type.	56
3.3 Rock type composition related to stratigraphic position at Watchet, and comparison with Lyme Regis.	58
3.4 Geochemical studies related to Lyme Regis.	59
3.4.1 Detailed geochemical profile.	59
3.4.2 Pyrite formation at Lyme Regis.	61
3.4.3 Stable isotopes at Lyme Regis.	66

Chapter 4 - Walsh power spectra: methodology and results for the basal Lias of South Britain.

4.1 Introduction.	76
4.2 Walsh power-spectral analysis of stratigraphic sections.	78
4.2.1 General Introduction to Walsh power spectra.	78

	<u>PAGE</u>
4.3.2 Sampling and time series generation.	80
4.3.3 Spectral estimation.	83
4.2.4 Testing the significance of spectral peaks.	85
4.2.5 Mathematical considerations.	87
4.2.6 Geological considerations.	89
4.3 Walsh power spectra for the basal Lias of Britain.	93
4.3.1 Time series, errors and dating.	93
4.3.2 Illustration of spectra.	96
4.3.3 The spectra.	97
4.3.4 Discussion.	102
<u>Chapter 5 Synthesis and conclusions for the basal Lias of South Britain.</u>	
5.1 Diagenesis.	105
5.1.1 Controls of limestone formation.	105
5.1.2 The nucleation of cement.	106
5.1.3 Diagenetic history for the basal Lias at Lyme Regis.	109
5.2 Environmental changes recorded in the basal Lias.	113
5.2.1 Changes in sediment composition.	113
5.2.2 Changes in bottom-water oxygenation.	115
5.3 Controls of sedimentation.	120
5.3.1 Climate.	120
5.3.2 Water-depth.	122
5.4 Models explaining the interbedding of light marl, dark marl and laminated shale.	126
5.4.1 Productivity model.	127
5.4.2 Stagnation model.	130
5.4.3 Stagnation model with productivity changes.	132
5.5 Synthesis: a general environmental model for the deposition of the basal Lias.	133
5.6 Conclusions.	138
<u>Chapter 6 Walsh power spectra for various open-marine sequences and power-spectral conclusions.</u>	
6.1 Introduction.	142
6.2 Boom Clay Formation (Lower Oligocene), Belgium.	
6.2.1 Introduction.	142
6.2.2 Spectral analysis.	144
6.3 Upper Kimmeridge Clay Formation (Upper Jurassic), Dorset, England.	
6.3.1 Introduction.	146
6.3.2 Spectral analysis.	149
6.4 Middle Pliensbachian-Toarcian of Breggia Gorge, Ticino, Switzerland.	
6.4.1 Introduction.	152
6.4.2 Toarcian section introduction.	153
6.4.3 Toarcian section spectral analysis.	154

	<u>PAGE</u>
6.4.4 Upper Pliensbachian section introduction.	155
6.4.5 Upper Pliensbachian section spectral analysis.	155
6.4.6 Middle Pliensbachian section introduction.	156
6.4.7 Middle Pliensbachian section spectral analysis.	157
6.5 Belemnite Marls (Lower Jurassic), Charmouth, Dorset, England.	
6.5.1 Introduction.	157
6.5.2 Spectral analysis.	159
6.6 'Siliceous shales' (Lower Jurassic), Robin Hood's Bay, Yorkshire, England.	
6.6.1 Introduction.	160
6.6.2 Spectral analysis.	161
6.7 Upper Birkhill Shales (Lower Silurian), Dob's Linn, Dumfries and Galloway, Scotland.	
6.7.1 Introduction.	162
6.7.2 Spectral analysis.	164
6.8 Discussion of power spectral results.	
6.8.1 Walsh power spectra.	165
6.8.2 Interpreting power spectra.	165
6.8.3 Spectral evolution.	169
6.9 Power spectral conclusions.	171
<u>References.</u>	175

CONTENTS OF VOLUME 1 - TABLES

	<u>Between</u> <u>Pages</u>
<u>Chapter 1:</u>	
1A Lithostratigraphic Units analysed using Walsh power spectra.	3 & 4
1B Biostratigraphic zonation of the Lias of Britain.	9 & 10
1C Reference list for descriptions of Lower Liassic Fossils.	9 & 10
 <u>Chapter 3:</u>	
3A Lyme Regis - Limestone geochemical results.	75 & 76
3B Lyme Regis - Light marl geochemical results.	75 & 76
3C Lyme Regis - Dark marl geochemical results.	75 & 76
3D Lyme Regis - Laminated shale geochemical results.	75 & 76
3E Lyme Regis - <u>Gryphaea arcuata</u> stable isotope results.	75 & 76
3F Watchet - Limestone geochemical results.	75 & 76
3G Watchet - Light marl geochemical results.	75 & 76
3H Watchet - Dark marl geochemical results.	75 & 76
3I Watchet - Laminated shale geochemical results.	75 & 76
3J Watchet - Laminated limestone geochemical results.	75 & 76
3K Watchet - Average geochemical values at Lyme Regis and Watchet.	75 & 76
 <u>Chapter 4:</u>	
4A Average errors for thickness measurements and minimum sedimentation rates for the basal Lias.	96 & 97

CONTENTS OF VOLUME 2 - FIGURES

	<u>PAGE</u>
<u>Chapter 1</u>	
1.1A	Location of the lithostratigraphic units listed in Table 1A. 1
1.2A	The nature of cyclic changes in orbital obliquity. 2
1.2B	The nature of cyclic changes in orbital eccentricity. 3
1.2C	The nature of cyclic changes in orbital precession. 4
<u>Chapter 2</u>	
2.1A	Map of basal Lias localities. 5
2.1B	Field photo of limestone nodule in Lang's bed 36, Lyme Regis. 6
2.1C	Field photo of limestone nodules in light marl bed passing laterally into a continuous limestone bed. 6
2.1D	Field photo illustrating the different rock types. 7
2.1E	Field photo illustrating the different rock types. 7
2.1F	Field photo of <u>Chondrites</u> burrow-mottles in a light marl and limestone bed. 8
2.1G	Field photo of <u>Diplocraterion</u> burrow-mottle in a limestone underneath a dark marl bed. 8
2.1H	Field photo of burrow-mottling in a dark marl and limestone bed. 9
2.1I	Field aspect of the basal Lias at Lyme Regis, Dorset. 9
2.1J	Field aspect of the basal Lias at Watchet, Somerset. 10
2.1K	Field photo of Palmer's beds C56-C82 near Blue Ben, Watchet. 10
2.1L	Field photo of Trueman's beds 9-33, <u>Pre-planorbis</u> beds - <u>planorbis</u> zone, Lavernock Point, Glamorgan. 11
2.1M	Field aspect of the basal Lias at Nash Point, Glamorgan. 12
2.1N	Field photo of Trueman's beds 1-7, <u>conybeari</u> subzone, <u>bucklandi</u> zone, Nash Point. 12
2.1O	Field photo of Clement's <u>et al.</u> 's beds 17k-23g, <u>angulata</u> zone, Long Itchington, Warwickshire. 13
2.2A	The Sutton Stone overlying the Carboniferous Limestone at Southerndown, Glamorgan. 14
2.2B	Close-up of the Southerndown beds at Southerndown, Glamorgan. 14
2.2C	The Brockley Down Stone overlying the Carboniferous Limestone at Lulsgate, Avon. 15
2.2D	Loose blocks of Brockley Down Stone at Lulsgate Quarry. 15
2.2E	Thin section photomicrograph of limestone. 16
2.2F	Thin section photomicrograph of limestone. 16
2.2G	Thin section photomicrograph of limestone. 17
2.2H	Thin section photomicrograph of limestone. 17
2.2I	Thin section photomicrograph of <u>Gryphaea</u> . 18
2.2J	Thin section photomicrograph of <u>Gryphaea</u> . 18
2.2K	Thin section photomicrograph of light marl. 19
2.2L	Thin section photomicrograph of light marl. 19
2.2M	Thin section photomicrograph of dark marl. 20
2.2N	Thin section photomicrograph of dark marl. 20

	<u>PAGE</u>
2.2O	Thin section photomicrograph of laminated shale. 21
2.2P	Thin section photomicrograph of laminated shale. 21
2.2Q	Thin section photomicrograph of beef calcite. 22
2.2R	Thin section photomicrograph of beef calcite. 22
2.2S	Thin section photomicrograph of laminated limestone. 23
2.2T	Thin section photomicrograph of laminated limestone. 23
2.3A	XRD trace for laminated shale whole-rock powder. 24
2.4A	SEM photomicrograph of limestone. 25
2.4B	SEM photomicrograph of light marl. 25
2.4C	SEM photomicrograph of light marl. 26
2.4D	SEM photomicrograph of dark marl. 26
2.4E	SEM photomicrograph of dark marl. 27
2.4F	SEM photomicrograph of dark marl. 27
2.4G	SEM photomicrograph of dark marl. 28
2.4H	SEM photomicrograph of laminated shale. 28
2.4I	SEM photomicrograph of laminated shale. 29
2.4J	SEM photomicrograph of laminated limestone. 29
2.5A	Relative thickness changes in the basal Lias studied. 30
2.5B	Field photo of limestone surface dominated by <u>Gryphaea</u> . 31
2.5C	Field photo of limestone containing limestone intraclasts. 31
2.5D	Field photo of isolated dark marl burrow-mottles. 32
2.5E	Photo of cut and polished block of limestone showing encrusted and bored surface. 33
2.5F	Photo of cut and polished block of limestone showing encrusted and bored surface. 33
2.5G	Negative prints of acetate peels from the encrusted and bored limestone surface. 34
2.5H	Negative prints of acetate peels from the encrusted and bored limestone surface. 34
2.8A	Stratigraphic variations in the average proportions of different rock types. 35
2.8B	Stratigraphic variations in the average proportions of different rock types. 36
2.8C	Correlation of %light marl/limestone with number of limestone beds and nodule horizons. 37
2.8D	Correlation in the basal Lias. 38
2.8E	Possible lithostratigraphic correlation for the lower part of the basal Lias. 39
2.8F	Possible lithostratigraphic correlation for the upper part of the basal. Lias. 40

Chapter 3

3.2A	Lower Lias whole rock composition according to rock type. 41
3.2B	TOC/CaCO ₃ relationship at Watchet and Lyme Regis. 42
3.2C	Clay/FeS ₂ /CaCO ₃ relationship at Watchet and Lyme Regis. 43
3.3A	Variations in whole rock composition at Watchet. 44
3.4A	Detailed geochemical profiles through Lang's beds 13-20 Upper <u>angulata</u> zone, Seven Rock Point, Lyme Regis. 45

	<u>PAGE</u>
3.4B	Field photo of Lang's beds 13-20, <u>angulata</u> zone, Seven Rock Point, Lyme Regis. 46
3.4C	Interpretation of S/DOP/Fe/TOC plots 47
3.4D	S/DOP/Fe/TOC relationships Upper <u>angulata</u> zone, Lyme Regis. 48
3.4E	Fe/S and S/TOC relationships at Watchet and Lyme Regis. 49
3.4F	Stable isotopes of carbonate from the <u>angulata-bucklandi</u> zone, Lyme Regis. 50
3.4G	Previously published stable isotopes from the <u>Pre-planorbis</u> beds- <u>semicostatum</u> zone, Lyme Regis. 51
3.4H	Stable isotopes in <u>Gryphaea arcuata</u> specimen BLG33. 52
3.4I	Stable isotopes in a limestone nodule from Lang's bed 37 <u>bucklandi</u> zone, Seven Rock Point, Lyme Regis. 53

Chapter 4

4.2A	Walsh power spectral estimates. 54
4.2B	The effect of hiatuses upon a perfectly regular time series. 55
4.2C	Time series: 16cm cycle plus 'random' gaps, for Fig 4.2B. 56
4.2D	Time series generated with random numbers. 57
4.2E	Spectrum of random time series. 58
4.2F	Time series generation. 59
4.2G	Choosing sample intervals. 60
4.2H	Testing the significance of spectral peaks. 61
4.2I	Harmonics. 62
4.3A	Basal Lias, Lyme Regis time series. 63
4.3B	Basal Lias, Lyme Regis power spectra. 64
4.3C	Basal Lias, Watchet time series. 65
4.3D	Basal Lias, Watchet time series. 66
4.3E	Basal Lias, Watchet time series. 67
4.3F	Basal Lias, Watchet power spectra. 68
4.3G	Basal Lias, Lavernock Point time series. 69
4.3H	Basal Lias, Lavernock Point power spectra. 70
4.3I	Basal Lias, Nash Point time series. 71
4.3J	Basal Lias, Nash Point power spectra. 72
4.3K	Basal Lias, Long Itchington time series. 73
4.3L	Basal Lias, Long Itchington power spectra. 74

Chapter 5

5.1A	Relationship between number of cemented horizons and zone thickness. 75
5.3A	Sea-level changes in the Early Jurassic in Britain. 76
5.4A	Productivity model. 77
5.4B	Stagnation model. 78
5.5A	General environmental model for the latest Triassic and earliest Jurassic in South Britain. 79
5.5B	Palaeogeography in the Hettangian and Early Sinemurian. 80

Chapter 6

6.2A	Field aspect of the Boom Clay Formation, Terhagen, near Antwerp.	81
6.2B	Boom Clay Formation time series.	82
6.2C	Boom Clay Formation power spectra - using five codes.	83
6.2D	Boom Clay Formation power spectra - using two codes.	84
6.3A	Field aspect of the Upper Kimmeridge Clay Formation, near Freshwater Steps, Kimmeridge, Dorset.	85
6.3B	Kimmeridge Clay Formation time series.	86
6.3C	Kimmeridge Clay Formation upper section power spectra.	87
6.3D	Kimmeridge Clay Formation lower section power spectra.	88
6.4A	Measured sections within the stratigraphy of Breggia Gorge, Ticino, Switzerland.	89
6.4B	Field aspect of the Toarcian section, Breggia Gorge.	90
6.4C	Breggia Gorge Toarcian section time series.	91
6.4D	Breggia Gorge Toarcian section power spectra.	92
6.4E	Field aspect of the Upper Pliensbachian section Breggia Gorge.	93
6.4F	Breggia Gorge Upper Pliensbachian section time series.	94
6.4G	Breggia Gorge Upper Pliensbachian section power spectra.	95
6.4H	Field aspect of the Middle Pliensbachian section Breggia Gorge.	96
6.4I	Breggia Gorge Middle Pliensbachian section time series.	97
6.4J	Breggia Gorge Middle Pliensbachian section power spectra.	98
6.5A	Field aspect of the Belemnite Marls, Charmouth, Dorset.	99
6.5B	Belemnite Marls time series.	100
6.5C	Belemnite Marls power spectra.	101
6.6A	Field aspect of the 'Siliceous Shales', Robin Hood's Bay, Yorkshire.	102
6.6B	'Siliceous Shales' time series.	103
6.6C	'Siliceous Shales' power spectra.	104
6.7A	Field aspect of the Upper Birkhill Shales, Dob's Linn, Dumfries and Galloway.	105
6.7B	Upper Birkhill Shales time series.	106
6.7C	Upper Birkhill Shales power spectra.	107

CONTENTS OF VOLUME 2 - APPENDICES

	<u>PAGE</u>
<u>For Chapter 2 - Stratigraphic logs for the basal Lias sections</u>	
Key to stratigraphic logs.	
2.1 Stratigraphic log for the basal Lias at Lyme Regis.	108
2.2 Stratigraphic log for the basal Lias at Watchet.	115
2.3 Stratigraphic log for the basal Lias at Lavernock Point.	138
2.4 Stratigraphic log for the basal Lias at Nash Point.	145
2.5 Stratigraphic log for the basal Lias at Long Itchington.	149
<u>For Chapter 3 - Geochemical methodology</u>	
3.1 Bulk sample preparation.	156
3.2 <u>Gryphaea</u> specimen preparation.	156
3.3 Determination of %CaCO ₃ , %TOC, and % FeS ₂ .	157
3.4 Determination of %Fe/R and DOP/R.	158
3.5 Determination of $\delta^{18}\text{O}$ and $\delta^{13}\text{C}$.	160
3.6 Reproducibility.	161
<u>For Chapter 4 - Computer Program for illustrating time series and generating Walsh power spectra</u>	
4.1 Listing of Program WPSPEC.	163
<u>For Chapter 5 - Publications</u>	
5.1 Weedon 1985.	168
5.2 Weedon 1986.	169
5.3 Weedon 1987.	184
<u>For Chapter 6 - Time series for various formations</u>	
6.1 Time series for the Boom Clay Formation.	186
6.2 Time series for the Upper Kimmeridge Clay Formation.	188
6.3 Time series for the Toarcian section at Breggia Gorege.	190
6.4 Time series for the Upper Pliensbachian section at Breggia Gorge.	193
6.5 Time series for the Middle Pliensbachian section at Breggia Gorge.	195
6.6 Time series for the Belemnite Marls.	196
6.7 Time series for the 'Siliceous Shales'.	197
6.8 Time series for the Upper Birkhill Shales.	198

ACKNOWLEDGEMENTS.

This thesis would have been impossible without considerable help and many ideas from my supervisor Dr. H.C. Jenkyns. The conception of the project was his at a time when the Milankovitch Theory was still new to most sedimentologists in this country. Professors A. Hallam and M.R. House suggested independently that I examine the Kimmeridge Clay Formation. Mr. C. Elders suggested spectral analysis of the Birkhill Shales and he and Prof. W.S. McKerrow helped with the relevant references. Dr. W.J. Kennedy helped my examination of a bored limestone block and supplied many references.

The project was supported by a NERC research studentship.

In the field Mark Burchell kindly drove me to and from Switzerland and helped me find exposures. In Belgium, Prof. Noel Vandenberghe of the Catholic University of Leuven introduced me to the Boom Clay Formation and provided a stratigraphic log which he had compiled over many years. I would like to thank various companies for allowing me to work in certain quarries. Permission to enter Lulsgate Quarry was granted by Mr. C.Hopkins of British China Clays Ltd. Mr. G. Benham of Rugby Portland Cement Co. and Blue Circle Industries enabled me to examine the Quarries at Long Itchington and Barnstone respectively.

On the technical side the staff of the B.G.S. Stable Isotope Laboratory at Gray's Inn Road, London were extremely helpful. I would particularly like to thank doctors P. Greenwood, L. Thrift, and B. Spiro. At Oxford, Richard McAvoy and Steve Baker helped me photographically and Steve also helped me with Cathodoluminescence. Colin Fagg helped me with the SEM whilst Clive Johnson and Steve Wyatt provided many hours of help with various types of geochemistry (Steve W. also threw in the odd wise-crack to cheer me up). Vivian Chamberlain, Andria Fowler and Sally Thompson were extremely helpful with secretarial problems.

Fellow research students Chris ('Frankie') Elders, Ghassan Al-Murani, Nigel Platt, Peter Jackson and Mark Burchell have been especially helpful in enabling me to discuss my ideas. Additionally, all the research students in Oxford have made my time in Oxford extremely enjoyable - even if they didn't like my red jumper!

My last abode in Oxford was inhabited by an eccentric bunch who employed a variety of diversionary tactics to stop me from working all the time. My thanks therefore to James, Malcolm, Christian and Maurice leChat.

Finally, Bowie provided the music, Star Trek supplied inspiration and Alexis gave me the love and support I needed.

CHAPTER 1

INTRODUCTION

1.1 Aim and Context

Open-marine 'cyclic' sequences are encountered frequently at outcrop and during deep-sea drilling (Dean et al. 1977, Einsele 1982b). They are characterized by centimetre-metre scale alternations of rock types which reflect vertical (stratigraphic) variations in the proportions of carbonate, organic carbon, clay or chert. Occasionally a dual geochemical variation is observed such as an antithetic relationship between %CaCO₃ and %TOC (total organic carbon). Examples of such 'cyclic' sequences, sometimes termed 'periodites' (Section 4.1), are known from most geological systems and were typically deposited in the open ocean or in the deeper parts of shelf/epeiric seas (Einsele 1982a and 1982b). (Geological cyclicity is discussed in Section 4.1; in this chapter the word cyclic does not necessarily imply regularity). Einsele (1982b), Arthur et al. (1984) and Fischer (1986) have reviewed open-marine cyclic sedimentation and sequences.

The mechanisms or processes that generated such small-scale cyclicity differ from those of 'turbidites' and 'tempestites' although all 3 may have contributed in a single section. Deep marine cyclic sequences carry chronostratigraphic information and correspond to the 'Type 1' cycles defined by Schwarzacher (1975). Thus more than just a few hours or days are needed to deposit a complete cycle. Variations in local biological productivity, supply of clastics, supply of organic matter, dissolution or hydrology (such as degree of circulation) may all be capable of generating primary centimetre-metre scale rock-type alternations. In any given case a variety of sometimes interrelated processes might have operated. The underlying controls might be climatic, tectonic or eustatic. Conceivably undescribed long-term biological controls might exist as well. These might act through changes

in, for instance, planktonic ecosystems with attendant changes in sediment composition. As biological controls remain entirely speculative at present, they will not be considered below. Again, several underlying controls might apply in one particular case because of the relationship between climate, tectonism and sea-level.

The Croll-Milankovitch Theory or Orbital Theory of climatic change was used as early as 1895 by Gilbert to explain Cretaceous limestone-shale alternations (Gilbert 1895, Fischer 1980). A few additional studies used the same explanation up to the mid 1970s (Section 1.2). Then palaeoclimatologists provided considerable support for the Orbital Theory with the use of sophisticated statistical techniques (power-, phase- and coherency-spectral analysis) (Section 1.2). Consequently sedimentologists took the Theory more seriously and the number of relevant publications has proliferated since, particularly in the mid-1980s. Phase- and coherency-spectra cannot be applied to ancient rocks (>2Myr) at present. However, power-spectral analysis has had some success as a way to identify objectively the regular cycles predicted by the the Milankovitch Theory. In fact, power spectra have also been applied by sedimentologists analysing varves, turbidites and sandstones possessing tidal-bundles (Anderson & Koopmans 1963, Martini et al. 1978, Williams & Sonnett 1985, Yang & Nio 1985).

The Milankovitch Theory may provide an explanation for the nature of a large proportion of cyclic marine rocks. Given the numerous examples of this group it was hoped that a detailed examination of one formation might provide a method for the routine interpretation of all such rocks. Therefore, the aim of this thesis has been to make a detailed case study of the basal Lias of Britain. This has involved petrography and sedimentology (Chapter 2), geochemistry (Chapter 3) and Walsh power

TABLE 1A: Lithostratigraphic Units analysed using Walsh Power Spectra (Chapters 4 & 6).

<u>AGE</u>	<u>LITHOSTRATIGRAPHIC NAME</u>	<u>LOCATION</u> (Fig 1.1A)	<u>CHAP.</u>
NP22-24, Rupelian, OLIGOCENE.	Boom Clay Formation.	Pits S.W. of Antwerp Belgium.	6
<u>P.elegans-P.pectinatus</u> zone, Kimmeridgian, JURASSIC.	Kimmeridge Clay Formation.	Kimmeridge Bay- Chapman's Pool, Dorset, England.	6
<u>P.davoei-D.levesquei</u> zone, Pliensbachian- Toarcian, JURASSIC.	Medolo Formation & Ammonitico Rosso.	Breggia Gorge, Morbio Superiore, Ticino, Switzerland.	6
<u>U.jamesoni</u> zone, Pliensbachian, JURASSIC.	'Belemnite Marls', Lower Lias Formation.	Charmouth, Dorset, England.	6
<u>O.oxynotus-</u> <u>E.raricostatum</u> zone, Sinemurian, JURASSIC.	'Siliceous Shales' Redcar Mudstone Formation.	Robin Hood's Bay, Yorkshire, England.	6
<u>A.bucklandi</u> zone, Sinemurian, JURASSIC.	Lower Lias Formation.	Nash Point, Glamorgan, Wales.	4
'Pre- <u>planorbis</u> Beds'- <u>A.semicostatum</u> zone, Rhaet.-Sine. TRI.-JUR.	Blue Lias Member, Lower Lias Formation.	Lyme Regis, Dorset, England.	4
<u>A.liasicus-A.bucklandi</u> zone, Hettangian- Sinemurian, JURASSIC.	Lower Lias Formation (inc. Blue Lias Mbr.).	Long Itchington, Warwickshire, England.	4
'Pre- <u>planorbis</u> Beds'- <u>A.bucklandi</u> zone, Rhaet. -Sine. TRIAS.-JURASSIC.	Lower Lias Formation (inc. Blue Lias Mbr.).	Watchet, Somerset, England.	4
'Pre- <u>planorbis</u> Beds'- <u>A.angulata</u> zone, Rhaet. -Sine. TRIAS.-JURASSIC.	Lower Lias Formation.	Lavernock Point, Glamorgan, Wales.	4
<u>M.sedgwickii</u> zone, Llandovery, SILURIAN.	Upper Birkhill Shales.	Dob's Linn, Dumfries & Galloway, Scotland.	6

spectral analysis (Chapter 4). As well as the spectral analysis of the basal Lias, Chapter 4 outlines the theory of Walsh power spectra applied to sedimentary rocks as this method is still extremely new to sedimentology. An attempt is made, in Chapter 5, to establish the nature of the fundamental control of the cyclicity in the basal Lias and to provide a model of the link between the control (climatic, tectonic or eustatic) and the sedimentary cycles. Chapter 5 ends with conclusions concerning the sedimentology of the basal Lias of South Britain. Chapter 6 concerns the spectral analysis of a variety of, mainly Liassic, cyclic sequences (listed in Table 1A and located on Fig 1.1A) and finishes with conclusions concerning spectral analysis in general. The present chapter is concluded with a summary of the Milankovitch Theory and an introduction to the basal Lias of Britain.

In this thesis appendices are numbered according to the chapter they are associated with and appendix section-numbers are independent of the text section-numbers. Figures are identified by the relevant text section-number followed by a specific capital letter. Tables are identified by a chapter number and then a specific capital letter.

1.2 The Milankovitch Theory, power spectra and cyclic rocks.

A good general introduction to the work of Croll and Milankovitch and palaeoclimatic investigations of the Pleistocene up to the late 1970s, is provided by Imbrie & Imbrie (1979). The most important paper to emerge in support of the Milankovitch Theory in the 1970s was undoubtedly that by Hays et al. in 1976. The volumes entitled 'Milankovitch and Climate' are a useful guide to the state-of-the-art in the mid 1980s and reflect the multidisciplinary nature of the field (Berger et al. 1984). Papers in the journal called 'Icarus' volume 50

parts 2 & 3 indicate the progress made in relating the layered-deposits of the Martian polar regions to changes in the orbit of Mars (eg Cutts and Lewis 1982). An introduction to climatology and meteorology can be found in Barry & Chorley (1982). Frakes (1979) and Crowley (1983) review the nature of Earth's climate during geologic time.

According to the Milankovitch^c Theory, cyclic changes in^{the} Earth's orbit induce climatic changes due to the redistribution of radiation (insolation) over the globe. Three different types of orbital cycles are involved, each possessing characteristic periods. The types of orbital cycles and the climatic effects associated with each are depicted schematically in Figs 1.2A-C. The most important periods involved are precession = 21kyr (21,000yr), obliquity = 41kyr and eccentricity = 100kyr and 410kyr. These orbital cycles do not significantly alter the total amount of radiation received by Earth in one year. Instead radiation is continuously redistributed according to latitude and season. Considerable discussion continues concerning the mechanism which links small changes in insolation to large changes in the world's climate. Shackleton & Pisias (1985) suggested that CO₂-levels in the atmosphere are controlled by insolation changes and actually amplify climatic variation.

The durations of the orbital cycles have been determined by modern astronomical observations and, using the equations of celestial mechanics, insolation values have been calculated for the last 1.6Myr (Berger 1984). The orbital cycles are caused by the movements of the planets and the Moon which gravitationally perturb the Earth in its orbit around the Sun. Ancient orbital cycles are likely to have retained the same periods for much of Earth history, but changes in the separation of the Earth and Moon suggest a slowly lengthening precession

cycle (Berger 1984). Significantly, Olsen (1984, 1986) found, using varves for dating, that in the late Triassic the precession cycle lasted about 20.8kyr and the eccentricity cycles 101.4 and 418.0kyr.

The regularity of the orbital cycles led Hays et al. (1976) to analyse $\delta^{18}\text{O}$ values from foraminifera in a deep-sea core with Fourier power spectra. Power spectra are used to detect regular cycles superimposed on a background of random variation (noise) (Imbrie 1985). Once a timescale had been constructed for the core, the power spectra revealed that regular cycles with durations of 21, 41 and 100kyr dominated variations in world ice-volumes (monitored by $\delta^{18}\text{O}$ recorded in foraminifera tests, Mix & Ruddiman 1984). Thus orbital control of ice-volumes was inferred. They tested this hypothesis by using phase spectra to compare calculated insolation values and $\delta^{18}\text{O}$ values. This demonstrated that changes in ice-volumes lagged changes in the orbit by a constant amount as predicted by the Milankovitch Theory. Recent work with coherency spectra has shown that 85% of the variation of ice-volumes at the Milankovitch frequencies (19, 23, 41 and 100kyr) are accounted for by orbital-forcing (Imbrie et al. 1984).

Gilbert (1885) hypothesised that orbital-precession forced sedimentation during the Cretaceous in North America (Greenhorn Formation). Bradley (1929) used varves in the Green River Formation (Eocene) to identify a 20kyr cycle in sedimentation. Other early studies which implied orbitally-controlled sedimentary cycles include that of Fischer (1964) on the Dachstein Limestone (Triassic) and of Van Houten (1964) on the Lockatong Formation (also Triassic). None of these studies utilized power-spectral analysis which is used nowadays to define regular cyclicity objectively.

Schwarzacher (1964) was probably the first to apply power spectra to cyclic sedimentary rocks. Both his work and that of Carss & Neidell (1966) concerned Carboniferous rocks. So, although both identified regular cycles with durations of tens of thousands of years, it is not clear whether sedimentation responded to local climatic variations or to glacio-eustatic changes related to changes in Carboniferous ice-volumes (Frakes 1979). The Mesozoic appears to have been ice-free (Frakes 1979) so that Dunn (1974), working on the Kimmeridge Clay Formation, was perhaps the first person to show that local orbitally forced climatic changes could have produced regular sedimentary cycles.

In 1982 three papers using power spectra were published. Anderson (1982 and 1984) demonstrated a 20kyr and possibly a 100kyr cycle in varved evaporites of the Permian Castile Formation. Schwarzacher & Fischer recognised cycles with periods of 20, 40 and 100kyr in the Cretaceous Maiolica and Scaglia Bianca of the Umbrian Apennines, Italy (see also Fischer & Schwarzacher 1984). De Boer (1982) and de Boer & Wonders (1984) analysed the Scisti a Fucoidi and the lower Scaglia Bianca of the same region and recognised cycles of 20 and 100kyr. Weedon (1985, 1986) published a Walsh spectral analysis for the basal Lias of Britain (reproduced in Appendix Sections 5.1 and 5.2). Herbert & Fischer (1986) used densitometer measurements from photographs of core from the Scisti a Fucoidi as well as %CaCO₃ measurements to produce power spectra. Curiously this and previous studies of the Italian mid-Cretaceous have not provided any firm spectral evidence for a 20kyr cycle, although all these authors believe that this would account for the limestone/marl couplets. Also in 1986, Olsen provided the first power-spectral analysis of the Lockatong and Passaic Formations (Norian, Triassic) from the Newark basin.

Important work which excluded spectral analysis includes the review by Cotillon & Rio (1984) of DSDP cyclic sequences and Fischer's (1986) wide-ranging review of climatic rhythms in strata. Additionally House (1985) proposed that orbitally-forced cycles be used to refine the absolute timescale and argued that most facies in the Jurassic of Britain contain evidence for orbital forcing of sedimentation (House 1986). Barron et al. (1984) have shown using a General Circulation Model (based on Cretaceous palaeogeography) how cycles in the Greenhorn Formation were linked to variations in runoff through changes in the density stratification of the waters of the mid-continental seaway of North America.

1.3 The basal Lias of Britain, selection for a case study and introduction.

The basal Lias of Britain (Pre-planorbis Beds - bucklandi Zone) has been selected as the case study for a variety of reasons. This group of rocks provides a fairly typical example of a Mesozoic cyclic marine formation deposited in a subtropical shelf sea (Hallam 1960a, House 1986). Additionally both primary and diagenetic processes contributed to the present cyclicity. The rocks are mud-grade with vertical variations in the major constituents: calcium carbonate, clay, organic matter and pyrite (Hallam 1964).

The Lower Lias Formation as a whole (Pre-planorbis Beds, Rhaetian - davoei zone, Pliensbachian) has exceptional biostratigraphic control and an extensively investigated fauna and flora. The shelf setting led to the presence of plankton, nekton, benthos and infaunal traces. It was hoped that this range of fossils/^{and trace fossils}would provide more environmental information than is available from most pelagic rocks (which often lack

benthonic fossils). Finally during the earliest Jurassic Pangaea remained intact and there is no evidence for ice on the globe at this time (Frakes 1979, Smith et al. 1981). These factors may have significantly reduced the number of palaeogeographic and palaeoclimatic variables involved if a climatic model is to be considered.

The Blue Lias Member belongs to the Lower Lias Formation and has a type section designated at Saltford railway cutting, Avon, (Section 2.1) (Cope et al. 1980, Donovan & Kellaway 1984). This member has diachronous upper and lower contacts and is vaguely defined at present by the proportion of limestone beds per unit thickness. The rest of the formation is characterised by calcareous and bituminous shales and marls with fewer limestone beds per unit thickness. The 'White Lias' has been included within the Lower Lias (Donovan & Kellaway 1984), but instead this study follows the London Geological Society Reports (Cope et al. 1980, Warrington et al. 1980) which include it in the Triassic Lilstock Formation. The base of the Jurassic has now been defined by the first appearance of the ammonite Psiloceras (Cope et al. 1980). Therefore the 'Pre-planorbis Beds' or 'Ostrea Beds' at the base of the Lower Lias are automatically defined as belonging to the Triassic. For convenience the 'basal Lias' is defined here as encompassing rocks from the base of the Pre-planorbis Beds to the top of the bucklandi zone of the Sinemurian. This is an informal definition referring to both the marginal and offshore facies (Section 2.1) although Chapters 2-5 concentrate on the offshore facies.

Lithostratigraphic descriptions are comprehensively referenced by Cope et al. (1980). Later descriptions include the work of Donovan & Kellaway (1984) on the Bristol district, of Hodges (1986) and Ager (1986) on the Welsh Lias and of Batten et al. (1986) and Amiri-Garroussi

1978) on the Triassic-Jurassic rocks of Scotland. The biostratigraphic zonation of the British Lower Lias as defined at present using ammonites, dinocysts and coccoliths is shown in Table 1B. Table 1C lists the sources of descriptions for most groups of fossils.

The key developments in the investigation into the sedimentology of the basal Lias are outlined below. As the work of Chapters 2-5 is limited to the offshore facies the discussion does not include clastic facies such as the Broadford Beds (Hallam 1959, Amiri-Garroussi 1978). The first rigorous investigations into the origin of the limestone/'shale' alternations of the Blue Lias Member were made by Richardson (in Lang et al. 1923). He observed that the limestone beds are progressively more separated moving up section from the Blue Lias and into the Shales with Beef at Lyme Regis, Dorset and noted the presence of elliptical limestone nodules. The nodules he concluded indicated a diagenetic origin for the limestones and, since he saw no limestone intraclasts, he believed the section lacked hiatuses. Thus based on separation of the limestones he compared limestone formation to Liesegang gels and believed that all the limestones formed simultaneously. Kent (1936) observed a Dapedius on its side (bedding parallel) with an oblique crossing of a limestone/'shale' contact. Two closely-spaced limestones were seen to change thickness - each at the expense of the other - but to maintain their combined thickness. So a diagenetic but 'replacive' and not 'displacive' origin was implied (the Dapedius was partly inside the limestone). The macro-fauna appeared to be identical in the 'shales' and limestones. Fossils were found crushed inside the shales and uncrushed inside the limestones so Kent implied that limestone formation preceded significant compaction. This in turn implied successive rather than simultaneous formation of limestones.

TABLE 1B: Biostratigraphic Zonation of the Lias of Britain.

<u>CALCAREOUS NANNOFOSSILS</u>	<u>AMMONITES</u>	<u>DINOCYSTS</u>	STAGE
(Hamilton 1982 cf Perch-Nielsen 1985)	(Dean et al. 1961)	(Wollam & Riding 1983 cf Williams & Bujah 1985)	
<u>E.britannica</u> (pars)	<u>D.levesquei</u> <u>G.thouarsense</u> <u>H.variabilis</u>	<u>M.semitabulatum</u> (pars)	TOARCIAN
	<u>H.bifrons</u> <u>H.falciferum</u> <u>D.tenuicostatum</u>		
<u>A.cylindratus</u>	<u>P.spinatum</u> <u>A.margaritatus</u>	<u>L.spinosa</u>	PLIENSACHIAN
	<u>P.davoei</u> <u>T.ibex</u>		
<u>C.crassus</u>	<u>U.jamesoni</u> <u>E.raricostatum</u> <u>O.oxynotum</u> <u>A.obtusum</u>	<u>L.variabile</u>	SINEMURIAN
<u>P.liasicus</u>	<u>C.turneri</u> <u>A.semicostatum</u> <u>A.bucklandi</u>	<u>D.priscum</u>	HETTANGIAN
<u>C.primulus</u>	<u>S.angulata</u> <u>A.liasicus</u>		
<u>A.arkelli</u>	<u>P.planorbis</u>		RHAETIAN

The relationship between the zones of different groups is schematic.

TABLE 1C: Reference List for Descriptions of Lower Liassic Fossils.

MACRO-FOSSILS:

Miscellaneous Invertebrates ----- Hallam 1960.

Ammonites ----- Wright 1878-1886, Donovan
1953.

Vertebrates ----- Owen 1861-1881.

Tracefossils ----- Hallam 1960, Sellwood 1970.

MICRO-FOSSILS:

Foraminifera ----- Copestake & Johnson 1981.

Ostracods ----- Field 1968, Lord 1978.

Palynomorphs ----- Wall 1965, Wollam & Riding
1983.

NANNO-FOSSILS:

Coccoliths ----- Hamilton 1982.

Intraclasts were noted in Nottinghamshire and demonstrated contemporary erosion.

Shukri (1942) showed that the concentration of limestones towards the base of the Blue Lias at Lyme Regis was not a result of downward-moving pore-waters as believed by Richardson (in Lang et al. 1923). Nevertheless, he agreed that the Liesegang ring mechanism could account for the limestones. He discounted Kent's (1936) arguments concerning compaction by asserting that by the end of bucklandi zone time the total thickness of the Lias was too small to have caused much compaction even at the base. Therefore he maintained that simultaneous formation of limestones could still be invoked. He reasoned that direct, primary carbonate-precipitation would be controlled by temperature and that, in turn, temperature would have been controlled by the 21kyr precession cycle. As the limestone bands change their separation up-section, he believed that this was inconsistent with an orbital control and therefore discounted primary mechanisms. (The idea that an orbital cycle produced the alternations but that sedimentation rates gradually increased, does not seem to have occurred to him.)

A geochemical investigation which concentrated mainly on heavy metals, showed that %TOC in the marls and shales is correlated with %CaCO₃ (LeRiche 1959). Note that the %TOC was expressed on a carbonate-free basis to remove the dilution-effect of the carbonate. This showed that little change had occurred in the relationship between the proportion of carbonate and organic matter since deposition (LeRiche 1959). If primary carbonate had dissolved in the marls and shales to form the limestones, there would be no correlation today (Section 3.2). Next Hallam (1960a, 1964) showed that burrow-mottling between the limestones and marls and primary lamination within the bituminous shales

revealed that a primary distinction existed between these rock types. The nodules and wavy contacts of some limestones he thought did indicate a diagenetic origin, but this must have emphasized a pre-existing distinction in sediment composition. On balance he favoured water-depth changes as the cause of cyclicity (Hallam 1964). Detailed petrographic and palaeontological studies showed that the bituminous shales had an impoverished and dwarfed benthos. The marls and limestones were shown to contain almost identical fossils when differences in preservation were considered (Hallam 1960a). Wobber (1965, 1966, 1967, 1968a, 1968b) investigated the sedimentation of the Sutton Stone and Southerndown Beds previously shown (Trueman 1922) to have accumulated in a near-shore environment in Glamorgan.

Sellwood (1970a and 1970b) pointed out that although very similar with respect to lithology, the Belemnite Marls of Charmouth, Dorset represent rocks which are much less altered diagenetically than the Blue Lias at Lyme Regis, Dorset. By analogy with the Belemnite Marls he believed the Blue Lias rhythms recorded the interplay of regional subsidence and small sea-level changes (Section 6.5). Later Kennedy and Garrison (1975) compared the cyclicity of the Chalk of Britain to the Blue Lias Member. Campos and Hallam (1979) published $\delta^{18}\text{O}$ and $\delta^{13}\text{C}$ values for limestones in the basal Lias which indicated formation during very early diagenesis. Donovan et al. (1979) showed that the vertical variation in the proportion of limestones in the Lower Lias, used by Hallam (1960a) and Palmer (1972) for correlation, could be related to relative and perhaps eustatic (Hallam 1981) changes in sea-level. They explained the cyclicity as the result of formation and destruction of thermoclines.

Jones (1981) studied the Pre-planorbis Beds and preferred Sellwood's (1970a and 1970b) explanation for the cyclicity and the explanation of Hallam and Bradshaw (1979) for the bituminous shales. Loughman (1982) used the scanning electron microscope to study the limestones for evidence of coccoliths without success. He inferred instead that green algae supplied the carbonate mud precursor for the limestone microspar and that a greater density of limestones indicated shallower water. He also discounted the evidence for a primary origin of the limestones and proposed a model for independent rhythmic unmixing of carbonate. Hamilton (1982) showed that the marls and shales contain a diverse coccolith assemblage which was used by her to develop a new zonal system. Gluyas (1983 & 1984) confirmed the findings of Campos and Hallam during a study, including $\delta^{34}\text{S}$ values for pyrite, of a group of formations that contain nodular limestones. Weedon's (1985, 1986) work is described in this thesis. House (1985, 1986) followed Weedon in ascribing the cyclicity of the basal Lias to orbital-control (Section 4.3.3a). Ebukanson & Kinghorn (1985, 1986) have recently studied the organic geochemistry of the basal Lias and suggested that the present kerogen-types are related to lithology and that the present organic geochemistry of different rock types was dependent on the levels of bottom-water oxygenation.

CHAPTER 2

FIELD OBSERVATIONS AND PETROGRAPHY OF
THE BASAL LIAS OF SOUTH BRITAIN.

2.1 Field description of rock types and exposures.

Introduction.

The basal Lias of South Britain consists of two main developments: the 'offshore' or 'Blue Lias' facies and the 'marginal' facies. The marginal facies is described in detail in Section 2.2.1. It has been examined at Southerndown and Lulsgate Quarry (Fig 2.1A). Much more prevalent is the offshore facies which has been examined at: Lyme Regis; Watchet; Lavernock Point; Nash Point; Saltford; Long Itchington; Barnstone and Redcar (Fig 2.1A). Generally this facies consists of interbedded limestone, calcareous mudstone and bituminous shale. Five different rock types (Figs 2.1B-E) have been distinguished at Lyme Regis, Watchet, Lavernock Point, Long Itchington and Barnstone. Bituminous shale ('dark, laminated shale' in this study) is missing at Nash Point and perhaps Redcar (Section 2.1.2). Only sections which are very well exposed with published biostratigraphic and lithostratigraphic descriptions have been measured in detail (logs in the Appendix for Chapter 2).

The term 'Blue Lias' is problematical because it lacks a precise definition. There is a complete gradation, within basal Lias rocks, from sections with nearly equal thicknesses of limestone and marl or shale (which is called Blue Lias), to sections which contain perhaps as little as 5-10% limestone. However it is defined, the Blue Lias has diachronous upper and lower contacts. The term Blue Lias is so well known that it is often incorrectly considered to be synonymous with the offshore facies. Cope et al. (1980) attempted to establish a type locality for the 'Blue Lias Formation' at Saltford Cutting in Avon (description in Donovan 1956), near to the area where William Smith originally described these rocks. Yet in the summer of 1984, this section had become almost totally

covered by soil and vegetation. Access is a problem, partly because the little rock that is still exposed is uncomfortably close to the railway line used by the '125' from Bristol to London. Recently the Blue Lias needed to be treated as a member within the Lower Lias Formation for mapping purposes, so this designation is used here (Donovan & Kellaway 1984). The term 'basal Lias' is used to refer to all types of rock which range in age from the Pre-planorbis Beds to the bucklandi zone. The bulk of the work for this thesis concerns the offshore facies.

2.1.1 Rock Type Descriptions.

2.1.1a Limestone.

This rock type forms elliptical nodules from 5 to 18cm thick by 7 to 100cm wide within light marl beds (Fig 2.1B). Nodules often contain bioclasts yet commonly there is no indication of any macro-fossils. In some instances isolated nodules within a particular light marl bed merge laterally to form continuous limestone beds (Fig 2.1C). Limestone beds reach a maximum thickness of 46cm and have planar or wavy (nodular) top and bottom contacts. The rock is homogeneous, blue/grey and compact with a conchoidal fracture. On weathered sections the limestone stands proud of the other rock types and possesses flat profiles that have bevelled edges and with irregularly-spaced vertical joints. Limestone beds with wavy contacts are frequently associated with light marl whereas plane contacts are most common when limestone beds are in contact with dark marl or laminated shale. All previous authors have described this rock type as limestone although only Hallam (1960a, 1964 & 1986) has distinguished it from laminated limestone.

In limestones, body fossils are largely preserved uncrushed in the original skeletal material or as neomorphic calcite moulds (especially the ammonites). Fossils include (Table 1C and Appendix for Chapter 2): wood (lignite), coccoliths (Section 2.4), dinoflagellates, acritachs, marine reptiles, fish, ammonites, nautiloids, belemnites (rare), bivalves, gastropods (rare), ostracods, echinoids, crinoids, brachiopods, and benthonic foraminifera.

Trace fossils are preserved as dark marl burrow-mottles near the top contacts of limestone beds and within limestone nodules. These are dominated by Chondrites (Fig 2.1F) although some horizons contain many examples of Arenicolites. Diplocraterion (Fig 2.1G) (presumably the same organism which made Arenicolites), Rhizocorallium and Thalassinoides and Kulindrichnus langi (Hallam 1960b) are also present.

2.1.1b Light Marl.

This rock type forms tabular beds 1-82cm thick with predominantly sharp contacts. The rock is light blue/grey, homogeneous and friable and weathers to produce a conchoidally fractured surface. The bedding planes of the light marl frequently separate around any limestone nodules present (ie the marls and shale are compacted round the nodules) (Fig 2.1B). Previous names for this rock type include (less common usage in brackets):

Conchoidal marl (Friable Marl)-----Lang 1924,
 Conchoidal marl-----Hallam 1960a,
 Light coloured 'marl'-----Sellwood 1970b,
 Marl (shale)-----Palmer 1972,

Marl (poorly laminated shale)-----Clements et al. 1975.

Fossils are sparser than in the limestones partly because aragonitic skeletons are not present except in the rare cases when ammonites are pyritized or preserved as limestone ^{moulds} (only one example of this is known to the author). Body fossils include: wood, pollen grains, coccoliths, dinoflagellates, acritachs, fish, ammonites, bivalves, ostracods, echinoids, crinoids, brachiopods and benthonic foraminifera.

Under laminated shales the upper contacts of light marl beds are planar and unburrowed. Contacts with limestone are mainly sharp on weathered surfaces, but at some contacts there is a gradation over a centimetre or two. Contacts with dark marl overlying light marl are sharp but burrow-mottled, with Chondrites dominant and Rhizocorallium and Thalassinoides present in some cases.

2.1.1c Dark Marl.

Beds are tabular and 1-149cm thick with sharp contacts. In a few instances, contacts with light marl and laminated shale are gradational over 1-3cm. The rock is dark blue/grey and friable, but unlike the light marl weathered surfaces have a crude bedding-parallel fissility. Sometimes lamination seems to be visible. Previous nomenclature includes:

Friable marl (conchoidal marl)-----Lang 1924,

Marly shale-----Hallam 1960a,

Dark coloured 'marl'-----Sellwood 1970b,

Shale-----Palmer 1972,

Well laminated shale-----Clements et al. 1975.

Body fossils are preserved with their original skeletal material or, in the case of ammonites, as rare crushed impressions. They include:

wood, pollen grains, coccoliths, dinoflagellates, acritachs, fish, ammonites, bivalves, ostracods, echinoids, brachiopods, and benthonic foraminifera.

Trace fossils occur as burrow-mottles below limestone and light marl beds (Fig 2.1H). Contacts are planar and unmottled below laminated shale. Most trace fossils are represented by Chondrites, but a few examples of Rhizocorallium and Thalassinoides are present.

2.1.1d Dark, Laminated Shale.

This rock type has sub-millimetre lamination and forms beds 1 to at least 270cm in thickness. In the Pre-planorbis Beds it is this rock type that frequently encloses laminated limestone beds. The rock is brown to black and when very calcareous even blue/grey. Fresh rock is usually friable, but it can be compact and almost as hard as limestone. Weathered laminated shale is extremely fissile; surprisingly this rock type often weathers 'proud' of the surrounding light and dark marl.

Previous terms are:

Paper shale-----Lang 1924,

Bituminous shale-----Hallam 1960a,

Bituminous shale-----Sellwood 1970b,

Paper shale (shale)-----Palmer 1972,

Paper shale-----Clements et al. 1975.

Body fossils are usually preserved with original skeletal material. In one bed at Watchet, however, the original iridescent aragonite is preserved in crushed Psiloceras specimens (Palmer 1972). Yet generally ammonites are preserved as flat impressions. Body fossils include: wood, pollen grains, coccoliths, dinoflagellates, acritachs, marine

reptiles, fish, ammonites, dwarfed bivalves (Hallam 1960a), ostracods, echinoids (as rare spines only) and benthonic foraminifera.

Laminated shales are rarely in contact with limestone beds. Under dark marl and light marl burrow-mottling is rare although Chondrites and Rhizocorallium burrows have been observed.

2.1.1e Laminated Limestone.

This rock type is comparatively rare except in the Pre-planorbis Beds and the planorbis zone although examples are known up to the bucklandi zone at Watchet (Appendix Section 2.2). The rock is dark blue/grey, compact and has a fetid odour when struck. The rock forms beds up to 43cm thick which have very sharp, planar contacts and in nearly every case laminated limestone beds are entirely enclosed by laminated shale. At Lavernock Point and Long Itchington, laminated limestone forms nodules with laminae which are pinched together at the edges (Appendix Sections 2.3 and 2.5). This rock type has only been distinguished by Hallam (1960a, 1964, 1986) previously, although sometimes there is disagreement with the definition used here.

Body fossils are very rare and seem to be limited to fish scales, uncrushed ammonite moulds, ostracods and benthonic foraminifera. No trace fossils have been observed.

2.1.2 Locality Descriptions (See Fig 2.1A).

2.1.2a Lyme Regis, Devon/Dorset.

The local lithostratigraphy was described by Lang (1924) and the biostratigraphy used for the stratigraphic log (Appendix Section 2.1) is based on Cope et al. 1980. The section was measured from the ledges exposed at low tide in Pinhay Bay to West Cliff (SY325908-332913). The

stratigraphic log spans Lang's beds H1-49 (Pre-planorbis Beds to reynesi subzone, semicostatum zone). Limestone beds are common throughout this section (Fig 2.1I) which has a comparatively high density of bioclasts and burrow-mottled contacts. All rock types are represented at this location. The limestone beds have been correlated with those exposed in Church Cliffs; a distance of 3km (Lang 1924).

2.1.2b Watchet, Somerset.

Lithostratigraphy was described by Palmer (1972) and Whittaker & Green (1983). The section measured for this study indicates that Palmer's log is more reliable so his biostratigraphy has been used, except that the base of the planorbis zone is set at the first appearance of Psiloceras (Cope et al. 1980). The stratigraphic log (Appendix Section 2.2) was measured in composite sections measured along 2km of coastline between St. Audrie's Cliff and Kilve Pill. Palmer's beds A1-C55 were measured between ST098434 and 103433; C56-C100 between 133441 and 134442; C101-D7 between 139443 and 141443. Beds C44-C55 were so poorly exposed that only the limestones and intervening sediment thickness (rather than intervening rock type) could be determined. The log spans Palmer's beds A1-D6 (Whittaker & Green's beds 1-188) and represents the Pre-planorbis Beds to the conybeari subzone, bucklandi zone. All rock types are present, but bioclasts are much less common than at Lyme Regis. The density of limestones varies markedly up section and is the basis of Palmer's lithostratigraphic divisions (Figs 2.1J and K)

/

(Section 2.8).

2.1.2c Lavernock Point, Glamorgan.

Lithostratigraphic and biostratigraphic descriptions can be found in Trueman (1920) and Donovan (1956) (Section 4.3.3c). The stratigraphic log in Appendix Section 2.3 spans Trueman's beds 5-74 or the Pre-planorbis Beds to mid the angulata zone. The section (at ST180678) was very degraded between beds 63 and 68. The density of limestone beds is high in the Pre-planorbis Beds (Fig 2.1L), decreasing in the planorbis and lower liasicus zones; limestones are virtually absent in the upper liasicus zone. In the mid angulata zone limestones are common (Section 2.8.1). All rock types are present in the lower part of the section, but laminated shale and laminated limestone beds are absent from the liasicus and angulata zones. Bioclasts are about as common as those in the Watchet section; burrow-mottles have only been observed in one limestone bed (bed 14 - Appendix Section 2.3).

2.1.2d Nash Point, Glamorgan.

This section was described by Trueman (1930). Beds 1-39 (conybeari subzone only) were measured (at SS918680) although the section was so nodular that the bed thicknesses quoted in the log (Appendix Section 3.4) do not correspond closely to those of Trueman (discussed in Section 4.3.3d). Very nodular limestones separated by light marl dominate the section (Figs 2.1M and 2.1N) with occasional dark marl beds. No laminated shale or laminated limestone is present. Bioclasts and burrow-mottles appear to be as common as at Lyme Regis, but the petrography (Section 2.2) reveals that unusually large amounts of silt-grade bioclastic fragments are present.

2.1.2e Southerndown, Glamorgan.

This coastal section (at SS839738) was described in general by Trueman in 1922 and consists of marginal facies limestones with Carboniferous Limestone intraclasts. The Sutton Stone limestones lie unconformably on the Carboniferous and grade laterally and vertically through the Southerndown Beds into the offshore facies which include limestone, light marl, dark marl and laminated shale beds. The section is described in more detail in Section 2.2.1.

2.1.2f Lulsgate Quarry, Avon.

This location (ST518659) was designated the type section for the Brockley Down Stone which lies unconformably on Carboniferous Limestone (Loughman 1982). Unfortunately this local marginal facies is no longer accessible (although loose blocks can be examined) and the quarry may soon be filled in.

2.1.2g Saltford Disused Railway Cutting, Avon.

The classic cutting through the centre of the town was proposed as the type section for the Blue Lias (discussion Section 2.1 Introduction). Because of the inaccessibility of that section the disused railway cutting nearby was examined instead. The railway has been replaced by a cycle track and the exposure is under a bridge at ST686678 and was described by Donovan (1956) (Section K19 in Donovan & Kellaway 1984). The section represents part of the lower bucklandi zone and although it is very small in area it yields the following log:

<u>Thickness</u>	<u>Rock Type</u>	<u>Notes</u>
~26cm	Homogeneous Limestone	Large, unbroken ammonite (5cm thick).

8cm	Dark Marl	Abundant sand-silt grade bioclastic-
		(
7cm	Homogeneous Limestone	<u>(fragments throughout.</u>
7cm	Dark, Laminated Shale	
13cm	Homogeneous Limestone	
12cm	Dark, Laminated Shale	
6cm	Dark Marl	Abundant sand-silt grade bioclastic-
		(
1cm	Dark, Laminated Shale	<u>(fragments throughout.</u>
18cm	Homogeneous Limestone	
20cm	Dark, Laminated Shale	Basal 5cm rich in sand-silt bioclasts
3cm	Dark Marl	Abundant sand-silt grade bioclastic-
		(
28-34cm	Homogeneous Limestone	<u>(fragments throughout.</u>

All the limestone beds have slightly undulose contacts. No burrow-mottling was observed. Apart from large uncrushed ammonites, the section is exceptionally rich in silt-sand-grade bioclastic fragments (Section 2.2).

2.1.2h Long Itchington Quarry, near Southam, Warwickshire.

This section (at SP423638) was described by Clements et al. (1975). The section measured during this study (Appendix Section 2.5) spans beds 10-231 and 31g-43; the intervening section is no longer exposed but represents 3.42m according to the published log. The top of the liasicus to the lower bucklandi zone is represented in the log produced here. Below bed 10, nine metres of laminated shale and laminated limestone, forming the liasicus zone, have been proved by quarrying and part of this has been included in the log. In the angulata and bucklandi zones all rock types are represented except laminated limestone (Fig 2.10) (Section 2.8). Bioclasts seem to be intermediate in frequency between

Watchet and Lyme Regis. Burrow-mottling is about as common as at Lyme Regis. The nearby quarry at Rugby is now disused.

2.1.2i Barnstone Quarries, Nottinghamshire.

These quarries (at SK739348) formed the type section for the 'Hydraulic Limestones' described by Kent (1936, 1937) and Loughman (1982). The northern quarries have been entirely filled in with council rubbish. The water-filled southern quarry is now of little use (except to the local fishermen), but on the very degraded walls all five rock types were identified.

2.1.2j Redcar, Teeside.

This section has received little attention but it spans the angulata to semicostatum zones (Lord 1971). The rocks are exposed at NZ600250 in very subdued ledges with no cliff section. The inclination of the beds is so low and the ledges so weakly developed, that it is impossible to produce a detailed stratigraphic log. The limestones have many horizons that are very bioclast-rich with Gryphaea being exceptionally common. Some horizons seem to contain limestone intraclasts (Section 2.5). The rock between the limestones is very poorly exposed, but light and dark marl could be distinguished. No evidence for burrow-mottles or laminated rock has been found to date.

2.2 Petrography.

This section describes the petrography of each rock type in turn. The cathodoluminescence work was carried out on standard polished sections with a Technosyn instrument using a cold cathode at 20kV in a helium atmosphere.

2.2.1 'Marginal Facies' Limestones.

Lying unconformably on the Carboniferous Limestone of Southerndown (Fig 2.1A), the conglomeratic Sutton Stone (Fig 2.2A) is overlain by the Southerndown beds which grade laterally and vertically into the 'Blue Lias' or 'offshore facies' (Trueman 1922). The petrography of these beds has been described in detail by Wobber (1965). The Sutton Stone contains large (up to 1m) clasts of Carboniferous Limestone at its base which are supported by a bioclastic and lithoclastic matrix. The lithoclasts decrease in size to an average diameter of 3cm about 2 m above the unconformity. Stylolites mark the decimetre-metre scale bedding. Bioclasts sometimes have micrite envelopes (Wobber 1965) and are dominated by echinoid and crinoid fragments with some lamellibranchs, solitary corals and lignite (Hallam 1960a).

The Southerndown beds have decimetre-scale beds picked out by stylolites and many horizons of concentrated chert and Carboniferous Limestone pebbles (≈ 2 cm average diameter) (Fig 2.2B). The matrix is usually a peloidal, bioclastic wackestone containing more clay than the Sutton Stone. Bioclasts include crinoid and echinoid fragments, bivalves, benthonic foraminifera, gastropods, bryozoa and occasional Thalassinoides and Rhizocorallium burrows. Some horizons are cross-stratified and oolitic (Wobber 1965, Loughman 1982). The adjacent and overlying 'Blue Lias' contains chert pebbles in nodular limestones separated by ^{pressure solution} seams. About 4m above the base of the Blue Lias exposed on Southerndown beach, the nodules are replaced by typical homogeneous limestones alternating with light and dark marls with unusually large amounts of bioclastic debris (for the offshore facies generally), and some calcarenitic beds. About 8m above the Southerndown Beds laminated shale enters the sequence.

The Sutton Stone and Southerndown Beds have been considered near-coastal deposits since Trueman's (1922) work. Clay contents increase towards the offshore facies which replaced the marginal facies within the horizontal distance of a kilometre or two. Wobber (1965) invoked local cliff collapse and slumping to introduce the lithoclasts into waters that must have been warm and clear to judge from the

corals (Hallam 1960a). Loughman (1982) believed that the water was generally calm and favoured cliff collapse during storms which supplied lithoclasts for the Sutton Stone and the transport of pebbles by rip-currents from a beach during the deposition of the Southerndown Beds. Ager (1986) thought that the whole of the Sutton Stone resulted from a single storm. This has been contested by Fletcher et al. (1986) who prefer a more protracted period of deposition perhaps involving many storms. The dispute will be settled by collection of many more biostratigraphically useful ammonites which are of course rare in these rocks.

The Brockley Down Stone exposed in the Bristol district lies unconformably on the Carboniferous Limestone (Fig 2.2C). Loose blocks collected in this study from Lulsgate Quarry revealed (Fig 2.2D) lithoclastic limestones (Carboniferous Limestone lithoclasts supported by bioclastic packstone) grading into bioclastic packstone dominated by prismatic bivalve fragments. Details of the petrography, lithostratigraphy and biostratigraphy were published by Loughman (1982) and Donovan & Kellaway (1984). These authors showed that deposition was on the very shallow Radstock Shelf which was swept by storm currents.

2.2.2 'Offshore' or 'Blue Lias' Facies.

2.2.2a Limestone.

Microspar with intimately mixed clay forms a matrix which supports 5-50% bioclasts. The vast majority of limestones are carbonate mudstones in terms of the abundance of bioclasts. Brachiopods and bivalves are often united and unbroken and were probably only disturbed by bioturbation. Bioclasts in general are not bored and they lack micrite envelopes; encrustation is rare and usually restricted to bivalves (Liostrea) on large specimens such as ammonites. Silt-grade quartz and small clusters of framboidal pyrite are scattered through the matrix. Often pyrite is associated with bioclasts, forming relict outlines of dissolved bivalves and filling the tests of benthonic foraminifera and ostracods. Only rarely are complete bioclasts replaced by pyrite so most fossils are preserved with their original skeletons or are now neomorphic calcite moulds (especially ammonites and ostracods). In the most bioclastic horizons, glauconite fills the centres of benthonic foraminifera and ostracods (Fig 2.2E).

The mean diameter of the microspar averages about 6 μ m and reaches a maximum of 50 μ m. Staining (Dickson 1965) shows that all the microspar is non-ferroan calcite (presumed low-Mg) (Fig 2.2E). The calcite which forms cavity-filling spar filling ammonite shell moulds is also non-ferroan (Fig 2.2F). Ammonite chambers are filled by sediment (microspar with small floating bioclasts and quartz silt) or cavity-filling spar that is non-ferroan calcite. In one section (sample BL105 from a loose block perhaps from bed 49 at Lyme Regis) the most central spar in the chamber is ferroan calcite (Fig 2.2F). This section also illustrates an unusual pelleted texture in the microspar matrix.

The microspar luminesces with a uniform yellow-orange colour with blue luminescent quartz silt. Cathodoluminescence of ammonite mould spar reveals at least two phases of cement or some variation in pore-water

chemistry during cementation (Figs 2.2G and 2.2H). Bivalve fragments which preserve their original texture do not luminesce (ie they are unaltered). As part of an isotopic study (Section 3.4.3a), two specimens of Gryphaea were sectioned and polished. The original foliated texture appears to be well preserved (Bathurst 1975) and it does not luminesce (Figs 2.2I and 2.2J). However, the cement which fills the gaps between growth layers and along cleavage traces and twin planes is luminescent. This diagenetic calcite makes up less than 5% of the total fossil calcite (visual estimation).

Samples of limestone from Saltford and Nash Point are unusually rich in small (0.75-0.04mm), broken bioclasts - particularly from echinoids, crinoids and bivalves - forming wackestones. Yet large, unbroken and thin-shelled ammonites are also preserved. Samples from Saltford (packstones) include isolated quartz sand grains and rare sandstone lithoclasts as well as abundant echinoid and crinoid fragments and large, unbroken ammonites. The very high proportion of bioclasts at these two localities does not seem to have resulted from burrowing because the homogeneity of limestones from all localities suggests thorough bioturbation. The most likely explanation is that deposition at Saltford and Nash Point was generally calm but broken bioclasts were exported from the nearby marginal facies (eg. from Southerndown to Nash Point and from Lulsgate to Saltford) perhaps during storms. Limestones from the Pre-planorbis Beds have many horizons which abound in fragments of Liostrea (Section 2.5). Occasionally these fossils form grain-supported horizons of bedding-parallel fragments that create a wavy-laminated appearance inside limestone beds.

2.2.2b Light Marl.

This rock type is dominated by homogeneous microspar with considerably more clay than the limestones, and considerably less bioclastic material probably due to preservational differences. Bioclasts in thin section are predominantly ostracods and benthonic foraminifera. Quartz silt grains and clusters of pyrite framboids ($\approx 50\mu\text{m}$ diameter) are scattered throughout. Staining shows that the microspar is non-ferroan calcite which produces a uniform yellow-orange luminescence (Fig 2.2K and 2.2L). At Nash point about 50% of the rock is composed of crinoid and echinoid fragments with ostracods.

2.2.2c Dark Marl.

This rock type is poorly laminated, but where light marl or limestone overlies dark marl, Chondrites burrows at the upper contact of the dark marl are filled with the overlying rock. The burrow-mottles have sharp edges, are slightly compressed and range from 1.55 by 3.92 to 0.41 by 0.93 millimetres in vertical section. The lamination has been deformed during compaction around the burrows (Fig 2.2M). The rock consists of four main components: microspar 'blebs', bioclasts, clay laminae and amorphous organic laminae.

The microspar blebs are elliptical in vertical section (long axis parallel to bedding) and range from 390 to 120 μm long by 100 to 50 μm thick; bleb microspar crystals average 25 μm in diameter (max. $\sim 40\mu\text{m}$). The blebs never contain bioclasts, clay or quartz silt, but sometimes pyrite framboids are present towards the edges, they frequently merge into each other when close together and sometimes horizons a few hundred microns thick are dominated by blebs* (Fig 2.2M). The blebs are surrounded by the clay and organic laminae which are themselves deformed

* The blebs are thought to represent altered faecal pellets (Section 2.6).

by the blebs. The laminae contain many ostracods (usually only visible using cathodoluminescence), fish scales, pollen grains, a few isolated microspar crystals, quartz silt and pyrite framboids. At Lyme Regis both the clay and organic laminae are about 30 μ m thick and always discontinuous (~200 μ m long). Staining shows that the microspar is non-ferroan calcite. However, although most microspar produces a uniform yellow-orange colour under cathodoluminescence, isolated rhombic microspar luminesces red with some zoning (Fig 2.2N). These crystals are probably euhedral dolomite whose presence in small amounts is indicated by X-ray diffraction (Section 2.3).

Dark marl samples from Nash Point are very bioclastic with ostracods ^{and} echinoderm fragments ^{as well as} Chondrites mottles and crude lamination defined by clay. At Saltford, abundant crinoid ossicles and echinoid spines are mixed with clay, quartz sand grains and lithoclasts of chert (sand-grade).

2.2.2d Dark, Laminated Shale.

Laminated shale is dominated by clay and amorphous organic laminae. Most of the rock is almost free of microspar blebs, but at some levels many blebs coalesce to form horizons 0.12-0.70mm thick (separated by bleb-free rock 0.37-2.00mm thick). Bleb-rich horizons are associated with the nanno-fossil Schizosphaerella in some samples (Section 2.4). Individual blebs often merge into each other, range up to 300 by 50 μ m and have microspar crystals 24 μ m on average (40 μ m max.). The clay and organic laminae are discontinuous; the most continuous lamina found in this study (sample LA4, see Appendix Section 2.3) is composed of clay, 32 μ m thick and traceable for 40mm. Clay laminae from Lyme Regis, Watchet and Lavernock Point are usually close to 30 μ m thick whereas organic

laminae range from 4 to 40 μ m. Ostracods, pollen grains, quartz silt, isolated dolomite microspar crystals (previous section) and pyrite framboids are dispersed throughout the clay and organic matrix (Figs 2.2O and 2.2P). Calcite 'beef' is especially common at Lyme Regis and is usually found towards the base of laminated shale beds. It forms bedding-parallel lenses up to 6mm thick, yet in most beds it is no more than a minor component. Staining reveals that most beef is non-ferroan with a little ferroan calcite towards the centre of beef veins; cathodoluminescence indicates at least two phases of cementation (Figs 2.2Q and 2.2R) (cf. Marshall 1982). At Saltford some horizons of laminated shale are very rich in silt-sand grade bioclastic fragments (Section 2.1.2g).

2.2.2e Laminated Limestone.

This consists predominantly of microspar mixed with clay with occasional discontinuous, bedding-parallel organic laminae about 8 μ m thick. Horizons relatively rich in clay 6.0-0.15mm thick alternate with relatively clay-free layers which are 1.9-0.1mm thick (Figs 2.2S & T). The relatively clay-free layers give a patchy appearance reminiscent of the bleb-rich horizons in the laminated shale. Calcite spheres about 60 μ m in diameter are more common in these more clay-free layers and might represent large Schizosphaerella (Section 2.4) (previously described as 'peloids' by Weedon (1986) in Appendix Section 5.2). Fossils are very rare, but ostracods are visible (as well as Schizosphaerella). Quartz silt and pyrite are dispersed throughout, although pyrite is more common in the relatively clay-free horizons. Microspar crystals produce a uniform luminescence and average 8 μ m in diameter (16 μ m max.). In the Pre-planorbis Beds some horizons (~2cm

thick) within the laminated limestones are rich in Liostrea fragments with a few echinoid spines.

2.3 X-ray Diffractometer Results.

XRD traces were produced simply to establish which minerals are present in the different rock types; no attempt was made to quantify the data. Powders prepared for the bulk geochemical determinations (outlined in Appendix Section 3.1) were reground using a small pestle and mortar. Acetone was added to produce a slurry that was evenly pipetted onto a thin section slide. The acetone was allowed to evaporate off and analysis then proceeded with a Philips PW1320 generator coupled to a PW1050 diffractometer. Copper tube radiation was used and the trace produced at 1°min^{-1} and scanned for $60^\circ 2\theta$. Because no effort was made to separate the clay by settling, only a crude idea of the clay minerals could be obtained. Nevertheless, to help identify clays, the same slides were glycolated and heated. Glycolation involved placing the slide in a desiccator with a flask of ethylene glycol and causing saturation of the internal atmosphere by gently heating the desiccator overnight. Analysis was undertaken immediately after removal of the slides from the desiccator. Heating the sample involved placing the slide on a flat copper plate in a furnace set for 500°C for 30 minutes. Interpretation of the clay mineral characteristics follows Loughman (1982) and the other minerals were identified from standard tables (Chao 1969).

The samples analysed were all from Lyme Regis (BL314-limestone; BL316-light marl; BL317-dark marl; BL318-laminated shale). An example of the results obtained is illustrated in Fig 2.3A. In each rock type calcite, quartz, and pyrite were identified. The most prominent peak for pyrite occurs at about $30.1^\circ 2\theta$ for all the traces and indicates pure

pyrite (FeS_2) rather than a formula produced by a mixture with pyrrhotite (Fe_7S_8 ; analogous peak at $33.8^\circ 2\theta$). This result has been employed during geochemical determinations of %pyrite from measurements of %S (Appendix Section 3.3). Small amounts of dolomite are present in the marls and shale (the shale seems to have the most from peak heights); dolomite might be present in limestone but the peak is virtually indistinguishable from the background noise. Gypsum was detected in laminated shale and might be present in the dark marl; as there is no evidence for hypersalinity in these rocks it probably results from minor surface weathering of pyrite (Appendix Section 3.3).

The clay minerals detected are illite and kaolinite which are present in the marls and shale and might have been detected in the limestone (where the clay concentration is too small to develop good peaks). The clay was investigated in some detail by Loughman (1982) who produced semi-quantified results for forty nine samples spanning the Pre-planorbis Beds to the semicostatum zone from twenty localities in Britain. His average composition is 45% illite, 35% mixed layers, 17% kaolinite and 3% smectite. Kaolinite concentration increases towards the North (the probable source area). Smectite was only recorded in Lincolnshire and Yorkshire although this mineral might have been converted to mixed-layer clays in most cases (Loughman 1982).

2.4 Scanning Electron Microscopy.

Small pieces of rock were freshly broken and stuck on to aluminium stubs before being coated with gold in a plasma chamber. Colloidal graphite was used to ensure good conduction of electrons from the gold coat to the earthed aluminium. The fracture surfaces were observed with an ISI40 scanning electron microscope.

2.4.1 Limestone.

Limestone is dominated by microspar which produces a rounded or fractured surface appearance with scattered clay flakes. Loughman (1982) was unable to find unequivocal evidence for coccoliths in the homogeneous limestones (he did not examine other rock types). However, during this study, very rare rings of calcite have been observed embedded in the ubiquitous microspar (Fig 2.4A). The diameter ($\approx 2.5\mu\text{m}$), elongate shape and crystallites which make up these rings strongly suggests that they are coccoliths. This is supported by the presence of abundant and undoubted coccoliths in the organic-rich lithologies described below. Yet the lack of a central cross-bar and the visibility of the crystallites in the ring illustrated in Fig 2.4A compared to the undoubted coccoliths, suggests that some dissolution has occurred in the limestone.

2.4.2 Light Marl.

Unlike the homogeneous limestone, fracture surfaces of light marl reveal considerable areas of clay which produces a flaky appearance (Fig 2.4B). The microspar sometimes forms discrete euhedral crystals as well as fused amalgamations (Fig 2.4C). Rare, elongate rings very similar to those seen in the homogeneous limestone are sometimes visible (Fig 2.4B). In some examples a vague cross-bar structure is present which confirms that the rings are coccoliths (ie. Staurorhabdus illustrated by Hamilton 1982). Calcite hemispheres 20-40 μm in diameter which are commonly associated with euhedral microspar crystals, represent the fossil Schizosphaerella punctulata. Kälin and Bernoulli (1984) considered that this fossil is most likely to represent a dinoflagellate (planktonic alga) which produced a calcareous test inside the cell wall.

They showed that initially the fossil consists of a latticework of low-Mg calcite laths with a very high porosity (eg. Fig 2.4H). During diagenetic cementation the wall porosity is infilled which leads to a smooth, slightly pitted surface (Fig 2.4C).

2.4.3 Dark Marl.

This rock type produces fracture surfaces dominated by clay and organic matter. In more calcareous specimens poorly preserved coccoliths similar to the the one in Fig 2.4B are present fairly commonly. The Schizosphaerella have almost smooth surfaces (ie considerable cementation) (Fig 2.4D). However, other specimens preserve many aggregates of coccoliths (Fig 2.4E and 2.4F). The aggregates are roughly elliptical and range from about 7 by 16 μ m to 80 by 40 μ m. Each aggregate consists of tightly packed coccoliths derived from several species and sizes of coccolithophore. Occasionally isolated coccoliths are observed, but the vast majority are contained in aggregates. The systematics and biostratigraphy of coccoliths from the basal Lias were described by Hamilton (1982). Because it is standard micropalaeontological practice to isolate coccoliths from the rock before examination, the aggregates were first reported during work for this thesis (Weedon (1986) in Appendix Section 5.2). The preservation of the coccoliths in Figs 2.4E and 2.4F appears to be very good. In some cases, however, coccoliths are preserved with microspar overgrowths which partially engulf the original calcite (Fig 2.4G).

2.4.4 Dark, Laminated Shale.

Clay and organics also dominate the fracture surfaces of laminated shale, but sometimes isolated euhedral microspar crystals are observed

(Fig 2.4H). Coccolith aggregates are frequently present but they are less common than those in the dark marl. Compared to the other rock types, there is much less cementation of the walls of Schizosphaerella. Although the wall remains fairly porous, microspar overgrowths nucleating on wall laths are present (Fig 2.4H) and some specimens are entirely embedded in microspar (Fig 2.4I). In Tethyan limestones Schizosphaerella provides the nucleation surface for radial fringes of calcite crystals, yet in marls, the clay inhibits fringe development (Kälin and Bernoulli 1984). Fig 2.4I demonstrates that radial fringes do not develop in these rocks. Nevertheless, the frequent association of large euhedral microspar crystals with Schizosphaerella in all the rock types studied here, suggests that these crystals developed locally on the surface of the fossil, in place of a fringe, wherever clay was unable to inhibit the process (eg. Fig 2.4D).

2.4.5 Laminated Limestone.

Fracture surfaces of this rock type are dominated by fused microspar crystals. As yet no coccoliths have been discovered; perhaps because only a little time was spent examining this comparatively rare rock type. Schizosphaerella specimens have nearly smooth, slightly pitted surfaces which indicates considerable wall cementation (Fig 2.4J).

2.5 Hiatuses.

Sadler (1981) has produced considerable evidence to show that regardless of rock type or environment, when sections span several ammonite zones (several million years) there is every reason to suspect gaps at the tens-of-thousands-of-years scale. Therefore, although in the basal Lias once deposition started in a particular place every ammonite

zone and subzone was represented by sediment (Cope et al. 1980), evidence for gaps should be expected. It has previously been suggested that when every ammonite zone is present in a section, large (in the order of 1 million year) gaps can be ruled out (Weedon 1986). This is erroneous because the ammonite zonation was originally established within South Britain so large gaps might yet be detected (Donovan pers. comm. 1986).

The absolute thickness of ammonite zones and subzones changes from place to place, which is most easily explained by variations in sedimentation rate. But the relative thickness of ammonite zones and subzones also changes from place to place (Fig 2.5A). Assuming that the biostratigraphy is reliable, this is most easily explained by variations in the amount of rock missing at hiatuses. All areas experienced simultaneous shifts in the proportion of different rock types (Section 2.8.1) so vertical variations in sedimentation rate and compaction cannot be invoked. Evidence for hiatuses is reviewed below.

Kent (1936 & 1937) recorded limestone nodules with borings as well as fossils and limestone intraclasts encrusted by serpulids from the Pre-planorbis Beds to the johnstoni subzone of Nottinghamshire. Loughman (1982) recorded thin (~1cm) graded beds of bioclasts and small scours (1cm deep by 9cm wide) in limestones from rocks of the same age and area. Hallam (1960a) illustrated a truncated burrow in a limestone bed packed with fossils and associated with unusually large amounts of glauconite and collophane (Lang's (1924) bed 49, Lyme Regis, reynesi subzone, semicostatum zone). Donovan's detailed work in the Bristol and Avon area has revealed that hiatuses in the offshore facies of the basal Lias are more common than previously thought (Donovan 1956, Donovan and Kellaway 1984). Thus the johnstoni subzone (planorbis zone) locally lies

directly on the Pre-planorbis beds. In some places a non-sequence has been recognised within the johnstoni subzone. The angulata and bucklandi subzones are missing over the Radstock Shelf probably as a result of a relative sea-level fall which might be eustatic in origin (Hallam 1960, Donovan & Kellaway 1984). The Calcaria Bed with abundant ammonites is well known in other parts of the Bristol and Avon area and suggests that this sea-level drop might have occurred during the conybeari subzone of the bucklandi zone (Section 2.8.2).

Several types of observation made during this study suggest that minor gaps occur throughout the sections for which detailed logs are given (Appendix for Chapter 2). The most frequent criteria for erosion are horizons which are unusually rich in broken bioclasts. Such horizons are found in every rock type and they probably indicate winnowing of the sediment (Kent 1937, Hallam 1960a). Hallam (1960a) distinguished these levels from horizons dominated by many specimens of one type of fossil (ammonites, Gryphaea, rhynchonellids or crinoid ossicles). These he argued were the product of biotic variations in productivity and competition. This is supported by the observation that specimens at these levels are usually unbroken and by the fact that double valved specimens (Gryphaea and rhynchonellids) are united (Fig 2.5B).

In the Pre-planorbis Beds there are many horizons of concentrated, broken Liostrea specimens (Section 2.2). Loughman (1982) argued that his Hydraulic Limestone Member (Pre-planorbis Beds to planorbis zone) was deposited in shallow, low-salinity water. His evidence for this included the scours and graded beds (see above), the lack of diverse fossils and the dominance of limestones with planar contacts which lacked burrow-mottles. But the lack of fossils, the contacts and lack of

burrow-mottles is easily attributed to the prevalence in this part of the basal Lias of laminated limestones associated with abundant laminated shale (Fig 2.1L and Appendix Sections 2.1-2.3). In fact Kent (1937) studied the fossils of the Hydraulic Limestones and showed that although the water was shallow, salinities were normal even for the Pre-planorbis Beds (^{without} ammonites). The abundance of bioclast-rich horizons in the Pre-planorbis Beds possibly indicates frequent winnowing caused by storms in water that was shallow compared to the rest of the basal Lias offshore facies.

Loose blocks of limestone with limestone intraclasts have been found at Lyme Regis (Fig 2.5B). At Watchet and Lyme ^{some} horizons of burrow-mottles filled with dark marl are entirely surrounded by light marl or limestone (Fig 2.5C). This indicates that the dark marl beds which supplied the burrow-fill material have been removed. Unusually thin (1-2cm) beds of dark marl and laminated shale can be used to demonstrate long-wavelength, low-amplitude scours. Thus in the conybeari and rotiforme subzones of the bucklandi zone ^{at} Lyme Regis (Appendix Section 2.1), such beds are locally cut out for up to 20m along strike, yet beds around 10cm thick occurring above and below the gaps are present everywhere.

Further evidence for erosion in the conybeari subzone at Lyme Regis is provided by a block collected from bed 25. This reveals a multiply bored and encrusted dome-shaped surface 3cm high and over 13cm long, which is entirely enclosed by limestone (Figs 2.5D-G). Initially the dome was exposed after some erosion demonstrated by the truncated bioclasts. The surface was hard enough to receive Trypanites borings (from bivalves - Bromley 1972) before a layer of sediment was deposited (~2mm thick). This sediment is now composed of microspar which becomes

coarser towards its outer surface. The sediment surface was then bored, probably by phoronids, to produce Talpina ramosa (250-150µm diameter, branching at 70° - Voigt 1972). Another layer of sediment was laid down (~1mm thick max.) but it was largely removed before encrustation by Liostrea (Fig 2.5H). These bivalves were bored by phoronids and algae or fungi (~25µm diameter, straight borings - Bromley 1970) both before and after another phase of encrustation.

The whole of this condensation surface is overlain by a packstone dominated by small gastropods which is, in turn, overlain by normal carbonate mudstone (Figs 2.5E and 2.5G). Interestingly gastropods are very uncommon in the offshore facies of the basal Lias except where deposited near the marginal facies (Nash Point - Appendix Section 2.4 and the Radstock Shelf - Donovan & Kellaway 1984). Therefore gastropods appear to indicate shallow water perhaps because these animals were algal grazers. The lack of micritic envelopes and boring generally in the offshore facies suggests deposition below the photic zone so algae and hence gastropods were excluded. Thus the packstone and condensed surface indicate shallow, agitated water. This evidence supports the suggestion of relative sea-level fall during the conybeari subzone (Section 2.8.2, Hallam 1960a, Donovan & Kellaway 1984).

The shape of the dome and the fact that it was hard suggests that an early diagenetic limestone nodule was exposed by erosion (cf Hallam 1969). The block with the condensation features was collected because in the field it appeared to contain a large encrusted ammonite. Later examination of this bed has failed to reveal any more condensation features other than large numbers of bioclasts. In general evidence for hiatuses is probably difficult to recognize because erosion did not usually expose consolidated levels. Even though hiatuses seem to be more

prevalent in the Pre-planorbis beds, the planorbis zone and conybeari subzone due to erosion in relatively shallow-water environments, evidence for gaps is found throughout the basal Lias (Pre-planorbis Beds - bucklandi zone). At present it is assumed that most gaps were generated during winter storms and hurricanes (Section 2.8.2, Loughman 1982, Marsaglia & Klein 1983, Pedersen 1985).

2.6 Origin of the microspar.

The elliptical microspar blebs observed in the dark marls, laminated shales and laminated limestone, are approximately the same size and shape as the coccolith aggregates (Sections 2.2.2c-e). This suggests that the blebs simply represent neomorphically aggraded coccolith aggregates. In fact the shape and size of these structures suggest that they are zooplankton faecal pellets as described from Cretaceous chalks and various organic-rich shales (Hattin 1975, Porter & Robbins 1981). It cannot be argued that the blebs are burrow-fills given their size and lack of features suggesting sediment infilling (bioclasts and quartz silt).

On the other hand, Hattin (1975) showed that in Cretaceous clay-rich chalk and marl, coccolith-rich faecal pellets had neomorphosed to microspar. Fig 2.4G shows that sometimes coccoliths are associated with microspar overgrowths indicating aggrading neomorphism. The single calcite microspar crystals scattered throughout the clay and organic matrix of the dark marl and shale might indicate the very tips of microspar blebs. Thus there is every reason to believe that zooplankton supplied carbonate to the dark marls and laminated shale in the form of faecal pellets packed with coccoliths derived from surface waters. Because these sediments were not bioturbated, the pellets retained their

integrity and during diagenesis some neomorphically aggraded to form microspar blebs.

The euhedral dolomite microspar crystals seen in thin section using cathodoluminescence and detected by XRD represents a tiny proportion of the carbonate present. Hallam (1960a) showed that less than 1% MgO is present in the limestones and marls. This small proportion of dolomite was ignored for simplicity during the geochemical determination of %CaCO₃ (Chapter 3 and Appendix Section 3.3). The dolomite probably formed during diagenetic sulphate reduction (Baker & Kastner 1981). Magnesium might have been supplied to the pore waters during dissolution of high-Mg calcite bioclasts or during cation exchange with clay minerals. It cannot be ruled out that some or all of the dolomite is actually detrital.

The microspar of the light marls and limestones is more problematical. That it is mainly neomorphic rather than clastic is indicated by the way it supports bioclasts and is tightly fused (Bathurst 1975). It does not represent cemented comminuted macrofossils considering its average diameter (~6µm) and uniform luminescence (no zoning). Accepting a neomorphic origin, primary grains are likely to have been either coccolithic or green algal particles which neomorphically aggraded (Folk 1965).

As Loughman (1982) was unable to find convincing evidence for coccoliths, ^{both} he and Hallam (1986) argued that the main source of carbonate mud was green algal and therefore aragonitic. Aragonitic carbonate mud neatly explains the neomorphism to microspar, but it is argued here that it is unlikely to have been a significant source for the offshore facies of the basal Lias. For instance, it has been shown that as strontium contents are very low in the limestones and marls, the original

carbonate mud was probably calcitic (Hallam 1960a). Substantial production of green algal carbonate would have required very shallow water (<20m). But the fauna and flora in the offshore facies contain common and diverse pelagic elements (ammonites, nautiloids, belemnites, ichthyosaurs, pleisiosaurs, fish, coccolithophores, acritachs and dinoflagellates - Table 1C). Additionally shallow-water criteria such as ooids, micritic envelopes, stromatolites, bird's eyes and evidence for exposure are absent, although some of these are found in the marginal facies (Section 2.2.1). And furthermore, the laminated organic-rich rocks are very unlikely to have accumulated in very shallow, yet fully marine waters.

Carbonate mud cannot have been transported to the offshore facies from the marginal facies as this would have produced carbonate mud laminae within the dark marl and laminated shale. On the other hand, sand- and silt-grade bioclasts were supplied from marginal facies to the adjacent areas (eg. Nash Point and Saltford Cutting - Section 2.2) and are now present in all rock types. Burrowing and ingestion of sediment by infauna may have generated some carbonate mud, but it is unlikely to have produced all of it as most particles macerated in this way would probably now be silt-sized. Schizosphaerella is present in the light marl (Fig 2.4C) and limestone, but thin sections indicate that the density never rises above five specimens per mm². It has been shown (Section 2.4.4) that instead of large calcite fringes developing, just a few euhedral microspar crystals are associated with this nanno-fossil.

Instead it is contended here that the carbonate mud of the light marls and limestones was largely coccolithic in origin. Support for this includes the occurrence of poorly preserved coccoliths in these rock types (Sections 2.4.1 and 2.4.2) and the abundant coccoliths present in

faecal pellets in the other rock types (Sections 2.4.3 and 2.4.4). Thus coccoliths are thought to have been ^{incorporated in the sediments} throughout the basal Lias, but oxidation of organic membranes and burrowing destroyed the pellets in the limestone and light marl. This hypothesis implies that neomorphism has largely altered the coccoliths in the bioturbated rocks.

This has been objected to on the grounds that coccoliths are low-Mg calcite and that ^{,for example,} in the coccolith-rich Chalk and Kimmeridge Clay of Britain, neomorphism is virtually absent (Loughman 1982, Hallam 1986-see discussion in Weedon 1987 and Hallam 1987 in Appendix 5.3). Yet it is known that water films on clays in clay-rich (>5%) limestones encourage the production of microspar (Folk 1965, Bathurst 1975). In North America, neomorphism of faecal pellet coccoliths in the Cretaceous is associated with high clay contents (Hattin 1975). Thus it is suggested here that the neomorphism of most coccoliths in the light marls and limestones was caused by the high clay contents (quantified in Chapter 3). There is in fact some evidence for an association between the neomorphism of coccoliths and the formation of nodular limestones in general (Jenkyns 1974).

The preservation of coccoliths in the dark marls and laminated shales might be considered surprising in view of the amounts of clay involved; but in these rocks organic-carbon contents were high (Section 3.2). In the Chalk, coccoliths were protected from pore-waters and diagenesis by individual organic membranes (Burki et al. 1982). Whole zooplankton faecal pellets are also enclosed by organic membranes (Honjo 1976, Porter & Robbins 1981) which might also account for the preservation of coccoliths in the dark marl and laminated shale. The same explanation might account for the preservation of coccoliths in the

coccolithic limestones of the Kimmeridge Clay (Section 6.3a) where clay contents are high but there is always more than 2.5% organic carbon (Farrimond et al. 1984).

Finally it should be noted that the limestone and laminated limestone represent the results of early diagenetic cementation (Sections 2.8, 3.4.3d and 5.1). Thus considerable volumes of pore-space would have been cemented during micrite formation, before neomorphism produced the microspar (Folk 1965, Raiswell 1971). This means that the bulk of the microspar from these rocks is likely to have started as early cement rather than coccolithic carbonate.

2.7 Primary and secondary considerations in the offshore facies.

There has been considerable speculation concerning the origin of the limestones in the basal Lias (reviewed by Hallam 1964). Some of the key developments in understanding have been summarized in Section 1.3. It is worth emphasising at the outset that the diagenesis of the basal Lias differed considerably from the simple Mesozoic limestone-marl alternations studied by Ricken (1985, 1986). He showed that carbonate redistribution during diagenesis was associated with the development of stylolites in relatively carbonate-poor horizons. The offshore facies of the basal Lias does not contain stylolites.

2.7.1 Evidence for diagenetic limestone formation.

Hallam (1964, 1986) has demonstrated convincingly that the limestones in the offshore facies of the basal Lias have a diagenetic origin; some of his evidence is discussed here. Limestone and laminated limestone nodules are unequivocal evidence for diagenetic migration of carbonate (Richardson in Lang et al. 1923, Hallam 1964, Raiswell 1971,

Hallam 1986). Marl and laminated shale beds are bent around limestone nodules (Fig 2.1B); carbonate contents decrease towards the edges of limestone nodules (Section 3.4.3d), and laminae pinch together at the edges of laminated limestone nodules. All these points indicate that nodule growth occurred during compaction (Raiswell 1971). Nodules in light marl beds are sometimes replaced laterally by a continuous limestone bed (Fig 2.1C). This and the nodular or wavy contacts of limestone beds suggest that continuous limestone beds were simply formed by the amalgamation of closely spaced nodules (Gluyas 1984).

The preservation of ammonites in limestone beds as uncrushed, neomorphic calcite moulds (Section 2.2.2a) suggests limestone beds formed before significant compaction and before the inversion of aragonite to calcite. There is good isotopic evidence that limestone beds formed during early diagenesis (Campos & Hallam 1979, Gluyas 1983 & 1984, Section 3.4.3). The isotopes also seem to imply that limestone bed cementation preceded limestone-nodule cementation (Section 3.4.3d). Therefore the continuity of limestone beds compared to the isolation of limestone nodules may be explained in terms of the speed of cementation and the separation of cementation nuclei or nodules.

Finally Hallam (1964, 1986) has shown that the size distribution of limestone bed thicknesses is independent of location and sedimentation rate which suggests that limestone bed thickness is controlled diagenetically. It has been speculated that this might be fortuitous (Weedon 1986). Thus if limestone formation proceeded by pore-space cementation, then this process might have ceased when porosities and permeabilities in the uncemented sediment were reduced to certain values by compaction. The rate of cementation might also have been proportional to the rate of pore-fluid expulsion (= rate of compaction). This would

mean that in areas of high sedimentation rate limestone growth would be rapid but short-lived. In areas of slow sedimentation limestone growth would be slow but long-lived. As a result the size distribution of limestone bed thicknesses would be more or less constant. Although the modal and mean size is independent of location and sedimentation rate, it should be noted that the shape of the size distribution recorded by Hallam is not remarkable (Schwarzacher 1975).

2.7.2 Evidence for limestone nucleation related to sediment composition.

Hallam (1964) argued that the limestones of the basal Lias, although diagenetic, were formed in locations determined by the primary sediment composition. Recently (1986), however, he has argued that many limestones formed in locations independent of primary sediment composition. This is contested here and it is argued that Hallam's earlier (1964) reasoning is closest to the truth (discussion in Weedon 1987 and Hallam 1987 - Appendix Section 5.3).

Limestone is associated with light marl; limestone beds with wavy contacts against dark marl or laminated shale commonly have light marl lenses preserved in the hollows. Limestone nodules are only found within light marl beds. Similarly laminated limestone beds and nodules are usually entirely surrounded by laminated shale. These observations suggest that limestone was formed by cementation of light marl and that laminated limestone formed by cementation of laminated shale. This is supported by a comparison of the petrographies of these pairs of rock types (Section 2.2). Limestone and light marl are homogeneous, whilst laminated shale and laminated limestone preserve lamination (even the bleb-rich horizons are preserved in laminated limestone). The fossils in

these pairs of rock types are also comparable in terms of diversity (Section 2.1.1) provided that allowance is made for preservational differences. Sections 3.2 and 3.3 show that, when expressed on a carbonate-free basis, organic carbon and pyrite contents are the same in the limestone and light marl and the same in the laminated limestone and laminated shale.

Because limestone apparently represents cemented light marl and laminated limestone cemented laminated shale, it appears that cementation was influenced by the composition of the sediment at that time (whether this composition was determined during very early diagenesis or during sedimentation). There is evidence that compositional variations during cementation were predominantly vertical (ie stratigraphic). Thus when limestone beds are entirely enclosed by light marl beds, they always occupy the same stratigraphic level. Limestone nodules occur at specific stratigraphic levels within light marl beds and laminated limestone beds and nodules also occupy specific stratigraphic levels within laminated shale beds. There is a discussion of the factors which might have controlled cementation in Section 5.1.

2.7.3 Evidence for a primary distinction of light marl, dark marl and laminated shale.

There are many observations which indicate that the marls and shales formed distinct sediment types on the sea-floor. In the field the diversity of bioclasts can be used. Laminated shale benthonic fossils include dwarfed bivalves (Hallam 1960a) whilst there is a lack of brachiopods; this sets apart this rock type from the light and dark marl. Dark marl has the same diversity of fossils as light marl which distinguishes it from laminated shale but, unlike the light marl,

crinoids are absent. There is no evidence for carbonate dissolution in these rocks because delicate structural features are well-preserved and coccoliths are found in the most organic-rich sediment which would be expected to be the most corrosive. Therefore, as the benthonic fossils are mainly calcitic, preservational factors probably cannot account for these differences in ^{benthonic} faunal diversity.

Burrow-mottles at the contacts of light marl and dark marl are very common. Mottling is rare at the top of laminated shale beds, but sometimes light or dark marl is piped down from the overlying rock. This type of burrow mottling indicates a primary distinction of sediment composition on the sea-floor (Hallam 1964, Arthur et al. 1984). But if burrowing were to have affected sediment which started lithification just below the sediment surface, mottling could have been produced where uncemented sediment was piped down into a partially cemented layer. However, this second type of mottling, which might be observed within limestone beds would not signify primary variations in sediment composition. Alternatively, burrows might in some circumstances have enhanced or inhibited cementation which would have produced indentations and lumps on the surfaces of limestone nodules and limestone beds (Loughman 1982). But burrows which affected, or were picked out by early diagenetic cementation are distinct from the burrow mottles associated with the contacts of marls and shales where distinct changes in petrography, biota and composition occur. Thus the burrow-mottling between light marl, dark marl and laminated shale indicates a primary difference in the composition of these rock types and cannot have been caused by early diagenetic cementation.

As mentioned above, petrography provides further evidence for a primary distinction between these rock types. Thus the light marl is

homogeneous whereas the dark marl and laminated shale are laminated (Section 2.2). Dark marl is distinguishable from laminated shale by the much greater proportion of microspar blebs and coccolith aggregates (ie faecal pellets - Section 2.6).

Conceivably, diagenesis could have caused a difference in the carbonate contents of the marls and shales, so %CaCO₃ cannot be used to prove primary distinction on it's own. Yet if the diluting effect of carbonate is allowed for by expressing other parameters on a carbonate-free basis (Section 3.1), useful information is available. The average %Total Organic Carbon (carbonate free) is different for the laminated shale, dark marl and light marl (Section 3.2). This is independent evidence for a primary distinction of these rock types. Additionally, there is a relationship between carbonate contents and %TOC (carbonate free) in the marls and shale which cannot have arisen from diagenetic unmixing of a homogeneous marl (Section 3.2). The relationship between %CaCO₃ and %TOC implies that primary carbonate, clay and organic-carbon contents varied according to the sediment type on the sea-floor.

2.8 Correlation.

A variety of techniques have been used for correlation in the basal Lias of South Britain, ie biostratigraphy (zone and subzone), vertical variations in the limestone/shale ratio and bed by bed. Biostratigraphy needs little comment except to state that ammonites have proved to be most useful and dinoflagellate and coccolith zonation is being used increasingly (Cope et al. 1980, Table 1B).

2.8.1 Large-scale correlation.

On a metre to tens-of-metres scale, variations in the ratio of limestone to shale have been used for correlation within a biostratigraphic framework (Hallam 1960a, Palmer 1972). But as the limestones were formed diagenetically (Sections 2.7 and 5.1), it is useful to investigate the dependence of limestone density upon the average proportion of the different sediment types.

It has already been shown that limestone beds and nodules were formed within light marl beds and laminated limestone beds and nodules within laminated shale (Section 2.7). Thus in the construction^{of} Figs 2.8A and 2.8B, three groups of rock types have been used: light marl/limestone beds, dark marl beds and laminated shale/laminated limestone beds. The average percentages of different rock types by thickness were found for fixed vertical intervals where detailed stratigraphic logs exist (Appendix for Chapter 2) (the Nash Point log was excluded because it only covers the conybeari subzone). The interval thickness was chosen so as to combine two light marl/limestone horizons and two laminated shale/laminated limestone horizons on average, in order to produce smooth vertical variations in the percentage of different rock groups.

As limestones and laminated limestones underwent less compaction than light marls and laminated shales, these diagrams (Figs 2.8A and 2.8B) do not represent the original proportions of light marl, dark marl and laminated shale as sediments. However, it is likely that the stratigraphic variation in the relative percentages of rock groups does reflect the original variation in the relative proportion of different sediment types.

Despite the differences in biostratigraphic resolution from place to place, it seems that variations in the original average percentages of different sediment types were synchronous. Thus the proportion of light marl decreased during the deposition of the Pre-planorbis Beds. A decrease in this percentage at the start of the planorbis zone was followed by an increase at the end. During the liasicus zone first lower and lower and then higher and higher proportions of light marl were accumulated. In the angulata zone it appears that the percentage of light marl deposited varied considerably, but overall a more or less constant proportion was maintained. During the bucklandi zone the amount of light marl deposited decreased, but only the log at Lyme Regis passes through the whole zone. These variations are summarized in Fig 5.3A.

Changes in the proportions of light marl were naturally offset by changes in the amounts of laminated shale combined with dark marl. Usually laminated shale and light marl deposition were inversely correlated. However, local changes in palaeogeography seem to have upset this relationship; at Lavernock Point laminated shale is absent from the liasicus and perhaps the whole of the angulata zone and at Long Itchington a large part of the liasicus zone contains laminated shale exclusively. In Section 5.3.2 it is argued that these anomalies and the synchronous basin-wide variations were related to local and basin-wide variations in water depth respectively.

The number of limestone beds and nodule horizons in the intervals used (Figs 2.8A and 2.8B) is directly correlated with the percentage of light marl (Fig 2.8C) (this is discussed further in Sections 5.1.1 and 5.3.2). The number of laminated limestone beds and nodule horizons is small, but generally highest in the Pre-planorbis Beds and the planorbis zone (Fig 2.8A and 2.8B) (Section 5.1.2).

2.8.2 Correlation bed by bed.

Many authors have been able to correlate single beds in the basal Lias over considerable distances. Thus Lyme Regis and Tolcis (11km apart) in Dorset, and in Glamorgan Lavernock Point and Bull Cliff (9km), and Stout Bay and Seamount (ie Southerndown Beach 17km apart) were shown to be pairs of locations where most beds could be correlated and the thicknesses remain very similar (Hallam 1960a) (Fig 2.8D). The Watchet section was correlated with the Brent Knoll borehole 26km away using individual limestone beds (Whittaker & Green 1983). And the Long Itchington and Rugby quarries, 15km apart, were shown to contain common limestone and laminated shale beds (Clements et al. 1975).

Single beds have also been traced over very large distances. For instance Hallam (1960a) correlated two groups of laminated limestone beds found at Lavernock Point and Lyme Regis (80km apart). (This correlation has been revised on Fig 2.8E on the assumption that the beds do not cross ammonite subzone boundaries.) Most impressive is the published correlation of the Calcaria Bed of the Avon district with elsewhere. Donovan (1956) and Donovan & Kellaway (1984) defined this bed as a thick limestone with many large ammonites on its top surface attributed to erosion during the conybeari subzone (Sections 2.5 and 5.3.2). It was tentatively correlated by Donovan (1956) with Lang's bed 29 at Lyme Regis although the only evidence proposed for erosion was the presence of many large ammonites. An alternative, suggested here, is that bed 25 at Lyme Regis correlates with the Calcaria Bed because conclusive evidence for erosion has now been documented (Section 2.5); there is no other evidence to support either correlation. Hallam (1960a) correlated Lang's bed 29 at Lyme Regis with a limestone bed near the top of the conybeari subzone in Glamorgan (perhaps Trueman's bed 21 at Nash

Point). In fact the bed in Glamorgan might correlate with the Calcaria Bed in Avon in which case it is suggested here that it also correlates with bed 25 not bed 29 at Lyme Regis. Even in the very thick section at Watchet, Palmer (1972) suggested that his bed C101 correlated with the Calcaria Bed. Therefore if these correlations are correct, the limestone bed known as the Calcaria Bed in Avon can be correlated over an area of 2750km². At Long Itchington, a 7cm thick packstone of bioclastic fragments 1-40mm long, including crinoid ossicles, at the top of bed 37c may likewise be correlated with the Calcaria Bed (Fig 2.8E, Appendix Section 2.5).

The possibility that more bed to bed correlations can be effected was investigated by using the detailed stratigraphic logs constructed in this study. The large number of limestone, light marl and dark marl beds meant that it was only practicable to correlate the comparatively small number of laminated shale beds. It has been assumed that the present biostratigraphy is reliable and that correlated laminated shale beds were deposited simultaneously everywhere so that individual beds do not cross ammonite zone and subzone boundaries. Of course, different assumptions in alternative schemes can be expected to produce different results. Data from Clements et al. (1975) were used to constrain the position of laminated shale beds (their 'paper shales') in the centre part of the Long Itchington section. Notice that where the log produced here and their log overlap, their 'marl' and 'shale' beds only sometimes correspond to light marl and dark marl beds respectively. Also beds less than a few centimetres were ignored by them.

The results of the attempted correlation are presented in Figs 2.8E and 2.8F including the suggested correlation of the limestone represented by the Calcaria Bed in Avon. Using the laminated shales it

was possible to correlate the Lyme Regis, Watchet and Lavernock Point sections in the planorbis and liasicus zones, and the Lyme Regis and Long Itchington sections in the angulata zone. The Pre-planorbis Beds could not be correlated perhaps indicating a diachronous base. At Watchet the angulata zone and conybeari subzone include many more laminated shale beds than at Lyme Regis and Long Itchington. This is discussed in Sections 4.3.3h and 5.3.2. These correlations demonstrate that the data are largely consistent with the hypothesis of simultaneous changes from light and dark marl deposition to laminated shale deposition over an area of 8000km² (Section 5.3.1).

CHAPTER 3

GEOCHEMICAL STUDY OF

THE BASAL LIAS OF SOUTH BRITAIN.

3.1 Introduction

This chapter concerns a detailed geochemical study of the basal Lias at Watchet and Lyme Regis. At Watchet seventy one samples from four ammonite zones and the Pre-planorbis Beds were analysed for the main rock constituents (excluding clay) %CaCO₃, %TOC (total organic carbon) and %FeS₂ ^{see} (Appendix Sections 3.1 and 3.3 for details of preparation and analysis). At Lyme Regis more detailed investigation involved collection of thirty five bulk samples and thirty one Gryphaea arcuata specimens over an interval 111cm thick near the top of the angulata zone. These samples were analysed for %CaCO₃, %TOC, %FeS₂, %Fe/R (using the hot HCl-method of Berner, 1970), $\delta^{18}\text{O}$ and $\delta^{13}\text{C}$ (Appendix for Chapter 3). Two supplementary studies were undertaken in order to help the interpretation of results from Lyme Regis. Thus, a series of bulk samples was collected from within and around an in situ limestone nodule from the bucklandi zone and eight powders were obtained from different portions of the same Gryphaea specimen.

The stratigraphic position of samples obtained from Watchet and Lyme Regis is indicated in the respective stratigraphic logs (Appendix Sections 2.1 and 2.2). The origins of the samples used in the supplementary studies are shown in Fig.3.4H and Fig.3.4I. All the geochemical results are listed according to locality and rock type in Tables 3A-3E (for Lyme Regis) and Tables 3F-3J (for Watchet) at the end of this chapter. Within each table the samples are listed in stratigraphic order with the youngest at the top. For each geochemical parameter the mean values are indicated in Table 3K and the reproducibility is discussed in Appendix Section 3.6.

The proportions of major constituents has been used to estimate the percentage of 'Clay' using the formula:

$$\% \text{'Clay'} = 100\% - ((\% \text{CaCO}_3) + (2.5 * \% \text{TOC}) + (\% \text{FeS}_2))$$

The component $(2.5 * \% \text{TOC})$ estimates the percentage of organic matter assuming an average composition close to CH_2O . In fact the 'Clay' component includes clay minerals and quartz, iron oxides, chlorite and perhaps some other trace constituents (eg glauconite, collophane, Section 2.2.2a). The gypsum detected by XRD (Section 2.3) has been treated as ^{an indirect} weathering product of pyrite here (Appendix Section 3.3). The small amounts of dolomite present have been expressed as calcite in view of the rarity suggested by staining, XRD (Sections 2.2 and 2.3) and Hallam's (1960a) measurement of MgO (<1%).

Values of $\% \text{TOC}$, $\% \text{FeS}_2$, $\% \text{Fe/R}$ and $\% \text{'Clay'}$ have been reexpressed on a carbonate-free basis using eg:

$$\% \text{TOCcarb. free} = \frac{\% \text{TOC}}{100\% - \% \text{CaCO}_3} * 100\%$$

This ensures that comparing results for samples with a large difference in carbonate contents is meaningful; it allows for the 'dilution' of the non-carbonate components by the carbonate.

3.2 Composition according to Rock Type

Fig 3.2A summarizes the variation in the values for $\% \text{CaCO}_3$, $\% \text{TOC}$ and FeS_2 as related to rock type and location. Each rock type is characterized by a particular mean (Table 3K), range and mode of composition although there is a substantial overlap of ranges. The sequence: light marl, dark marl, laminated shale involves on average a decrease in carbonate contents and an increasing proportion of organic carbon and pyrite. The homogeneous and laminated limestones possess much higher and mutually comparable carbonate contents. However, organic carbon contents (carbonate free) of the homogeneous and laminated

limestones are very similar to those of the light marl and laminated shale respectively; this is consistent with limestone formation through the cementation of light marl or laminated shale. Because the pyrite contents follow this relationship as well, it can be concluded that pyrite formation preceded carbonate cementation (cf. Gluyas 1984). The very different proportions of organic carbon and pyrite (whether carbonate-free or not) in the light marl compared to the laminated shale shows that these components did not determine whether cementation into limestone took place.

The relationships between different constituents is illustrated in Fig 3.2B and 3.2C. Both depositional and diagenetic processes could account for the overlapping fields of the marls and shale (Section 3.4.1). Excluding one value near 50% carbonate, all the limestone values lie in discrete fields as shown by Hallam (1964). Early diagenetic cementation involves the infilling of pore-spaces (Raiswell 1971). Thus if the percentage porosity of uncemented and uncompact sediment is much larger than the primary carbonate content of that sediment, the final carbonate content of the limestone (primary carbonate plus porosity-filling carbonate) is inevitably much larger than that of the uncemented rock (primary carbonate only). Hence, the distinct limestone fields merely indicate that the porosity of the light marl and laminated shale was probably greater than 50% during cementation.

LeRiche (1959) observed a correlation between %CaCO₃ and Log₁₀(%TOC (carb. free)) in the marls and shales of the Lower Lias. On Fig 3.2B an inverse relationship is suggested for rocks with less than 60% calcium carbonate although there is a large scatter. The correlation of LeRiche was used by him to argue against rhythmic unmixing as an explanation for the limestones of the Lower Lias. Consider a homogeneous marl on the

sea-floor; both organic carbon and carbonate contents would be more or less constant. After a phase of hypothetical rhythmic unmixing, limestone would have differentiated into discrete beds. The organic carbon contents (carbonate-free) of the marl or shale between the limestones would now be spread in a horizontal band on a plot of $\text{Log}_{10}(\% \text{TOC})$ v $\% \text{CaCO}_3$ (ie no correlation). Rhythmic unmixing independent of primary composition is therefore unable to account for the inverse correlation seen on Fig 3.4B, and this relationship implies the deposition of sediment with a range of compositions on the sea-floor (Section 2.7.3).

The most significant constituent after calcium carbonate is 'Clay' in these rocks, so there is an inverse relationship between the $\% \text{CaCO}_3$ and $\% \text{'Clay'}$. But, because there is a relationship between the $\% \text{CaCO}_3$ and $\% \text{TOC}$ (carb. free), there is also an inverse relationship between the amount of 'Clay' and organic carbon (carb. free) (compare Fig 3.2B with 3.2C and see Fig 3.4A).

3.3 Rock type composition related to stratigraphic position at Watchet and comparison with Lyme Regis.

The variation in carbonate contents is large for all rock types at all levels of the 90m section studied at Watchet (Fig 3.3A). There is no clear relationship between stratigraphic position and carbonate content for homogeneous limestone, light marl or laminated limestone. However, for dark marl and laminated shale a slight increase in values is apparent in the Pre-planorbis Beds and in the lower part of the bucklandi zone.

The percentage organic carbon and pyrite is higher, regardless of rock type, in the Pre-planorbis Beds and the lower bucklandi zone.

Carbonate-free values of these components are very similar when light marl is compared to homogeneous limestone, and when laminated shale is compared to laminated limestone. This correspondence of values confirms that homogeneous limestone represents cemented light marl and laminated limestone is cemented laminated shale. The link between pyrite and organic carbon contents is discussed later (Section 3.4.2a).

The relative proportion of particular rock types in a section is related to its stratigraphic position (Section 2.8.1). At Watchet (Fig 2.8A) a greater proportion of laminated shale is found in the Pre-planorbis Beds and hucklandi zone than in intervening zones. Hence, the average composition of particular rock types at particular stratigraphic levels is related in some way to the proportion of laminated shales around that level.

The samples collected at Lyme Regis mainly come from the top of the angulata zone. If Lyme Regis follows the same relationship between rock composition and stratigraphic position, the values at Lyme should fall in the middle of the stratigraphic variation exhibited at Watchet. Support for this hypothesis comes from the varying proportion of laminated shales at Lyme Regis which follows that at Watchet (Fig 2.8A). Indeed the %CaCO₃ and %TOC values at Lyme Regis and Watchet have more or less the same averages (Table 3K). However, the pyrite results are a little higher, on average, at Lyme Regis for all rock types (cf. Palmer 1972 p8-9 and Section 3.4.2b for discussion).

3.4 Geochemical Studies related to Lyme Regis.

3.4.1 Detailed Geochemical Profile.

The relationship between a variety of geochemical parameters and rock type on a centimetre scale is shown in Fig 3.4A. Most of this

section is shown in the photograph of Fig 3.4B. Although rock type does control the relative composition of particular samples, the absolute value of one parameter is not always diagnostic of the rock type involved. For example the %CaCO₃ in the lowest dark marl bed is lower than the light marl directly above it, but it is identical to the next light marl higher in the succession (Fig 3.4A).

A different situation is represented by a dark marl sample (BL327) obtained from between the two limestone beds at the top of the section (Figs 3.4A+B). In this case the carbonate content exceeds the organic carbon content of most light marl samples. Additionally the organic carbon and pyrite contents are lower than most light marl samples whether or not the comparison is made on a carbonate-free basis (Tables 3B and 3C). Thus the content of pyrite and organic matter does not make this bed appear dark (Fig 3.4B). Presumably the separation of organic matter, clay and carbonate into a crude lamination in the dark marl rather than the homogeneous mixture found in light marl, accounts for some of the difference in colour. This means that the classification of these rocks in the field (Section 2.2) reflects petrographic characters which are associated with distinct average geochemical compositions. However, there is no reason why different petrographies or rock types should not have the overlapping compositional ranges observed here (Section 3.2).

The geochemical profiles of Fig 3.4A also show an inverse relationship between the percentage of clay and organic matter on a carbonate-free basis. Yet the proportion of organic matter clearly correlates with the amount of reactive iron or Fe/R (Section 3.4.2a) and pyrite (Section 3.4.2b). Laminated shale sample BL319 contains 57% CaCO₃

which, because it is exceptionally high, might indicate the inclusion of a certain amount of calcite 'beef' (Sections 2.2.2d).

3.4.2 Pyrite formation at Lyme Regis.

3.4.2a Pyrite - Introduction.

The following introduction relates to work by Berner (1970) and Raiswell & Berner (1985). Pyrite formation starts once H₂S is available to combine with iron. In normal marine sediments oxygen is used up by the bacterial decomposition of organic matter which then allows the reduction of pore-water sulphate to form H₂S. Thus the greater proportion of organic matter, the more H₂S is formed and ultimately the more pyrite is produced (Raiswell & Berner 1985). This is carbon-limited pyrite formation. Consequently plots of %S (a proxy-measure for %pyrite) against %TOC possess a sloping line passing through the origin (ie zero percent organic matter prevents pyrite formation) (Fig 3.4Ca). In these circumstances, the more H₂S which is available, the more the available iron is converted to pyrite. The proportion of converted iron is measured by the 'degree of pyritization' (Berner 1970):

$$\text{DOP} = \frac{\% \text{Fe/pyrite}}{\% \text{Fe/pyrite} + \% \text{Fe/rest of sediment}}$$

In sediments with high organic carbon contents (>1%) so much H₂S can be produced that pyrite formation continues until all the iron in a very reactive form is used up; pyrite formation becomes iron-limited.

In the Black Sea pyrite formation is associated with anoxic bottom-water and organic-rich sediments, yet it remains organic-limited (Raiswell & Berner 1985). The H₂S present in the bottom-water produces pyrite before burial and causes a positive intercept on the %S v %TOC plot. But after burial the amount of organic matter controls the amount

of H_2S generated and hence further iron is ^{bound into pyrite} λ so both the %S and DOP are correlated with TOC (Fig 3.4Cb). The intercept on the %S v %TOC graph can be used to infer anoxic bottom-waters provided that pyrite formation is demonstrably carbon-limited (denoted by the correlation between DOP and %TOC).

Sediments with high organic contents and low concentrations of iron (particularly in carbonate-rich sediments) are likely to involve iron-limited pyrite formation (Berner 1970, Raiswell & Berner 1985). In these cases the DOP is independent of %TOC because all the readily converted iron is pyritized and a greater supply of H_2S cannot convert any more. Thus the %S v %TOC plot follows the %Fe v %TOC plot instead of the DOP v %TOC plot. If the amount of iron is unrelated to the amount of organic matter, horizontal trends appear on the %Fe and %S v %TOC plots (Fig 3.4Cc). However, iron deposition can be linked to organic matter through colloids causing the correlation of %Fe and %TOC. In this case the correlation of %S with %TOC is related to the association of iron and organic matter rather than a correlation between DOP and %TOC (Fig 3.4Cd) (Raiswell & Berner 1985). Iron-limited pyrite formation can be associated with bottom-waters possessing low oxygen levels or anoxia or fluctuating oxygen contents (Raiswell & Berner 1985).

The limiting factor in pyrite formation and in some cases environmental data, can be gleaned from these plots (Fig 3.4Ce). Thus it was hoped that by measuring %Fe/R for the Lyme Regis samples, it would be possible to decide whether the light marl was deposited in normal marine and the laminated shale in anoxic bottom-waters.

Pyrite determinations in these rocks uses the measurement of sulphur contents and assumes a formula FeS_2 (Section 2.3 for the formula and Appendix Section 3.3 for a discussion of the assumptions involved).

Berner (1970) developed the 'hot HCl method' for the determination of the amount of iron able to react with H₂S (%Fe/R or reactive iron). The method was developed to exclude very unreactive iron structurally bound within clays for example. This method was adopted here (Appendix Section 3.4) and measures all the iron from haematite, limonite, chlorite and iron adsorbed onto clay (Berner 1970). Pyrite is left virtually unaffected (Appendix Section 3.3) by this treatment leading to the definitions:

$$\%Fe/R = (\%Fe \text{ in pyrite}) + (\%Fe \text{ soluble in HCl}).$$

and

$$DOP/R = \frac{\%Fe/pyrite}{\%Fe/R} .$$

3.4.2b Pyrite - Results and Discussion.

The values for %S, DOP/R, %Fe/R and %TOC are given in Tables 3A-3D. The values plotted in Fig 3.4D are all expressed on a carbonate-free basis even though only the DOP v %TOC plot is affected by this adjustment of the data, this allows comparisons between plots to be made more easily. The points form one consistent trend on each graph in spite of the different rock types involved (Fig 3.4D). This suggests that the mode of pyrite formation was not controlled by the sediment type deposited at any particular time.

The trends on all the plots produce positive intercepts with the vertical axes. Both the sulphur and iron plots have a significant positive slope whereas the DOP plot is virtually horizontal (especially if compared with the plots in Raiswell & Berner 1985). The slopes of these plots indicate iron-limited pyrite formation which explains the very similar distribution of points on the Fe v. TOC and S v. TOC graphs. The slope of the iron plot indicates a link between the amount

of iron and organic matter rather than the deposition of iron predominantly absorbed onto clay (Fig 3.4A).

The DOP values are high (average = 0.73) compared to normal marine sediments; probably reflecting either anoxia or low oxygenation levels in the bottom-waters during deposition of all sediment types (Raiswell & Berner 1985). Since the light marl (and homogeneous limestone) was not deposited under anoxic bottom-water considering the degree of bioturbation (Section 5.2.2), deposition probably occurred in bottom-waters with low oxygen contents. This helps to explain the amount of organic matter in the light marl because it is higher than might be expected for a normally oxygenated sediment. It is not possible to decide from this study whether the dark marl and laminated shale were deposited in anoxic bottom-waters (Section 5.2.2).

Fig 3.4Ea shows the relationship between Fe/R and sulphur in these rocks. The slope corresponds to the weight ratio of iron to sulphur according to the pyrite formula Fe:S_2 (ie 56:2*32). The intercept reflects a constant proportion of iron soluble in HCl (about 0.8% Fe/R).

Gluyas (1983,1984) investigated the $\delta^{34}\text{S}$ of pyrite at Lyme Regis and the proportions of framboidal and euhedral morphologies in a limestone bed (Lang's bed 50) and the adjacent light marl. His isotopic results indicated that pyrite formation in light marl was associated with an open system and a low organic-carbon budget. Pyrite in the limestone was associated with a progressively more restricted supply of sulphate. Apparently a phase of framboidal pyrite formation preceded cementation, whereas euhedral pyrite formed during cementation.

Fig 3.4Eb shows that when all the sulphur and organic-carbon results for Lyme Regis are combined with those for Watchet, the same %S v %TOC

correlation as Fig 3.4D results. Therefore pyrite formation at Watchet was probably iron-limited also (though strictly this should be checked with a DOP plot). So deposition at Watchet may well have occurred in poorly oxygenated or anoxic bottom-waters. The C/S ratio of sediments can be used to measure palaeosalinities (Berner and Raiswell 1985). Part of the stratigraphic study at Watchet was designed to establish whether the salinity of the sea during deposition of the Pre-planorbis Beds was fairly low (perhaps explaining the lack of ammonites). Unfortunately, this method can-not be applied to rocks with iron-limited pyrite formation because the C/S ratio is controlled by the Fe/TOC relationship (Berner & Raiswell 1984).

In Section 3.3 it was shown that pyrite contents at Watchet were consistently lower than at Lyme Regis. The organic carbon contents are not significantly different, however, so if pyrite formation at Watchet was also iron-limited, the source of iron must have differed from Lyme Regis. Palmer (1972 p9) suggested that low pyrite contents at Watchet ruled out substantial anoxia. In fact, the pyrite contents are only a little lower than at Lyme (Section 3.3) and no conclusions concerning anoxia can be reached from the pyrite content alone.

It is interesting to compare the results obtained here for the Blue Lias at Lyme Regis with those published for the Black Ven Marls slightly higher up the succession (turneri and obtusum zones, Sinemurian - Table 1B). The Black Ven Marl results also indicate iron-limited pyrite formation, but iron deposition was not linked to the deposition of organic matter at that time (Raiswell & Berner 1985). This and the comparison with Watchet suggests a variety of sources of iron in the south of England during the Hettangian and Sinemurian (Section 5.5).

3.4.3 Stable Isotopes at Lyme Regis.

3.4.3a Isotopes - Gryphaea Results.

Before the results from the single specimen and stratigraphic study can be interpreted, the primary or secondary nature of the values must be assessed. On Fig 3.4F all the Gryphaea values lie close to the origins of both axes, indicative of a normal marine signature. Diagenetically altered results are often correlated, but no such correlation is present here. Two left (lower) valves were sectioned, one longitudinally and one transversely, to investigate the texture of the specimens. The foliated, low-Mg calcite appears to be well preserved (Bathurst 1975) and is not luminescent (Fig 2.2I and 2.2J) supporting the suggestion that the results were not altered during diagenesis. However, partings between growth layers (<0.1mm), cleavage traces and twin planes (about 50µm) and cracks confined to the margins of one specimen investigated, are all filled with luminescent (and therefore diagenetic) calcite. Overall there is less than about 5% diagenetic calcite in the shells so the results are regarded here as essentially unaltered by diagenesis.

Isotopic ratios in specimen BLG33 have been contoured in Fig 3.4H. All the powders for the Gryphaea studies were collected by drilling through several growth layers (Appendix Section 3.2). Nevertheless, clear patterns emerge with $\delta^{18}\text{O}$ and $\delta^{13}\text{C}$ becoming lighter towards the margin of the shell; the contours frequently cross the growth lines. The patterns might indicate a greater proportion of diagenetic calcite along wider cracks at the margin of the shell. Only five out of thirty one specimens used for the stratigraphic study could not be sampled at position A shown on Fig 3.4H (Appendix Section 3.2). Most results come from the isotopically heaviest and therefore the least altered part of

the shell. Diagenetic alteration cannot account for the slightly different $\delta^{18}\text{O}$ and $\delta^{13}\text{C}$ patterns or for the lack of correlation between these two ratios. Thus a combination of metabolic fractionation parallel to the growth lines (Lowenstam & Epstein 1954, Jones et al. 1986) and a greater proportion of diagenetic calcite in cracks at the edges may explain the patterns.

The $\delta^{18}\text{O}$ values in Gryphaea can be used to calculate palaeotemperatures providing it is assumed that the ratios obtained in the stratigraphic study are unaltered and not significantly fractionated metabolically. The thirty one results (Table 3E) have a mean value for $\delta^{18}\text{O}$ of -0.85 ± 0.81 per mil. The 'error' quoted here is calculated as $2\sigma_{n-1}$ on all 31 specimen ratios and reflects the range of values determined. The Craig palaeotemperature equation, updated by Shackleton and Kennett (1975), has been used with their value for the isotopic composition of ocean water on an ice-free globe (-1.2 per mil). The calculated average palaeotemperature is $15.4 \pm 3.5^\circ\text{C}$. The palaeolatitude of S. Britain was about 40°N during the ^{Early Jurassic} (Smith et al. 1981). Today, temperatures at sea-level, over the ocean at 40°N range from $20-10^\circ\text{C}$ during the year (Barry & Chorley 1982). The temperature implied by the Gryphaea results agrees very well with this range and supports the suggestion that the isotopes are not altered because diagenetic processes would have led to 'unreasonably' high palaeotemperatures.

The range of $\delta^{18}\text{O}$ results in the stratigraphic study is considerably greater than the range in a single specimen (Fig 3.4A). Assuming unaltered values, $\delta^{18}\text{O}$ could have monitored both palaeotemperature and palaeosalinity. Yet salinity changes would have related to freshwater alone (from rivers) as there is no evidence for evaporites or

hypersaline water. Therefore, the salinity changes would be restricted to the surface of the sea and would not have been recorded by Gryphaea on the sea-floor. The range of temperatures suggested above (7°C) seems rather high for average temperature changes from year to year; thus the samples probably record part of the yearly (seasonal) temperature range even though each sample powder represents an amalgamation of different growth layers.

The $\delta^{18}\text{O}$ values are not related to the rock type matrix nor are they correlated with the $\delta^{13}\text{C}$ results (except for the top few results where the sampling density is low). On the other hand the $\delta^{13}\text{C}$ values do appear to be related to the matrix and like the oxygen ratios show a much larger range stratigraphically than within a single specimen. The carbon ratios are inversely correlated with the %TOC results (compare the %'Clay' or inverse of the %TOC curve with $\delta^{13}\text{C}$ on Fig 3.4A). Unfortunately Gryphaea specimens were not collected from exactly the same levels as the bulk samples and except for the top few centimetres, Gryphaea is absent from laminated shales. The correlation between $\delta^{13}\text{C}$ and %TOC is discussed in Section 5.2.2.

3.4.3b Isotopes - Bulk Sample Results - Primary versus Secondary.

All the bulk sample isotopic ratios determined in this study are shown in Fig 3.4F and previous determinations (Campos & Hallam 1979 and Gluyas 1983) are plotted in Fig 3.4G. The main difference between the new and published results is that the range of limestone bed values is greater in previous studies (more positive $\delta^{13}\text{C}$ and more negative $\delta^{18}\text{O}$). The published ratios showed that the limestone values lie fairly close to normal marine ratios ($\delta^{13}\text{C}\sim 0$, $\delta^{18}\text{O}\sim 0$). The evidence for lack of compaction within the limestone was combined with these results to argue

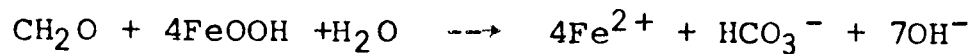
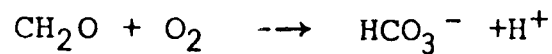
for early cementation (Campos & Hallam 1979, Gluyas 1984). The Gryphaea results here have been shown to be largely unaltered (Section 3.4.3a) yet they have much heavier isotope values than any bulk sediment results, implying that the bulk samples record a diagenetic overprint.

The correlation of isotopic ratios in the limestone beds, marls and shale could arise from primary processes. The coccolithic matter in all rock types could have recorded surface changes in salinity (monitored by $\delta^{18}\text{O}$) and consequent productivity changes (monitored by $\delta^{13}\text{C}$) (Barron et al. 1985). Yet, if the Gryphaea values recorded bottom-water $\delta^{13}\text{C}$ and the bulk samples recorded surface-water $\delta^{13}\text{C}$; times of completely mixing water-columns would produce identical values and stratified water would cause an inverse relationship (Mckenzie 1982). Neither of these circumstances occur; the carbon isotopes are always lighter in the bulk samples, the range of values is different and there is no correlation between the two. Thus as the Gryphaea values have been shown to be primary and the bulk sample microspar is luminescent, it appears that all the bulk sample $\delta^{13}\text{C}$ results were modified during diagenesis. The correlation of the two isotopic ratios in the bulk samples implies diagenetic modification of the oxygen results as well.

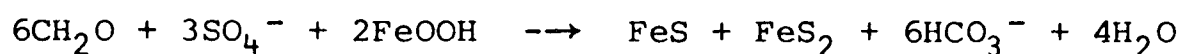
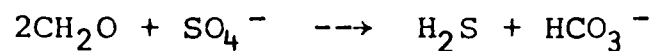
3.4.3c Isotopes - Theoretical diagenetic history and pore-water isotopic evolution.

A summary of the likely diagenetic processes involved and the changes in pore-fluid composition is given here to aid the interpretation of bulk sample results. Irwin et al. (1977) demonstrated a series of zones involved in the diagenesis of organic-rich rocks which relate depth and burial history to pore-water isotopic development. Zone

I involves oxidation of organic matter and a rise in pH summarized in the equations (from Irwin et al. 1977 and Irwin 1980):

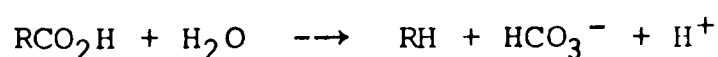


The transition to Zone II represents the exhaustion of free oxygen and involves the generation of carbonate ions with very light $\delta^{13}\text{C}$ values (~ -25 per mil) from the decomposition of organic matter by bacterial oxidation and sulphate reduction. The pH falls in this zone and the reduction of iron and sulphate ions allows the formation of pyrite:

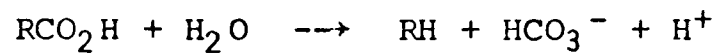


Work on early diagenetic limestone nodules introduced an extra element into the isotopic evolution of pore-waters in the sulphate reduction zone (Zone II) (Hudson & Friedman 1974). During the later stages of sulphate reduction, the initial drop in $\delta^{13}\text{C}$ can be reversed and rises to around 0 per mil because of the progressive dissolution of unstable bioclasts (aragonite and high-Mg calcite). This is associated with a lightening of $\delta^{18}\text{O}$ which is related to temperature increases, ultrafiltration by clays and closed-system depletion of ^{18}O (Hudson & Friedman 1974).

Bacterial fermentation (Zone III) starts once the supply of sulphate has run out and generates, overall, carbonate ions with heavy carbon ratios ($\sim +15$ per mil). As ammonia is generated as well as methane, the pH rises in this zone (Irwin 1980):



Further burial leads to a temperature increase which causes decarboxylation (Zone IV) and carbonate ions with a light carbon ratio (~-10 to ~-25 per mil):



Pyrite forms the main sink for iron during sulphate reduction so any precipitating calcite is non-ferroan (Gluyas 1984). During fermentation and decarboxylation however, the only sink for iron is in carbonate so ferroan calcite, dolomite, ankerite and siderite can form (Gluyas 1984).

3.4.3d Isotopes - Bulk Sample Results and Interpretation.

A little ferroan calcite is found in the innermost parts of ammonite cavity fillings (Section 5.1.3) and in parts of the calcite 'beef' of the basal Lias at Lyme Regis (Section 2.2.2d). Marshall (1982) studied the beef in the Shales with Beef overlying the Blue Lias Member near Lyme. Most beef seems to have formed during early and late stages of sulphate reduction; the ferroan portions formed near the end of sulphate reduction or the start of fermentation when $\delta^{13}\text{C}$ values were around zero. However, as the microspar which forms the principal carbonate component of the basal Lias is non-ferroan, and the $\delta^{18}\text{O}$ values are more positive than -5.6 per mil, most diagenesis probably occurred during or before sulphate reduction.

The isotopic ratios of the limestone beds, marls and shale produce a different trend to the limestone nodules (Figs 3.4F&G) so these groups are treated separately. Carbon and oxygen ratios for an in situ limestone nodule and the surrounding light marl from Lang's Bed 37 have been contoured in Fig 3.4I. Unfortunately samples could not be obtained from the centre of the nodule (short of collapsing the entire cliff!) so

the full diagenetic history of the nodule is unknown. This nodular horizon passes laterally into a continuous limestone bed (Fig 2.1C). Carbonate contents in the light marl away from the nodule (samples A4 and A5 - Table 3B) average 38.7%. If this value mainly represents the original light marl carbonate content, then the extra carbonate in the limestone nodule reflects porosity in the uncemented, uncompact sediment (Raiswell 1971). The values of %CaCO₃ of samples A16 and A14 (Table 3A) suggests that the porosity during cementation decreased from at least 71% to 50%; indicating progressive compaction. The proportion of early cement will have decreased towards the edge of the nodule so results from the edge are less representative of the pore-water isotopes than samples in the centre. The general nature of changes in pore-water isotopes is faithfully recorded, however; $\delta^{18}\text{O}$ was decreasing and $\delta^{13}\text{C}$ increasing during cementation. Thus nodule growth took place during the latter part of sulphate reduction when $\delta^{13}\text{C}$ was slowly increasing due to the dissolution of bioclasts (Section 3.4.3c).

Campos & Hallam (1979) reported two ratios from a nodule from Lang's bed 15 which occurs at the base of the detailed stratigraphic section studied here. The trend observed (Fig 3.4G) from inside to the outside of the nodule agrees with the trend obtained for the nodule in bed 37 here, but both $\delta^{18}\text{O}$ and $\delta^{13}\text{C}$ are much heavier in the published case. This difference is unlikely to have resulted from differences in proportions of cement. One possibility is that the published case indicates cementation in a partially closed system.

In the model suggested here the closed system allows much higher values of $\delta^{18}\text{O}$ than normal to be developed. Thus in the case of the nodule from bed 15 (from the hypothetically closed system), most bicarbonate might have been derived from dissolving bioclasts rather

than from sulphate reduction of organic matter. Initially then, both oxygen and carbon values would rise. Then fractionation could have produced the usual falling values of $\delta^{18}\text{O}$ when the rate of supply of bicarbonate ions from bioclast dissolution slowed down. However, the $\delta^{13}\text{C}$ in the pore-water would have remained high and rising as elsewhere. In the case of the nodule from bed 37 (from the hypothetically open system), however, some bicarbonate would have been supplied from sulphate reduction as well as from dissolved bioclasts, but whilst the carbon values were rising, the oxygen values were lighter than the closed system and continued to lighten. The nodules of bed 15 are closely overlain and underlain by continuous limestone beds whereas bed 37 is separated from the nearest limestone beds by much more sediment (Appendix Section 2.1). Thus, if limestone beds cemented prior to nodule growth, a partially closed system might have developed between beds that were closely spaced (eg. bed 15).

The trend of isotopic values for light marl, dark marl and laminated shale (Fig 3.4F) could have arisen as a mixing line between sediment with normal marine isotopes (near the Gryphaea field) and cement formed from pore-waters with lighter oxygen and carbon ratios. This phase of cementation presumably relates to the formation of micrite from carbonate mud grains or to the neomorphic aggradation of micrite to microspar (Folk 1965). The presumed composition of the cementing pore-waters combined with the observation of ubiquitous non-ferroan microspar, implies a phase of cementation and microspar formation during the latter stages of sulphate reduction. Limestone nodule formation occurred when porosities were still high (>50% - see above) yet the cementation which produced microspar in the marls and shales must have occurred when porosities were low, otherwise limestone would have

formed. Therefore, microspar formation post-dated limestone nodule growth.

The lack of compaction of the continuous limestone beds suggests early diagenetic cementation and, as for the limestone nodules, the isotopic signature mainly represents the isotopic composition of the limestone bed cement. The phase of cementation which produced limestone beds cannot have been simultaneous with nodule growth otherwise identical isotopic trends would have resulted. The trend of the limestone bed isotopes (Fig 3.4F) corresponds to that of the marls and shale. But limestone beds cannot have formed at the same time as microspar was formed in the marls and shales because field observations show that, unlike these other rocks, limestone beds were cemented prior to significant compaction and aragonite inversion (Section 2.7.1). The question is therefore why do all the limestone bed, light marl, dark marl and laminated shale isotopic ratios lie on the same trend?

This problem can be resolved by suggesting very early cementation of light marl into continuous limestone beds during the earliest stages of sulphate reduction. Isotopic values of the resulting micrite would be normal marine and lie in or near the Gryphaea field. Neomorphism of the micrite in the marls, shale and limestone beds during the latter part of sulphate reduction would have generated the mixing-line correlation of isotopes and microspar with the same luminescent properties regardless of rock type. Presumably, because the limestone beds possessed less porosity than the marls and shale during neomorphism, the limestones retained the heaviest isotopic ratios of the group. The cementation of the laminated shale into laminated limestone beds might have been at the same time as the cementation of the homogeneous limestone. However, the only laminated limestone analysed (bed H1 at Lyme Regis, by Campos &

Hallam 1979) has a relatively heavy carbon-isotopic ratio (Fig 3.4F) perhaps indicating neomorphism at the start of fermentation. Section 5.1.3 summarizes the diagenetic history.

TABLE 3A LYME REGIS - Limestone Geochemical Results. Stratigraphic Log in Appendix Section 2.1.
(cf = Carbonate Free Basis)

Bed Number	Sample	%CaCO ₃	%TOC	%TOCcf	%S	%Scf	%Fe/R	%Fe/Rcf	%FeS ₂	%FeS ₂ cf	'Clay'	'Clay'cf	DOP/R	δ ¹⁸ O ‰ PDB	δ ¹³ C ‰ PDB
37	A11	77.7	0.77	3.45	-	-	-	-	-	-	-	-	-	-5.26	-2.04
37	A13	76.9	0.89	3.85	-	-	-	-	-	-	-	-	-	-5.29	-2.04
37	A14	69.6	0.90	2.96	-	-	-	-	-	-	-	-	-	-5.45	-1.90
37	A15	81.5	0.62	3.35	-	-	-	-	-	-	-	-	-	-4.32	-3.27
37	A15													-4.35	-3.17
37	A16	82.3	0.59	3.33	-	-	-	-	-	-	-	-	-	-4.43	-3.52
37	A12	76.6	0.87	3.72	-	-	-	-	-	-	-	-	-	-5.15	-2.16
36e	BL226	75.8	0.55	2.27	-	-	-	-	-	-	-	-	-	-	-
32b	BL5	73.7	0.73	2.78	-	-	-	-	-	-	-	-	-	-	-
31	BL33	65.9	1.10	3.23	-	-	-	-	-	-	-	-	-	-	-
31	BL36	81.0	0.50	2.63	-	-	-	-	-	-	-	-	-	-	-
31	BL37	66.5	0.75	2.24	-	-	-	-	-	-	-	-	-	-	-
29	BL103	82.7	0.55	3.18	-	-	-	-	-	-	-	-	-	-	-
27	BL110	83.6	0.40	2.44	-	-	-	-	-	-	-	-	-	-	-
19	BL329	80.5	0.30	1.54	0.42	2.15	0.56	2.87	0.78	4.00	18.0	92.3	0.65	-3.50	-1.12
19	BL332	85.7	0.40	2.80	0.43	3.00	0.55	3.85	0.80	5.59	12.5	87.4	0.68	-2.00	-0.41
19	BL328	83.9	0.33	2.05	0.43	2.67	0.51	3.17	0.80	4.97	14.5	90.1	0.73	-2.55	-0.58
19	BL326	70.4	0.27	0.91	0.79	2.67	0.92	3.11	1.48	5.00	27.5	92.9	0.75	-4.19	-1.15
19	BL325	76.1	0.21	0.88	0.53	2.22	0.68	2.85	0.99	4.14	22.4	93.7	0.68	-4.15	-1.16
17	RL314	80.0	0.41	2.05	0.51	2.55	0.64	3.20	0.95	4.75	18.0	90.0	0.69	-3.28	-0.76
17	BL313	84.3	0.29	1.85	0.41	2.61	0.52	3.31	0.76	4.84	14.2	90.5	0.69	-1.86	-0.22
17	BL312	86.3	0.37	2.70	0.64	4.67	0.69	5.04	1.21	8.83	11.6	84.7	0.82	-1.82	-0.25
13	BL301	73.5	0.42	1.59	0.76	2.87	0.86	3.25	1.42	5.36	24.0	90.6	0.77	-2.58	-0.47
														-4.59	-1.24

TABLE 3B LYME REGIS - Light Marl Geochemical Results. Stratigraphic Log in Appendix Section 2.1.
(cf = Carbonate Free Basis)

Bed Number	Sample	%CaCO ₃	%TOC	%TOCcf	%S	%Scf	%Fe/R	%Fe/Rcf	%FeS ₂	%FeS ₂ cf	'Clay'	'Clay'cf	DOP/R	δ ¹⁸ O ‰ PDB	δ ¹³ C ‰ FDB
37	A9	33.7	3.35	5.05	-	-	-	-	-	-	-	-	-	-3.85	-1.13
37	A7	35.3	2.22	3.43	-	-	-	-	-	-	-	-	-	-3.89	-1.40
37	A10	36.5	1.74	2.74	-	-	-	-	-	-	-	-	-	-4.28	-1.38
37	A1	37.3	1.98	3.16	-	-	-	-	-	-	-	-	-	-4.01	-1.49
37	BL221	39.1	1.78	2.92	-	-	-	-	-	-	-	-	-	-	-
37	A3	45.6	1.92	3.53	-	-	-	-	-	-	-	-	-	-4.84	-1.70
37	A4	39.7	1.82	3.02	-	-	-	-	-	-	-	-	-	-4.38	-1.49
37	A5	37.7	2.00	3.21	-	-	-	-	-	-	-	-	-	-4.50	-1.32
37	A2	38.2	2.11	3.42	-	-	-	-	-	-	-	-	-	-4.21	-1.23
37	A6	40.7	1.91	3.22	-	-	-	-	-	-	-	-	-	-4.39	-1.26
37	A8	33.2	4.41	6.62	-	-	-	-	-	-	-	-	-	-4.43	-1.03
32	BL15	26.7	1.94	2.65	-	-	-	-	-	-	-	-	-	-	-
32	BL17	35.5	3.47	5.38	-	-	-	-	-	-	-	-	-	-	-
32b	BL119	55.7	1.10	2.48	-	-	-	-	-	-	-	-	-	-	-
20	BL335	43.2	1.31	2.31	1.28	2.25	1.53	2.69	2.40	4.23	51.1	90.0	0.73	-5.15	-1.86
20	BL333	48.8	1.13	2.21	1.22	2.38	1.43	2.79	2.28	4.45	46.1	90.0	0.75	-3.82	-1.12
18a	BL316	37.9	1.15	1.85	1.32	2.13	1.64	2.64	2.47	3.98	56.8	91.5	0.70	-4.19	-1.70
18a	BL315	41.9	1.06	1.82	1.25	2.15	1.58	2.72	2.34	4.03	53.1	91.4	0.69	-4.84	-1.74
15c	BL308	25.7	0.59	0.79	1.51	2.03	1.90	2.56	2.83	3.81	70.0	94.2	0.70	-4.09	-1.20
15c	RL307	38.2	0.61	0.99	1.27	2.06	1.54	2.49	2.38	3.85	57.9	93.7	0.72	-1.99	-0.25
15c	BL306	34.3	1.49	2.27	1.37	2.09	1.74	2.65	2.57	3.91	59.4	90.4	0.69	-4.67	-1.47
15a	BL330	43.7	0.61	1.08	1.18	2.10	1.50	2.66	2.22	3.94	52.6	93.4	0.69	-4.20	-2.11
15a	BL304	46.1	0.38	0.71	1.39	2.58	1.61	2.99	2.60	4.82	50.4	93.5	0.75	-3.86	-1.36

TABLE 3D LYME REGIS - Dark, Laminated Shale Geochemical Results. Stratigraphic Log in Appendix Section 2.1.
(cf = Carbonate Free Basis)

Bed Number	Sample	%CaCO ₃	%TOC	%TOCcf	%S	%Scf	%Fe/R	%Fe/Rcf	%FeS ₂	%FeS ₂ cf	%Clay'	%Clay'cf	DOP/R	δ ¹⁸ O ‰ PDB	δ ¹³ C ‰ PDB
32	BL9	25.4	3.48	4.67	1.39	1.86	1.91	2.56	2.60	3.49	63.3	84.9	0.64	-	-
	BL9						1.86	2.49							
32	BL117	22.6	5.38	6.95	2.51	3.24	3.25	4.20	4.71	6.09	59.2	76.5	0.68	-	-
32	BL12	28.4	4.37	6.10	2.58	3.60	3.92	5.48	4.84	6.76	55.8	77.9	0.58	-	-
32c	BL30	29.0	4.66	6.56	2.21	3.11	3.13	4.41	4.13	5.82	55.2	77.8	0.62	-	-
	BL30						3.11	4.38							
18c	BL331	27.4	4.74	6.53	2.38	3.28	2.75	3.79	4.47	6.16	56.3	77.6	0.76	-3.94	-1.55
18c	BL320	26.1	4.66	6.31	2.25	3.05	2.64	3.57	4.22	5.71	58.0	78.5	0.75	-4.54	-2.00
18c	BL319	57.0	4.81	11.19	1.61	3.74	1.96	4.56	3.01	7.00	28.0	65.1	0.72	-5.03	-1.67
18c	BL318	20.1	12.30	15.39	4.84	6.06	5.17	6.47	9.08	11.36	40.1	50.2	0.82	-5.18	-1.78
16b	BL310	15.4	3.87	4.58	4.37	5.17	4.51	5.33	8.19	9.68	66.7	78.8	0.85	-4.76	-2.64
16b	BL309	20.7	10.66	13.44	5.41	6.82	5.72	7.21	10.13	12.77	42.5	53.6	0.85	-5.54	-1.93

TABLE 3E LYME REGIS - Gryphaea arcuata Stable Isotope Results.
 Stratigraphic Log in Appendix Section 2.1.

(* = Sample not collected from position A)

(- defined on Fig 3.4H and in Appendix Section 3.2).

(L = Limestone Bed Nod = Limestone Nodule LM = Light Marl)

(dkM = Dark Marl ldSh = Dark, Laminated Shale)

Bed Number	Sample	Rock Matrix	$\delta^{18}\text{O}$ ‰ PDB	$\delta^{13}\text{C}$ ‰ PDB
20	BLG11	LM	-1.08	+1.22
20	BLG54	dkM	-1.03	+1.34
19	BLG13*	L	-0.68	+1.67
19	BLG12*	L	-1.00	+1.28
19	BLG1	dkM	+0.28	+2.45
	BLG1	-----	+0.33	+2.49
18d	BLG14	dkM	-0.53	+1.79
18d	BLG15	dkM	-1.33	+1.21
	BLG15	-----	-1.33	+1.23
18d	BLG53	dkM	-0.54	+1.00
18c	BLG52*	ldSh	-0.83	+1.02
18a	BLG17*	LM	-0.85	+0.50
18a	BLG21	LM	-0.86	+1.71
17	BLG25	L	-1.00	+1.24
18a	BLG19	LM	-0.93	+1.69
18a	BLG20	LM	-1.05	+1.35
17	BLG26	L	-0.95	+1.66
17	BLG27*	L	-0.76	+1.92
16c	BLG23	dkM	-0.69	+1.31
16c	BLG28	dkM	-0.41	+1.72
16b	BLG32	ldSh	-0.42	+1.34
16b	BLG33H*	ldSh	-0.84	+1.66
	BLG33H*	-----	-0.82	+1.61
	BLG33G*		-0.80	+1.44
	BLG33F*		-0.84	+1.06
	BLG33E*		-0.63	+1.42
	BLG33D*		-0.52	+1.64
	BLG33C*		-0.54	+1.78
	BLG33B*		-0.41	+1.31
	BLG33B*	-----	-0.37	+1.28
	BLG33A		-0.33	+1.64
15c	BLG37	LM	-1.46	+1.15
15c	BLG38	LM	-1.34	+1.44
15c	BLG41	Nod	-0.11	+2.31
15c	BLG39	LM	-1.28	+1.26
15b	BLG49	dkM	-1.31	+0.79
15b	BLG51	dkM	-0.92	+1.10
15a	BLG42	LM	-0.66	+1.20
15a	BLG43	Nod	-0.85	+1.83
14	BLG44	dkM	-1.66	+1.34
14	BLG48	dkM	-0.83	+1.17
13	BLG46	L	-0.84	+1.42

TABLE 3F WATCHET - Limestone Geochemical Results. Stratigraphic Log in Appendix Section 2.2.
(cf = Carbonate Free Basis, Height = Metres above the base of the Lower Lias)

Height /m	Bed Number	Sample	%CaCO ₃	%TOC	%TOCcf	%S	%Scf	%FeS ₂	%FeS ₂ cf	%Clay	%Clay'cf
79.48	C111	BW104	88.7	0.35	3.10	0.31	2.74	0.59	5.22	9.8	86.7
74.55	C101	BW97	85.4	0.58	3.97	0.18	1.23	0.33	2.26	12.8	87.7
69.28	C93	BW79	86.2	0.38	2.75	0.49	3.55	0.91	6.59	11.9	86.2
65.66	C83	BW69	79.3	0.54	2.61	0.53	2.56	0.98	4.73	18.4	88.9
63.61	C81	BW66	74.7	0.52	2.06	0.74	2.93	1.38	5.46	22.6	89.3
59.80	C71	BW62	51.0	0.59	1.20	1.08	2.20	2.02	4.12	45.5	92.9
56.41	C59	BW54	84.9	0.37	2.45	0.24	1.59	0.46	3.05	13.7	90.7
47.46	C39	BW52	83.1	0.44	2.60	0.24	1.42	0.46	2.72	15.3	90.5
28.38	B12	BW32	64.4	0.50	1.40	0.69	1.94	1.30	3.65	33.1	93.0
7.24	A24	BW7	85.1	0.35	2.35	0.53	3.56	1.00	6.71	13.0	87.3
3.29	A12	BW125	80.4	1.64	8.37	0.41	2.09	0.77	3.93	14.7	75.0

TABLE 3G WATCHET - Light Marl Geochemical Results. Stratigraphic log in Appendix Section 2.2.
 (%cf = Carbonate Free Basis, Height = Metres above the base of the Lower Lias)

Height /m	Bed Number	Sample	%CaCO ₃	%TOC	%TOCcf	%S	%Scf	%FeS ₂	%FeS ₂ cf	%Clay	%Clay'cf
85.88	D1	BW110	55.9	0.58	1.32	0.99	2.25	1.85	4.20	40.8	92.5
79.70	C112	BW105	59.5	0.82	2.03	1.01	2.49	1.90	4.69	36.6	90.4
73.04	C96	BW95	42.1	1.17	2.02	1.66	2.87	3.11	5.37	51.9	89.6
68.04	C88	BW74	50.7	0.87	1.77	0.86	1.74	1.60	3.25	45.5	92.3
61.93	C78	BW65	36.4	0.93	1.46	1.24	1.95	2.33	3.66	59.0	92.8
58.54	C66	BW58	40.4	1.18	1.98	0.73	1.22	1.36	2.28	55.3	92.8
55.90	C56	BW53	38.5	1.16	1.89	1.69	2.75	3.17	5.16	55.4	90.1
43.97	C32	BW49	40.6	0.90	1.52	0.17	0.29	0.31	0.52	56.8	95.6
39.35	C18	BW44	46.9	0.81	1.53	0.82	1.54	1.54	2.90	49.5	93.2
33.40	C2	BW39	43.1	0.79	1.39	0.81	1.42	1.51	2.65	53.4	93.9
29.83	B14	BW34	62.1	0.32	0.84	0.65	1.72	1.23	3.25	35.9	94.7
24.01	B8	BW28	56.7	0.54	1.25	0.79	1.82	1.47	3.40	40.5	93.5
19.04	B5	BW26	40.5	1.07	1.80	1.32	2.22	2.48	4.17	54.4	91.4
12.81	A39	BW20	51.0	0.83	1.69	1.93	3.94	3.62	7.39	43.3	88.4
9.53	A27	BW12	35.3	1.24	1.92	1.50	2.32	2.81	4.34	58.8	90.9
5.45	A19	BW115	34.6	3.21	4.91	1.13	1.73	2.11	3.23	55.3	84.6
2.46	A9	BW127	49.3	3.01	5.94	1.49	2.94	2.80	5.52	40.4	79.7

TABLE 3H WATCHET - Dark Marl Geochemical Results. Stratigraphic Log in Appendix Section 2.2.
(cf = Carbonate Free Basis, Height = Metres above the base of the Lower Lias)

Height /m	Bed Number Sample	%CaCO ₃	%TOC	%TOCcf	%S	%Scf	%FeS ₂	%FeS ₂ cf	%Clay	%Clay'cf
89.04	D5 BW112	46.9	2.75	5.18	2.28	4.29	4.27	8.04	42.0	79.1
84.06	C119 BW109	44.9	2.08	3.78	1.38	2.51	2.58	4.68	47.3	85.8
75.10	C102 BW100	46.3	1.59	2.96	1.47	2.74	2.75	5.12	47.0	87.5
71.14	C94 BW89	36.8	2.79	4.42	1.00	1.56	1.88	2.98	54.4	86.1
68.98	C92 BW76	39.0	1.08	1.77	1.72	2.82	3.23	5.30	55.1	90.3
61.36	C78 BW63	33.8	2.92	4.41	0.70	1.06	1.31	1.98	42.4	64.1
57.92	C66 BW56	36.1	1.35	2.11	0.68	1.06	1.27	1.99	59.3	92.8
47.06	C38 BW51	33.3	2.09	3.13	0.66	0.99	1.24	1.86	60.2	90.3
38.39	C14 BW43	23.7	1.72	2.25	0.77	1.01	1.44	1.89	70.6	92.6
30.60	B15 BW35	27.0	1.12	1.53	1.11	1.52	2.08	2.85	68.1	93.3
25.26	B9 BW29	24.4	1.01	1.34	1.24	1.64	2.33	3.08	70.8	93.7
18.23	B4 BW25	47.5	1.12	2.13	0.95	1.81	1.79	3.41	47.9	91.2
14.23	B1 BW21	19.6	5.02	6.24	2.17	2.70	4.07	5.06	63.81	79.4
10.32	A31 BW13	41.4	1.61	2.75	1.25	2.13	2.34	3.99	52.2	89.1
5.06	A17 BW116	22.2	4.04	5.19	2.11	2.71	3.96	5.09	63.7	81.9
4.21	A15 BW119	39.6	5.59	9.25	1.54	2.55	2.88	4.77	43.6	72.2

TABIE 3I WATCHET - Dark, Laminated Shale Geochemical Results. Stratigraphic Log in Appendix Section 2.2. (cf = Carbonate Free Basis, Height = Metres above the base of the Lower Lias)

Height /m	Bed Number	Sample	%CaCO ₃	%TOC	%TOCcf	%S	%Scf	%FeS ₂	%FeS ₂ cf	%Clay	%Clay'cf
90.16	D6	BW113	38.1	6.35	10.26	2.15	3.47	4.04	6.53	42.0	67.9
87.12	D3	BW111	60.7	1.53	3.89	1.01	2.57	1.90	4.84	33.6	85.5
81.98	C116	BW107	49.1	4.74	9.31	1.45	2.85	2.72	5.34	36.3	71.3
77.21	C108	EW101	48.1	10.57	20.37	2.14	4.12	4.02	7.75	21.5	41.4
73.58	C100	BW96	46.4	3.14	5.86	1.64	3.06	3.08	5.75	42.7	79.7
70.70	C94	BW88	44.4	2.62	4.71	1.42	2.55	2.66	4.78	46.4	83.5
68.71	C92	BW75	25.6	7.28	9.79	2.77	3.72	5.20	6.99	51.0	68.6
66.14	C86	BW72	30.9	3.95	5.72	1.95	2.82	3.66	5.30	55.6	80.5
61.56	C78	EW64	34.6	3.34	5.11	1.72	2.63	3.23	4.94	53.8	82.3
59.46	C70	BW60	28.1	3.04	4.23	1.07	1.49	2.01	2.80	62.3	86.7
58.29	C66	BW57	29.0	3.26	4.59	0.84	1.18	1.57	2.21	61.3	86.3
42.53	C30	BW47	30.8	2.26	3.27	1.39	2.01	2.60	3.76	61.0	88.2
31.50	B15	BW36	34.3	3.93	5.98	1.37	2.09	2.57	3.91	53.3	81.1
25.63	B10	BW30	11.6	4.84	5.48	2.58	2.92	4.84	5.48	71.5	80.9
21.34	B7	BW27	20.7	5.20	6.56	3.52	4.44	6.59	8.31	59.7	75.3
17.46	B4	BW24	26.9	3.73	5.10	2.09	2.86	3.91	5.35	59.9	81.9
11.93	A39	BW19	33.1	7.76	11.60	3.62	5.41	6.78	10.14	40.7	60.8
8.21	A25	EW9	44.8	10.80	19.57	3.21	5.82	6.01	10.89	22.2	40.2
4.60	A17	BW118	28.8	5.79	8.13	1.73	2.43	3.25	4.57	53.5	75.1
2.57	A9	EW126	37.5	7.75	12.40	2.48	3.97	4.64	7.42	38.5	61.6
1.19	A3	BW132	42.4	6.08	10.56	2.42	4.20	4.54	7.88	37.9	65.8
0.16	A3	EW134	28.3	3.14	4.38	2.06	2.87	3.87	5.40	60.0	83.7

TABLE 3J WATCHET - Laminated Limestone Geochemical Results. Stratigraphic Log in Appendix Section 2.2. (cf = Carbonate Free Basis, Height = Metres above the base of the Lower Lias)

Height /m	Bed Number	Sample	%CaCO ₃	%TOC	%TOCcf	%S	%scf	%FeS ₂	%FeS ₂ cf	'Clay'	'Clay'cf
70.33	C94	BW86	62.4	1.41	3.75	1.70	4.52	3.20	8.51	30.9	82.2
41.79	C29	BW46	74.7	1.01	3.99	0.43	1.70	0.81	3.20	22.0	87.0
11.12	A36	BW16	85.2	1.05	7.10	0.72	4.87	1.34	9.05	10.8	72.8
3.70	A13	BW123	69.3	3.00	9.77	1.02	3.32	1.91	6.22	21.3	69.4
1.66	A4	BW131	86.5	1.39	10.30	0.48	3.56	0.89	6.59	9.1	67.4

TABLE 3K Average Geochemical Values at Lyme Regis and Watchet.

cf = Carbonate Free Basis, N = Number of analyses
 Nb. Average %Clay'cf = 100% - ((2.5 * Average %TOccf) + Average %FeS₂cf)

Location	Geochemical Determination	Limestone Beds + Nodule	N	Light Marl	N	Dark Marl	N	Laminated Shale	N	Laminated Limestone	N
Lyme Regis	%CaCO ₃	77.9	22	38.9	23	36.4	15	27.2	10	-	-
Watchet		78.5	11	46.1	17	35.2	16	35.2	22	75.6	5
Both		78.1	33	42.0	40	35.7	31	32.7	32	75.6	5
Lyme Regis	%TOccf	2.54	22	2.82	23	3.76	15	8.17	10	-	-
Watchet		2.99	11	2.07	17	3.65	16	8.04	22	6.98	5
Both		2.69	33	2.50	40	3.71	31	8.08	32	6.98	5
Lyme Regis	%FeS ₂ cf	5.28	9	4.11	9	5.41	11	7.48	10	-	-
Watchet		4.40	11	3.88	17	3.88	16	5.92	22	6.71	5
Both		4.80	20	3.96	26	4.51	27	6.41	32	6.71	5
Lyme Regis	%Clay'cf	88.4	-	88.8	-	85.2	-	72.1	-	-	-
Watchet		88.1	-	91.0	-	87.0	-	74.0	-	75.8	-
Both		88.5	-	89.8	-	86.2	-	73.4	-	75.8	-
Lyme Regis	%Fe/Rcf	3.41	9	2.69	9	3.29	11	4.74	10	-	-
Lyme Regis	DOP/R	0.72	9	0.71	9	0.76	11	0.73	10	-	-
Location	Geochemical Determination	Limestone Bed	N	Limestone Nodule	N	Light Marl	N	Dark Marl	N	Laminated Shale	N
Lyme Regis	δ ¹⁸ O‰ PDB Bulk Sample	-3.20	9	-4.99	6	-4.19	19	-4.19	11	-4.83	6
Lyme Regis	δ ¹⁸ O‰ PDB <u>Gryphaea</u>	-0.87	6	-0.48	2	-1.02	10	-0.83	10	-0.53	3
Lyme Regis	δ ¹³ C‰ PDB Bulk Sample	-0.80	9	-2.49	6	-1.38	19	-1.38	11	-1.93	6
Lyme Regis	δ ¹³ C‰ PDB <u>Gryphaea</u>	+1.53	6	+2.07	2	+1.29	10	+1.40	10	+1.33	3

CHAPTER 4

WALSH POWER SPECTRA: METHODOLOGY AND ANALYSIS FOR
THE BASAL LIAS OF SOUTH BRITAIN.

4.1 Introduction

According to the Milankovitch Theory changes in Earth's orbital geometry can induce climatic change (see Section 1.2 for a discussion). The cyclic changes in orbital geometry have nearly constant periods of 410, 100, 41, and 21kyr (Berger 1984). Any stratigraphic sequence with cyclicity induced by orbitally forced climatic change should possess evidence for one or several regular cycles with the durations listed above. Two problems are faced by geologists wishing to test a hypothesised Milankovitch origin for sedimentary cycles. Firstly regular cyclicity must be demonstrated and secondly any regular cycles present must have their periods estimated.

It is now well established that regular cyclicity is readily demonstrated using the statistical technique called power-spectral analysis (Hays et al. 1976 and many papers in Berger et al. 1984). Fourier power spectral analysis is normally applied to stratigraphically-ordered geochemical determinations (%CaCO₃ for instance). However, the data used for analysis, called time series, can be generated by digitising stratigraphic logs and in such cases Walsh power spectral analysis is applied instead (Schwarzacher 1985, Weedon 1985, 1986 in Appendix Sections 5.1 and 5.2). The Walsh technique is still extremely new to sedimentology so this chapter is partly devoted to an explanation of the mathematical methodology used and includes a discussion of geological considerations such as the effect of hiatuses. The second part of this chapter (Section 4.3) is devoted to Walsh power spectra generated using time series from the basal Lias of Britain. The explanation of power-spectral analysis is made diagrammatically as many texts already exist to give rigorous mathematical treatment (Beauchamp 1975, Jenkins & Watts 1968, Schwarzacher 1975). A computer program,

'WPSPEC', listed in the appendix for this chapter provides a straightforward method for generating Walsh power spectra. It is stressed that it is important to understand the pitfalls of the time series generation and spectral interpretation stages.

Once regular cyclicity has been demonstrated, some method is needed to estimate the periods or durations of the cycles involved. This is usually solved by the use of varves or by some reference to a radiometric time scale (Section 4.2.6e). The estimated periods are often poorly constrained. However, if demonstrably-regular sedimentary cycles possess periods in the order of tens of thousands of years, orbitally-forced climatic changes can be inferred (Crowley 1983, Schwarzacher 1964, Schwarzacher 1975).

The nomenclature of 'cyclic' sequences has not yet been formalized (Duff et al. 1967, Merriam 1964, Schwarzacher 1975). The words 'cyclic', 'periodic' and 'rhythmic' have no universally accepted definitions. 'Periodite' is a recent term with unfortunate genetic implications (Einsele 1982b). It has been applied to sequences which lack a sedimentological or spectral analysis and the use of this term should not, in the author's opinion, be assumed to indicate the product of orbitally forced climate as, for instance, limestone/shale series might be generated entirely diagenetically in some cases (Eder 1982). Schwarzacher (1975, pp288-296) extensively reviewed the concept of geological cyclicity. Many would agree that Carboniferous cyclothem are geologically cyclic whether or not the order of rock types is constant or some Markov property is present or whether power spectra have been used to indicate regularity (Schwarzacher 1975). Schwarzacher defined geological cyclicity as an oscillating random process.

To avoid confusion I use the term 'regular cycle' ^{ic} (ity) as a sedimentary cycle of constant wavelength which has been recognised using power spectral analysis. Further I use the term 'interbedded' if two or more rock types occur many times stratigraphically in a section; regardless of whether any regularity is present.

4.2 Walsh power spectral analysis of stratigraphic sections.

4.2.1 General introduction to Walsh power spectra.

The interpretation of power spectra at first sight is deceptively simple. The recognition of peaks on a spectrum is achieved in the same way as the recognition of peaks on an X-ray diffraction trace. The spectra of real data have an element of 'noise' or random elements, but a particularly well-developed peak indicates that a regular cyclicity occurs with a certain frequency or wavelength (cycle thickness). The complications start with the decision of whether a peak is 'well developed' or 'significant' and whether it's existence is related to other 'significant' peaks present (Section 4.2.5).

All time series can be represented as the summation of different regular waves. Each component regular wave has a particular wavelength and amplitude. In Fourier analysis the component regular waves are sine and cosine waves. In Walsh analysis they are SAL and CAL functions (which are both types of Walsh functions, Beauchamp 1975). Sine and cosine waves of a particular wavelength are identical in shape but are phase-shifted by 90° relative to each other - SAL and CAL functions have an analogous relationship. In Fig 4.2A the Walsh power spectrum of a sine wave is shown with the component Walsh functions. Notice that the peak corresponding to a regular cycle of 8cm (12.5 cycles per metre) was produced from both a SAL function of 8cm and a CAL function of 8cm.

Power is calculated as the sum of the squares of the amplitude of each paired SAL and CAL component (Beauchamp 1975). In Fig 4.2A the amplitude of the 8cm components is much greater than the 2.6cm components and hence the 8cm peak is dominant on the spectrum.

In Fig 4.2B a time series composed of a regular cycle 16cm thick and repeated 128 times (giving 2048 points) has been used to produce a Walsh power spectrum with a single peak. A new time series was then produced by using a table of random numbers to generate 'hiatuses'. The first column in the random number table was used to determine the separation of hiatuses (00-99cm) and the second column was used to determine the thickness of section removed (00-99cm). The new time series is illustrated in Fig 4.2C. The resulting power spectrum shows that the original regular time series has been distorted producing small peaks around the 16cm peak (which can be described as noise) (Fig 4.2B).

In Fig 4.2D random numbers have been used to generate an entire time series. For each row of the random number table, the first column was used to determine the number of points given a code of +1 (ie an even number in the second column) or -1 (ie an odd number in the second column). The spectrum of the 'random' time series is illustrated in Fig 4.2E and shows that random data produce small and no particularly dominant peaks in the low-frequency part of the spectrum (<10 cycles per metre) (cf. Figs 4.2E & 4.3B drawn to the same scale). The power spectra of geological time series with regular cyclicity lie between the extremes of spectra with very dominant peaks (Fig 4.2B) and spectra without dominant peaks (Fig 4.2E).

Walsh functions have been used to analyse the sine wave in Fig 4.2A. If a Fourier power spectrum had been calculated instead, then a single peak indicating a single component sine wave of 8cm would have resulted.

Either technique can be applied to any time series, but the Walsh method is best applied to discontinuous or stepped data (Beauchamp 1975 p89). Continuous data such as % calcium carbonate values are best analysed using the Fourier method.

4.2.2 Sampling and time-series generation.

By definition a time series is composed of observations made at sample points placed at equal intervals of time or thickness. The method of time-series generation used here is illustrated in Fig 4.2F. Measured sections are digitized by assigning a different numerical code to each rock type. The codes must lie on both sides of 0 so two rock types would be coded +1 and -1 and three might be coded +1, 0 and -1 etc. This digitization of stratigraphic sections is similar to that of Carss & Neidell (1966), but they analysed their time series with Fourier power spectra. Schwarzacher & Fischer (1982) and deBoer (1982) used successive limestone bed-thickness measurements to generate Fourier power spectra. Their method of time-series generation ignored the small thickness of intervening shale; thus their interpretation of the spectra produced in terms of the Milankovitch Theory, is based on a comparison of the time series with only one side of modern insolation curves.

A major difference in time series generation used here by comparison with Pleistocene studies is that a thickness-scale is used instead of a time-scale. In Pleistocene work a constant sedimentation rate is assumed between radiometrically-dated horizons and a 'time-depth function' is calculated by linear interpolation (Hays et al. 1976). This is not possible for ancient rocks, but the use of a thickness scale can be justified by reference to Sander's 'Rule' (Sander 1936, Schwarzacher 1975 p288-296).

Schwarzacher translated Sander's 'Rule' as "Cyclicity in space indicates cyclicity in time, but the absence of cyclicity in the stratigraphic record does not indicate the absence of time cyclicity" (Schwarzacher 1975 p288). Schwarzacher also derived a mathematical proof of this 'Rule' and showed that a stratigraphic record with regular cyclicity cannot result from an independent random process in time. Thus the detection of regular sedimentary cycles via the use of a stratigraphic thickness scale implies regular cyclicity in time. Yet it cannot be concluded that any set of regular sedimentary cycles must indicate orbitally-forced climatic change; some form of dating is needed first. The absence of regular sedimentary cycles might be the result of a host of geological processes which have had the effect of damping a regular climatic signal (Section 4.2.6). Alternatively there may have been no regular climatic signal in the environment of deposition.

The digitization of stratigraphic sections generates just a few discrete values and the transition from one code number to another is step-like and treated mathematically as instantaneous (Fig 4.2F). The conditions required for the generation of such a time series are listed below:

- 1) Laterally continuous beds.
- 2) Few distinct rock types interbedded.
- 3) Continuous exposure vertically (stratigraphically).
- 4) Sharp contacts (ie thinner transition-layers than the sample interval).
- 5) 'Type 1' cycles, as defined by Schwarzacher (1975 p281), are

present. Viz the thickness of beds is related to the duration of deposition in some way and accumulation was not geologically instantaneous.

These conditions are usually only met within pelagic, hemipelagic, evaporitic and deep-lacustrine sequences. In sequences that only fulfill conditions 1), 3) and 5), Fourier power spectra can be applied instead if geochemical determinations are made at constant intervals (Dunn 1974). The considerable advantages of the Walsh over the Fourier method stem from the ease of generation of time series as well as computational factors concerning the speed of processing and ^{size} the of storage space required (Beauchamp 1975 p63).

Sample intervals must be carefully chosen according to the thickness of the beds. In order to use sampling to represent oscillations in the data correctly, ^{at} least two samples per oscillation are needed. If less than two samples are used then 'aliasing' results whereby spurious lower frequency (longer wavelength) cycles are generated (Fig 4.2G). Using digitization of measured sections, aliasing can be avoided by choosing a sample interval which is the same or smaller than the thickness of the smallest bed present. Thus if the smallest bed is 2cm thick then all beds must be measured to the nearest 2cm or some smaller value. The sample interval should also be chosen, when possible, so that it is greater than the thickness of any gradational contacts. When some beds have gradational contacts thicker than the thinnest bed, there are likely to be measurement errors (Section 4.2.5e), so a Fourier method might be more appropriate.

All peaks on a power spectrum have the same frequency-resolution or bandwidth (indicated as a horizontal bar labelled BW on the spectra shown here). This means the wavelengths of regular cycles are less well

constrained towards the low-frequency end of power spectra. For example the peak on spectrum C on Fig 4.2H labelled 16cm might have received power from regular cycles from 15.74 to 16.27cm during spectral estimation. The number of sample points in a time series controls the bandwidth of a spectrum if the sample interval is kept constant. Doubling the number of points halves the bandwidth.

The sample interval is equal to half the thickness of the smallest cycle which can be detected. In all the spectra for this chapter the sample interval is 1cm, so the highest frequency value calculated (called the 'Nyquist frequency') is 50 cycles per metre corresponding to a wavelength of 2cm. The longest complete, regular cycle possessing a power value on a Walsh spectrum has a wavelength equal to the length of the time series used.

4.2.3 Spectral estimation.

The calculation of a power spectrum is necessarily performed with a computer given the number of operations involved. Power values for spectra of real data are called 'spectral estimates' because only infinitely long time series could be used to calculate perfect spectra. Generating Walsh power spectra involves at least three stages:

- a) Generation of time series.
- b) The Walsh transform operation.
- c) Spectral estimation.

Additional stages used here are:

- d) Normalization with the sum of the squares of the power values.
- and

e)Smoothing with a 3-point Hanning window (Section 4.2.4).

A time series can be considered to be a representation of data in the 'time domain'. The Walsh transform or operation re-expresses the time series in the 'frequency-domain' in terms of the frequency and amplitude of the component SAL and CAL functions. Strictly, the term 'Sequency' should be used (ie half the average number of zero-crossings per unit interval, Beauchamp 1975), but in order to keep the explanation clear 'frequency' has been retained. Pairs of SAL and CAL amplitudes are squared and added (Fig 4.2A) to yield spectral estimates (the 'periodogram' approach, see the formulae given by Beauchamp 1975 p100).

The algorithm for the Walsh transform has been taken from Kanasewich (1981 pp395-396). A computer program called WPSPEC has been written in FORTRAN to run on a VAX computer and expresses the frequency in 'cycles per metre'. The program is listed in Appendix Section 4.1 and uses GHOST80 library-file subroutines to produce the graphics (power spectra and/or plots of time series).

The algorithm used for the Walsh transform uses a number of nested DO-loops. The number of repetitions of the outermost DO-loop is controlled by the number of points in the time series in such a way that the number of points must be an integer power of 2 (ie $N=2,4,8,\dots,512,1024,2048,\dots$). As well as satisfying this condition, the number of points in a digitized time series is also controlled by the sample interval, the thickness of continuously exposed section and the thickness of section exhibiting the same interbedded rock types. In order to maximize the frequency-resolution of the spectrum (ie minimize the bandwidth); the more points in a time series the better.

4.2.4 Testing the significance of spectral peaks.

A variety of procedures can be used to test the significance of spectral peaks. Firstly a visual appraisal of a spectrum can be made to decide whether a particular peak appears above the background noise-level. Spectra are usually very spiky making it difficult to distinguish noise peaks from small 'significant' peaks. This problem can be partly solved by 'smoothing' the estimates. A 3-point Hanning window (weighted 0.25, 0.5, 0.25) has been used here following Beauchamp (1975 p205). The smoothing operation is similar to the application of a moving average; it flattens all the peaks, but only 'noise' peaks disappear altogether. The visual appraisal of the spectrum becomes more reliable after smoothing, but unfortunately the bandwidth is automatically doubled (the 'degrees of freedom' rise from 2 to 4, Beauchamp 1975 p100). The top spectrum (A) of Fig 4.2H shows the same spectrum as Fig 4.2B generated by introducing 'random' hiatuses into a time series that was originally a perfect 16cm cycle. Spectrum B (Fig 4.2H) was generated by smoothing spectrum A and shows that some of the noise peaks have been eliminated.

Statistical confidence levels can be applied to test the significance of peaks against some form of random model. If the spectral noise possesses approximately equal power from one end of the spectrum to the other, called 'white noise', then the peaks emerging from the noise level are investigated using Fisher's test (Nowroozi 1967). This requires normalization of the spectral estimates (excluding the zero cycles per metre value Section 4.2.5d). Next a confidence level is selected and the corresponding power value is obtained from a table (NB. the power depends on the number of spectral estimates $((N/2)+1)$, Nowroozi 1967). Spectrum B of Fig 4.2H shows the 95% confidence level

suitable for 2048 points. Peaks below this level are not significantly distinguishable from white noise, whereas peaks above can only be considered significant with 95% confidence.

If the power of the background noise rises progressively at the low frequency end of the spectrum it is termed 'red noise' and a different test is applied (Jenkins & Watts 1968, Schwarzacher 1975 p210-212). The spectrum is displayed with $\text{Log}(\text{power})$ v. frequency and a confidence interval dependent on the degrees of freedom (=4 for smoothed Walsh power spectra) is read from a ' $\chi^2/\text{degrees of freedom}$ ' table. To be distinguishable from red noise, the peak to be tested must exceed the average power for its region of the spectrum by more than the confidence interval. Unfortunately, the statistics of Walsh power spectra are imperfectly known (Pestiaux & Berger 1984a). Therefore the basis for this test - that noise peaks are randomly distributed around the mean power on a log power plot - might be erroneous.

To test further the significance of peaks on a power spectrum, subspectra can be calculated (Negi & Tiwari 1984). The power (or amplitude) of regular cycles can vary with the position in the time series for both climatic and mathematical reasons (Beauchamp 1975, Ruddiman et al. 1986). However, geologically and climatically meaningful regular cycles should be present throughout the time series. The amplitude of the component Walsh functions used to calculate power is equal to the average amplitude for the whole time series. Therefore it is possible for a peak to appear on a spectrum despite the fact that the corresponding regular cycle is only present in half the time series. To eliminate such peaks subspectra are calculated for each half of the time series; only those peaks on the main spectrum which possess peaks on both subspectra are accepted as meaningful. Thus in Fig 4.2H the two

subspectra 'bottom' and 'top' prove that the peak on the main spectrum labelled '16cm' is present in both halves of the time series. The other peaks were caused by the hiatuses and did not generate components with anywhere near power of the 16cm cycle. The peak labelled '?17cm' would be considered genuine using the criteria used here. However, this peak is so much weaker than the 16cm peak it would probably not be distinguished if the background noise were more uniformly distributed across the spectrum than in this idealised case. Before a spectral peak can be considered to be significant in terms of the Milankovitch theory, there are certain mathematical and geological processes which must be considered first.

4.2.5 Mathematical considerations.

4.2.5a Sidebands.

All time series of real data start and end abruptly. In Fourier analysis these truncations are difficult to represent with sine waves and cause additional minor peaks associated with every natural peak on a spectrum (called sidebands). In Walsh analysis truncations are easily represented with Walsh functions so sidebands are not generated. No sidebands are produced by smoothing with a 3-point Hanning window.

4.2.5b Harmonics.

Harmonics are generated when some regular oscillation is asymmetric with one short and one long portion for each otherwise regular cycle (Fig 4.2I). The wavelength of a harmonic is always some integer divisor of the fundamental. For instance the asymmetric cycle 16cm long in Fig 4.2I, called the fundamental, has three harmonic peaks associated with it of 16/2cm, 16/3cm and 16/4cm. Pisiyas & Leinen (1984) demonstrated

that a Pleistocene sedimentary cycle with a duration of 23kyr was not related to orbital precession but was instead generated as the second harmonic of the 41kyr orbital obliquity cycle.

4.2.5c Combination tones.

Two types of combination tone exist and indicate the interaction of two different regular cycles. Summation and difference tones possess, respectively, frequencies equal to the sum or the difference in frequency of the two generating cycles. A peak generated as a combination tone satisfies this frequency relationship and has less power than one or both of the generating cycles. Ruddiman et al. (1986) may have detected combination tones of 54 and 31kyr duration in Pleistocene sea surface temperature records.

4.2.5d Zero cycles per metre or trend power value.

During the normalization of spectral estimates for Fisher's test for white noise, the zero cycles per metre power value is excluded (Nowroozi 1967). Therefore, during the smoothing of normalized spectra this value must be excluded, otherwise the low-frequency values are incorrectly biased. In Fig 4.2I (and Weedon 1986) the zero cycles per metre value was indicated, although it was not included during the smoothing operation. To avoid incorrect interpretation of the lowest frequency values, the spectra which follow are drawn without this value (eg Negi & Tiwari 1983).

4.2.5e Inaccuracies in time series generation.

Whilst measuring a section in the field, the wrong rock type might be assigned to a bed and/or an inaccurate thickness might be recorded.

The classification of rock types should not present problems if a consistent set of characteristics are employed. Inaccurate measurements may arise due to, for example, difficulties with exposure such as variable slope. Because each spectral peak is associated with a bandwidth, or range of wavelengths which contribute power, small errors are not important. However, larger errors will cause damping of significant peaks if the errors are random. Nevertheless, significant peaks on a power spectrum are extremely unlikely to result from errors (cf. discussion of Sander's 'Rule' Section 4.2.2).

4.2.6 Geological considerations.

The Milankovitch Theory was developed during studies of the Pleistocene with an accurate time-scale and well constrained orbital periods. In pre-Neogene studies, however, a thickness-scale must be substituted for a time-scale. Inevitably any record of climatic processes displayed in terms of rock thickness instead of time will cause some form of change in the theoretical spectral shape. If certain sediment types represent certain climatic states, there are a number of processes which might influence the shape of the spectrum. Relevant factors and processes include bioturbation, variations in sedimentation rate, variations in compaction and diagenetic processes and hiatuses.

4.2.6a Bioturbation.

Burrowing smooths out geochemical variation in deep-sea cores, although methods are available for removing this effect during Fourier studies (Pestiaux & Berger 1984b, Schiffelbein 1984). Burrowing causes 'reddening' of power spectra, in other words, all the peaks are reduced in size or damped by an amount which increases at higher frequencies

(Dalfes et al. 1984). Burrowers destroy very thin beds (unless inhibited by anoxic bottom-waters) and they make sharp contacts become more gradational.

4.2.6b Variations in sedimentation rate.

Irregular variations in sedimentation rate have the effect of distorting regular stratigraphic signals because each regular cycle in time would be recorded as beds with irregular variations in thickness (Pestiaux & Berger 1984b). On the spectrum the peaks related to regular cycles in time would be less pronounced or entirely indistinguishable from the background noise as a result. If sedimentation rates gradually increase or gradually decrease, regular cycles in time are again damped. So if the sedimentation rate gradually increased for instance, each regular cycle in time would be recorded by thicker and thicker beds and the expected peaks would consequently be flattened. Significant peaks on a power spectrum cannot have been generated by irregular variations in sedimentation rate.

On the other hand, systematic variations in sedimentation rate produce harmonics (Section 4.2.5b) which can now be removed quite simply during Fourier analysis (Schiffelbein & Dorman 1986). At present harmonic removal has not been pursued for Walsh studies. As an example of systematic variations in sedimentation rate consider a regular 21kyr climatic cycle represented by 10.5kyr of shale- and 10.5kyr of limestone sedimentation. The shale is likely to have a very different sedimentation rate to the limestone and therefore a regular, but asymmetric, sedimentary cycle (eg. thick limestone beds and thin shale beds) would result, producing harmonics on the spectrum (Section 4.2.5b, Fig 4.2I).

4.2.6c Differential compaction and diagenetic processes.

Precisely the same relationships exist for differential compaction as for variations in sedimentation rate. If irregular variations in compaction occur then regular signals are distorted, causing flattening of the peaks associated with regular cycles in time. Alternatively, systematic variations in compaction might produce harmonics. (Systematic variations in compaction may enhance or counteract harmonics generated by systematic variations in sedimentation rate.) In carbonate-rich sequences, stylolite formation and early diagenetic cementation represent typical diagenetic processes which could produce regular or irregular distortions of a thickness scale.

The importance of demonstrating the primary origin of interbedded rock types is emphasized here. It has been contended, although it remains to be shown, that regular 'rhythmic unmixing' can occur within a homogeneous marl sequence. Thus a regular limestone/shale sequence could have a purely diagenetic origin (Hallam 1964, 1986, Eder 1982, Ricken 1985, 1986). Burrow-mottling and primary lamination can be used to demonstrate the primary distinction of rock types (Hallam 1964, Arthur et al. 1984). However, diagenetic enhancement of rock types (systematic changes in thickness) does not prevent or invalidate power spectral-analysis.

4.2.6d Hiatuses.

A corollary of Sadler's (1981) work is that sections which span several million years contain hiatuses at the tens of thousands of years scale whether or not they are recognisable (Section 2.5). Hiatuses which occur randomly (ie random spacing and random thickness of section lost) cause distortion of regular time series (Fig 4.2B & 4.2C). In the time

series of Fig 4.2C the hiatuses were spaced between 0 and 99cm. If the spacing had been less on average, then the 16cm cycle is less likely to have remained detectable. If hiatuses occur systematically, at regular intervals and with a regular thickness of missing strata, then a regular time series might or might not become distorted. If hiatuses form preferentially within one rock type then harmonics might be generated.

4.2.6e Estimating the periods of regular sedimentary cycles.

At present, two methods are available for estimating the periods of regular sedimentary cycles. Average varve thicknesses can be used to calculate sedimentation rates (assuming that each varve indicates a single year, eg. Olsen 1986). Or some relationship to an absolute chronology can be inferred by utilizing biozones (eg. Schwarzacher & Fischer 1982) or radiometrically-dated tuffs within the measured section (eg. Barron et al. 1984). For instance in the Jurassic, on average ammonite zones represent about 1Myr :

<u>Reference</u>	<u>Duration of the Jurassic</u>	<u>Average duration of 74 ammonite zones:</u>
Van Hinte 1976	57Myr	1.30Myr
Armstrong 1978, 1982	64Myr	1.15Myr
Harland <u>et al.</u> 1982	69Myr	1.07Myr
Kennedy and Odin 1982	74Myr	1.00Myr
Hallam <u>et al.</u> 1986	70Myr	1.06Myr

This allows sedimentation rates to be calculated. Unfortunately, it is unlikely that biozones represent equal time intervals (House 1985). Thus it is better to use data from several biozones rather than only one. Stratigraphic sections spanning several million years are very likely to possess hiatuses at the tens of thousands of years level. This

is because Sadler (1981) showed that, for a given rock type, the longer time interval employed, the lower the sedimentation rate calculated. In other words a section representing a few million years is quite likely to have sediment preserved from each million year interval. On the other hand the same section is much less likely to have sediment preserved from every 20-100kyr interval. Hence the biozone method can only provide a maximum estimate for the periods of regular cycles because the sedimentation rates for intervals of tens of thousands of years are probably underestimated. Provided that regular cycles have periods estimated in the order of tens of thousands of years, then orbitally forced sedimentation can still be inferred (Crowley 1983 pp867-868, Schwarzacher 1964, Schwarzacher 1975 pp311-320). Additionally, glacio-eustatic control of sedimentation can be discounted and local orbitally-forced climatic change can be proposed if ice was absent from the globe during deposition.

An indirect method for the dating of regular sedimentary cycles uses the inference that orbital cycles were responsible for them if they have periods between 410 and 20kyr. Thus the wavelength ratio of orbital cycles (41/21, 100/21, 410/21 etc.) can be compared with the wavelength ratio of regular sedimentary cycles detected with power spectra (Hays et al. 1976, Olsen 1986). This method is largely independent of the other methods of dating.

4.3 Walsh power spectra for the basal Lias of Britain.

4.3.1 Time series, errors and dating.

The time series (including the sources of the biostratigraphic data) and the Walsh power spectra for the basal Lias of Britain are illustrated in Figs 4.3A-L. A description of rock types was given in

Chapter 2 and the geochemistry was discussed in Chapter 3. Detailed stratigraphic logs for the sections yielding time series used here are illustrated in the Appendix for Chapter 2.

Evidence for the primary distinction of rock types was discussed in Section 2.7.3 and centers on the presence of burrow-mottled bed contacts and primary lamination. Thus it is meaningful to apply power-spectral analysis in order to test orbital-forcing of sedimentation (Section 4.2.6c). All the spectra were generated using a sample interval of 1cm and the codes: limestone=+1.5, light marl=+1.0, dark marl=0.0, dark, laminated shale=-1.0, and laminated limestone=-1.5 (Fig 4.2F). The average error for the thickness measurements are indicated on Table 4A. The average errors are within 10% of published stratigraphic logs for all locations except Nash Point. This suggests that the errors are probably too small to have seriously damped spectral peaks by distortion of the time series (compare with Nash Point discussion Section 4.3.3d).

During early diagenesis, at the horizons with highest primary carbonate contents (Section 5.1.2), limestone beds formed within some light marl beds and laminated limestone beds formed within laminated shale beds. So five rock types were produced from three sediment types. Because this process occurred prior to significant compaction, the light marl and laminated shale beds were compacted much more than the limestone beds. Therefore, early diagenesis must have altered the hypothesized proxy-climatic record by forming extra rock types and distorting the thickness-scale. In Section 4.2.6c it was shown that compactional processes can cause damping of regular signals or introduce harmonic components, but these processes cannot generate entirely new spectral peaks. So, the detection of significant peaks on the following

spectra cannot be attributed to differential compaction related to early diagenesis.

Nevertheless, it might be thought that the introduction of extra rock type codes would affect the spectral shape. This problem was tackled by Weedon (1986 - Fig 7, Appendix Section 5.2). Thus it was shown that if the code values quoted earlier (+1.5, +1.0, 0.0, -1.0, -1.5) are replaced by the codes +1.0, +1.0, 0.0, -1.0, -1.0, the shape of the spectra are virtually unchanged. In Section 6.2.2, concerning the Oligocene Boom Clay Formation, the codes -1.0, -0.5, 0.0, +0.5 and +1.0 were replaced by the codes -1.0, -1.0, -1.0, +1.0 and +1.0. Again the spectral shape is hardly affected by these changes. The reason for this appears to be that the spectral shape is mainly controlled by the position of 'zero-crossings' in the time series. So it is most important, whilst choosing code values for rock types, to establish the major factors in the classification (ie. which rocks are given positive and which rocks negative codes) rather than the details (ie. the particular positive or negative code to use). Ideally some attempt should be made to remove the distortions caused by differential compaction, but that is beyond the scope of the thesis. Instead it is simply assumed that the spectral results have been degraded by the effects of early diagenesis.

Dating was based on the assumption that ammonite zones in the Jurassic represent 1Myr each (Section 4.2.6e). Although undoubtedly inaccurate, this assumption does provide what is probably a reliable estimate of the order of duration of the regular cycles detected. The Pre-planorbis Beds have been omitted from this analysis as there appears to be some difference in the nature of the facies, individual beds cannot be correlated and the base of this unit might be diachronous

(Section 2.8.2). The relative, as well as the absolute thickness of ammonite zones and subzones varies considerably from location to location (Fig 2.5A). This probably indicates that substantial thicknesses of section are missing due to the presence of hiatuses. Evidence for hiatuses is outlined in Section 2.5. All the zones are likely to contain hiatuses (Sadler 1981, Section 4.2.6e); hence the sedimentation rates calculated using ammonite-zone thicknesses provide minimum values. To obtain the highest, and presumably most reliable, sedimentation rate the thickest ammonite zone included in the main time series of each location is used for this calculation. Minimum sedimentation rates for intervals of tens of thousands of years are indicated for each location on Table 4A. 'Varving' within laminated shale at Lyme Regis provides a partial check for this method of dating (Section 4.3.3a).

4.3.2 Illustration of Spectra

Weedon (1986), following Negi & Tiwari (1984), tested peaks on Walsh power spectra using Fisher's test for white noise. It was assumed that peaks too small to pass this confidence level did not represent a significant proportion of the variance of the time series. However, Dafles et al. (1984) showed that bioturbation produces a 'reddening' of spectra by reducing the power of peaks particularly towards the high-frequency end of the spectrum. When plotted on a logarithmic scale the spectra for the basal Lias (Figs 4.3B, F, J, H and L) have a background of red noise up to 12 Cycles per metre and thereafter a background of white noise. This suggests that it would be most meaningful to test peaks on these spectra using a red noise model.

TABLE 4A Average errors for thickness measurements and minimum sedimentation rates for the basal Lias.

Ave. error:

Average error in thickness, calculated as % difference in thickness between corresponding beds, as compared to published logs.

Min. sed. rate:

Minimum sedimentation rate (at the tens-of-thousands of years scale) for each location. Calculated using thickness of thickest ammonite zone (in brackets) occupied by the main time series, divided by 1 million years.

<u>Location</u>	<u>Author</u>	<u>Bed No.s</u>	<u>Thickness</u>
<u>LYME REGIS</u>	Cope et al. 1980	H1-49	25.06m
	This Study	H1-49	24.36m
Ave. error=-2.8% Min. sed. rate=0.92cmkyr ⁻¹ (using <u>bucklandi</u> zone)			
<u>WATCHET</u>	Palmer 1972	A1-D6	98.28m
	This Study	A1-D6	90.77m
Ave. error=-7.6% Min. sed. rate=3.96cmkyr ⁻¹ (using <u>angulata</u> zone)			
<u>LAVERNOCK POINT</u>	Trueman 1920	5-74	33.13m
	This Study	5-74	35.51m
Ave. error=+7.2% Min. sed. rate=0.79cmkyr ⁻¹ (using <u>lasicus</u> zone)			
<u>NASH POINT</u>	Trueman 1930	1-38	20.52m
	This Study	1-38	15.95m
Ave. error=-22.3% Min. sed. rate=4.86cmkyr ⁻¹ (using <u>conybeari</u> subzone)			
<u>LONG ITCHINGTON</u>	Clements et al. 1975	13-43	21.72m
	This Study	13-43	20.03m
Ave. error=-3.2% Min. sed. rate=1.07cmkyr ⁻¹ (using <u>angulata</u> zone)			

Unfortunately, the statistics of Walsh power spectra are too poorly known at present to be sure that the test for red noise is reliable (Pestiaux & Berger 1984a) (Section 4.2.4). Consequently, greatest reliance has been placed here on the use of subspectra to test the stability of spectral peaks. Additionally, the position of peaks possessing durations of less than 20kyr is indicated on the spectra. Peaks to the right of this position do not belong to the Milankovitch band of orbital-cycles (410-20kyr).

The time series used are illustrated in Figs 4.3A, C-E, G, I and K. All the spectra are smoothed. The uppermost spectrum on each figure uses the maximum number of points and a linear power scale. The lowest spectrum on each figure is derived from the same time series but it is illustrated with Log power and a different range of frequencies. The 95% confidence levels (CL, for white noise) and 95% confidence intervals (CI, for red noise) are indicated respectively on these spectra. Spectra in an intermediate position, labelled with letters, are calculated using time series half the length of the main time series. These subspectra possess poorer frequency-resolution (larger bandwidths) and can be used to trace the vertical development of the time series in the frequency domain. The two subspectra from the main time series are superimposed on each other in order to test the stability of peaks on the main spectrum.

4.3.3 The spectra.

4.3.3a Lyme Regis.

The spectrum for Lyme Regis (Fig 4.3B) reveals power concentrated at a few discrete peaks by comparison with a spectrum generated using random numbers (Figs 4.2D & E). Two peaks are common to both subspectra.

These peaks are distinguishable from both white and red noise (at the 95% level).

The maximum period estimated for these cycles (93 & 56kyr) is indicated and utilizes the minimum sedimentation rate from Table 4A. A further constraint on the period of these cycles is provided by Hallam's (1960a) figure for the average thickness of laminae in dark, laminated shales (0.03mm). The simplistic assumption is made that half the thickness of the 85cm cycles is represented by laminated shale. If the laminae represent varves (Anderson & Koopmans 1963), then the 85cm cycles represent over 14,167 years ($425/0.03$), and the 51cm cycles represent more than 8,500 years ($255/0.03$).

These ranges (93-14kyr and 56-9kyr) suggest that the peaks probably correspond to the precession and obliquity cycles (41 and 21kyr). This is borne-out by the wavelength ratio ($85/51=1.7$) which is closer to the ratio for the 41 and 21kyr orbital-cycles rather than any other combination (discussed further in Section 4.3.4).

House (1985) concluded that the obliquity cycle was present at Lyme Regis by simply dividing the total duration of the section (using: 1 ^{zone} ammonite=1Myr) by the total number of limestone/nonlimestone alternations. This technique is erroneous as;

- a) No regard was paid to the possibility of purely diagenetic alternations.
- b) Some of his limestone parts of the alternations are merely horizons of nodules.
- c) No consideration for regularity with superimposed noise was made (ie some limestones might have arisen due to random climatic - or other - fluctuations).

d) It was assumed that every limestone/nonlimestone alternation originally present was partially preserved despite his estimate that the section is only about 37% complete.

The completeness of the section at Lyme Regis can be estimated very crudely by comparing the minimum sedimentation rate of Table 4A (0.92cmkyr^{-1}) with the rate implied using $85\text{cm}/41\text{kyr}$ (2.07cmkyr^{-1}). Thus the section is in the order of 44% complete at best (ie. $0.92/2.07 \times 100$).

4.3.3b Watchet.

The main spectrum for Watchet (Fig 4.3F) possesses two closely spaced peaks which cannot be resolved on the subspectra. Nevertheless, the subspectra indicate concentration of power at the corresponding frequencies. Although other well-defined peaks are present on the main spectrum, none appear to be present on both subspectra.

The stable peaks represent durations of <207 and $<129\text{kyr}$ and cannot as yet be dated more precisely. The wavelength ratio of the regular cycles is 1.6, suggesting that the orbital-precession and -obliquity cycles are the best explanation. The minimum sedimentation rate (3.96cmkyr^{-1}) compared with the implied rate ($819/41=20.0\text{cmkyr}^{-1}$) indicates a section about 20% complete.

Subspectrum C indicates much smaller-scale interbedding in the angulata zone and the conybeari subzone, even though this upper part of the sequence is greatly expanded by comparison with the lower zones (Fig 2.5A). It appears that the shift in power towards high frequencies in subspectrum C reflects the presence of an unusually large number of laminated shale beds (Section 2.8.2). The anomalously large number of these beds is explained in Section 5.3.2.

4.3.3c Lavernock Point.

The biostratigraphy for this section was previously based (Weedon 1986) purely on Trueman's (1920) data. However, Donovan (1956) showed that the base of the angulata zone was placed too low; consequently the liasicus zone obtains a greater proportion of the section. Additionally, the main time series does not pass into the angulata zone and therefore the liasicus zone has been used here for the calculation of minimum sedimentation rate (Table 4A).

Two peaks are stable according to the subspectra on the main spectrum. Weedon (1986) excluded the 33cm peak as not significant. But considering the 'reddening' effect of bioturbation (Section 4.3.2) the main emphasis has been placed on stable peaks as defined with subspectra. Both peaks recognised here as indicating regular sedimentary cycles are distinguishable from white and red noise.

The wavelength ratio of the peaks (=10.3) might be explained by the 410 (eccentricity) and 41kyr (obliquity) orbital cycles. But this would imply that the section is 95% complete which seems unlikely considering the evidence for hiatuses (Section 2.5, Appendix Section 2.3) and the completeness estimates for the other sections (20-40%). Therefore it is more likely that the 341cm cycle had a shorter period. If this peak represents a 41 or 21kyr period as found at Lyme Regis, Watchet and Long Itchington, then the presence of only one peak might be because of the low wavelength resolution of this part of the spectrum (Weedon 1986).

4.3.3d Nash Point.

No peaks on the main spectrum for Nash point (Fig 4.3J) are stable excluding a peak with an duration of <4kyr. The section spans just one subzone (of the three within the bucklandi zone); the minimum

sedimentation rate was estimated assuming that it represents 333kyr. Unless this sedimentation rate is incorrect by a factor of more than five, this peak can be excluded from discussion as it does not lie within the Milankovitch range of cycles.

The lack of regular cyclicity in the Milankovitch frequency-band was attributed to the proximity of the palaeo-shoreline (Hallam 1960a, Loughman 1982, Wobber 1965) by Weedon (1986). Another possibility is that the average measurement error (-22%, Table 4A) is so large that any regularity in thickness has been destroyed (Section 4.2.5e). Although each bed described by Trueman (1930) was recognised during section measuring, the nodularity of nearly every limestone bed made it difficult to assign representative thicknesses (Section 2.1.2d).

4.3.3e Long Itchington.

The peak labelled 205cm on the main spectrum for this locality (Fig 4.3L) seems to have considerable power on the subspectra. The subspectra peaks lie either side of the correct frequency, but their bandwidths (ie frequency resolution) overlap suggesting that the peak corresponding to a cycle 205cm long probably is stable.

The shifting of the power on the subspectra towards higher frequencies up-section indicates a decrease in sedimentation rate near the base of the angulata zone. This probably reflects the change from continuous dark, laminated shale deposition to cyclic sedimentation just below the base of this zone at Long Itchington (Appendix Section 2.5).

The 205cm cycle has an estimated period of <186kyr which cannot be further constrained. This peak might represent either the precession or obliquity cycles apparently detected at Lyme Regis and Watchet. The small discontinuity at 0.781 cycles per metre might indicate a regular

cycle at 128cm. The frequency ratio with the other peak would be 1.6 (205/128) in agreement with the results for Watchet and Lyme and suggest that the two peaks have periods of 41 and 21kyr. A longer time series is really needed in order to investigate the stability of these peaks.

4.3.4 Discussion.

Despite the field evidence for hiatuses (Section 2.5), and the estimates that the sections are 20-40% complete at best, significant peaks are present for four localities out of five. The hiatuses probably caused distortions of the time series, but the spectral peaks have not been entirely removed. If sedimentation rates had been the same across the whole basin then the regular cycles would have had identical wavelengths everywhere. Also thin ammonite zones would indicate locally increased erosion. Yet a comparison of the wavelengths of the regular cycles detected, with the relative thicknesses of the zones at different localities (Fig 2.5A), shows that longer wavelength cycles are found in more expanded sections. Therefore the local thickness of a given ammonite zone was at least partly determined by local sedimentation rates assuming that thicker beds and longer wavelength regular cycles were formed where sedimentation rates were higher. The estimates of completeness quoted for each location above are extremely crude partly because it is assumed that the periods of the regular cycles are correct and partly because it is assumed that each ammonite zone represents 1Myr. Nevertheless it appears that that all the sections are similarly incomplete. This might indicate that the bottom-relief in the basin was fairly subdued.

Either the obliquity or both the obliquity and precession cycles seem to have been detected at Lyme Regis, Watchet, Lavernock Point and

Long Itchington. The use of ammonite zones for dating is unavoidable at present and it almost certainly produces inaccurate estimates of the maximum periods of the regular cycles. But the presence of regular cycles possessing periods in the order of tens- to hundreds-of-thousands of years which were stable for millions of years, are strong indication of orbital forcing of sedimentation (Section 4.1). Therefore the Walsh technique appears to be a useful method for the detection of Milankovitch cyclicity in stratigraphic sections. But although the spectral results obtained here are consistent with orbital forcing there is room for improvement in the dating in this case and it is still possible that some other process could be stable and regular enough to produce the same spectral results (Section 5.3.1). More conclusions concerning the interpretation of power spectra can be found in Sections 6.8 and 6.9.

Two regular cycles appear to have been detected at Lyme Regis, Watchet and Long Itchington (at Lavernock Point the resolution is too poor to demonstrate more than one regular cycle). It has been assumed that the frequency (or wavelength) ratio of 1.6 indicates that the two cycles are related to precession and obliquity (wavelength ratio of about 1.95). The difference between the expected and observed ratios might be explained by hiatuses acting as a sort of filter which altered the separation of the peaks (Coe pers. comm. 1986). The only support for this idea to date comes from Fig 4.2B where the peak originally at 6.25 cycles per metre (16cm) was shifted to 6.21 cycles per metre (16.1cm) by the introduction of gaps in the original time series. Another possibility suggested by Weedon (1986) is that the longer period peaks actually corresponds to a cycle of about 30kyr. Such a cycle was predicted by Berger (1984) and has been detected in Pleistocene data

although the strength of the peak is enigmatic at present (Ruddiman et al. 1986). Recently Olsen's (1986) Fourier power spectra for Triassic strata from Newark, U.S.A., revealed cycles of 120, 29 and 22kyr. As varves were used for dating this appears to be confirmation that a 30kyr cycle should be considered whilst interpreting power spectra. But until more work has been done on the effect of hiatuses on the structure of power spectra, and the dating for the basal Lias has been improved, the cause of this frequency ratio will remain uncertain.

All the log power spectra, regardless of sedimentation rates, exhibit a discontinuity in the power distribution at or near 12.5 cycles per metre (8cm). To the right of the discontinuities the spectra conform to white noise. This observation is compatible with the smoothing of time series due to uniform mixing by burrowing to a common compacted depth (8cm) (Pestiaux & Berger 1984b). It could also be explained by measurement errors which are more likely to have damped high frequency peaks than low frequency peaks (Herbert & Fischer 1986).

CHAPTER 5

SYNTHESIS AND CONCLUSIONS FOR
THE BASAL LIAS OF SOUTH BRITAIN.

5.1 Diagenesis.

5.1.1 Controls of limestone formation.

Section 2.7 discusses the evidence for the diagenetic formation of limestone and laminated limestone beds and nodules. The nodules themselves and the stable isotopes of the limestone beds indicate formation by early diagenetic infilling of pore-space. The carbonate ions for this process were supplied during the bacterial decomposition of organic matter and from dissolution of aragonite and high-Mg calcite bioclasts. This conclusion is based on the isotopes (Section 3.4.3). There is good evidence that limestone beds and limestone nodules were formed by cementation of light marl beds; their petrography, organic-carbon contents (carbonate free) and biota are identical. Similarly, laminated limestone beds and nodules seem to have formed by cementation within laminated shale beds (Section 2.7). On the other hand, light marl, dark marl and laminated shale seem to represent different sediment types. Their benthonic fossils, organic-carbon contents and petrographies are distinct (Section 2.7.3).

Hallam (1964, 1986) showed that the number of limestone beds in a certain ammonite zone, at a particular place, is related to the thickness of the zone at that location. However, a more complete compilation of relevant data (Fig 5.1A) reveals that, although this relationship is generally correct, there are important exceptions. Thus in the planorbis and liasicus zones at Watchet there are far fewer limestones than expected. This discrepancy can be resolved if it is accepted that limestone beds were only formed by the cementation of light marl. At Watchet there is a correlation between the number of limestone beds and nodule horizons and the proportion of light marl within a certain thickness (Fig 2.8C). Therefore the unexpected paucity

of limestone beds at Watchet merely reflects the unusually low proportion of light marl (cf. Weedon 1987).

The stratigraphic logs for Lyme Regis (Appendix Section 3.1) and Watchet (Appendix Section 3.2) show that light marl beds that are only a few decimetres thick contain just one limestone bed or nodule horizon; thicker light marl beds often have several horizons of nodules or limestone beds. This reflects the way that limestone beds tend to maintain the same, fairly limited, thickness distribution regardless of sedimentation rate (sedimentation rate did of course affect the average thickness of light marl, dark marl and laminated shale beds) (Section 2.7.1, Hallam 1964, 1986). In a given ammonite zone or subzone, the number of limestone beds and nodule horizons depends on the proportion of light marl whereas the number of limestone beds and nodule horizons within a particular light marl bed depends on the thickness of the bed in question. This relationship between the density of diagenetic limestones and facies explains why plots of percentage limestone against thickness can be used for correlation (Section 2.8.1, Hallam 1960a, Palmer 1972).

5.1.2 The nucleation of cement.

Limestone beds and nodules and laminated limestone beds and nodules are not centred on large bioclasts that once contained decaying organic matter; some other explanation for the nucleation of cementation must be sought. In some cases at least, limestone beds formed by the lateral coalescence of isolated nodules (Gluyas 1984, Section 2.7.1). Limestone beds with planar contacts might represent horizons where cementation was especially rapid; all the sediment available for cementation was

cemented prior to compaction so that no hint of nodularity is preserved, the corollary of this being that such beds should have constant carbonate profiles rather than slowly decreasing carbonate contents towards the contacts. Because limestone and laminated limestone beds and nodules always occupy the same stratigraphic level within light marl and laminated shale beds, it can be assumed that sediment composition controlled cementation (Section 2.7.2). The most likely candidates for this critical composition are surface effects, primary organic-carbon contents and primary carbonate contents.

The infilling of pore-space during early diagenesis would have required carbonate surfaces for seeding and nucleation. Thus horizons that contained an exceptionally high density of suitable carbonate surfaces might have nucleated cementation^{preferentially}. Prior to cementation the seeding surfaces must have been bioclasts, suggesting an intimate link with primary carbonate contents. Conversely, during the discussion of neomorphic aggradation of coccoliths (Section 2.6) and Schizosphaerella (Section 2.4) it was shown that organic matter and clay might have inhibited cementation and aggradation. Thus primary organic carbon contents (Section 5.2.1) might have indirectly controlled cementation. It cannot be demonstrated that the availability of nucleation surfaces was a controlling factor, but if it was, then it was probably related to primary organic-carbon or primary carbonate contents.

Direct or bacterial oxidation of organic matter liberates carbonate ions and causes a rise in pH (Irwin 1980, Section 3.4.3c). The carbonate liberated would have been encouraged to precipitate where the pH was high and thus perhaps where organic-carbon contents were high. Yet the most organic-rich sediments were the laminated shales; and the proportion of cemented laminated shale (ie laminated limestone) is very

much lower than the proportion of cemented light marl (limestone). As light marl contains and contained much less organic matter, this candidate for the control of carbonate cementation can be rejected. Conversely, high organic carbon contents might be thought to have impeded cementation by preventing seeding. This would explain the predominance of cementation in light marl beds, but it fails to explain why laminated shale beds were cemented in spite of their high organic carbon contents. (Note that, on a carbonate-free basis, laminated limestone beds have higher organic carbon contents than light marl and dark marl beds - Tables 3J and 3K). Thus it appears that primary organic carbon contents were not the main control upon cementation.

Primary carbonate contents are only able to affect the pH of pore-waters passively by dissolving when the pH is low and creating a buffered system (Irwin 1980). During oxidation and fermentation the pH would have been rising slowly, but during sulphate reduction it was probably falling despite the production of bicarbonate ions (Section 3.4.3c). Clearly the pH never became high enough to cause cementation in all parts of every rock type. Therefore, if the pH was generally low during cementation, cementation might have favoured horizons where the pH was kept relatively high by high primary carbonate contents. This hypothesis can explain the cementation of light marl and laminated shale. On average carbonate contents in light marls are higher than dark marls and laminated shales (Table 3K) so cementation was most frequent in this rock type.

In laminated shales the carbonate contents are generally low, but up to 60% CaCO_3 has been recorded (Tables 3D and 3I) (probably associated with abundant ostracods - Fig 2.2P). This shows that primary carbonate contents in laminated shales were probably locally high enough to

encourage cementation. Interestingly, most laminated limestone beds are found in the Pre-planorbis Beds and the planorbis zone where there are many horizons of concentrated bioclasts (Section 2.5, Figs 2.8A and 2.8B) suggesting unusually high primary carbonate contents. Dark marl does not usually contain limestone nodules or limestone beds presumably because primary carbonate contents remained low. However, in Palmer's bed A15 ^{at Watchet} in the Pre-planorbis Beds, a 4cm thick lens of tightly-packed bivalves has been cemented to form a limestone nodule. Additionally at Nash Point, Trueman's beds 3 and 32 include dark marl beds with limestone nodules. These nodules might have formed because the abundant small broken bioclasts at Nash Point (Section 2.2.2c) caused unusually high primary carbonate contents.

Although carbonate contents may have controlled local pH during diagenesis, another possibility is that high carbonate contents produced unusually large numbers of surfaces suitable for seeding cement. It is concluded that primary carbonate content was the principal control on the nucleation of early diagenetic cement in the basal Lias.

5.1.3 Diagenetic history of the basal Lias at Lyme Regis.

The following discussion is based on conclusions from Sections 2.6, 2.7, 3.4.2, 3.4.3, 5.1.1 and 5.1.2. The stable isotopes of limestone beds form a mixing line between the field of Gryphaea (normal marine) values and the marl and laminated shale values. This is interpreted as indicating that neomorphism of the limestone beds occurred simultaneously with neomorphism of the marls and shale, and that the isotope values of the limestone beds were close to bottom-water values prior to neomorphism (Section 3.4.3). Before neomorphism, limestone carbonate would have been dominated by early diagenetic cement, but as

the isotope ratios at this time were probably typically marine in nature (Section 3.4.3d), cementation of the limestones must have occurred before diagenesis altered the pore-water isotopes. On the other hand, pyrite occurs within the limestone beds (Section 3.4.2b, Gluyas 1984) so limestone bed cementation must post-date the start of sulphate reduction. To reconcile this point with the isotopes it is necessary to suggest that the formation of limestone beds started just after the initiation of sulphate reduction.

It is assumed here that the isolated, euhedral dolomite microspar crystals found in the marls and shale (Section 2.6) were formed authigenically and that the magnesium required was supplied by dissolution of high-Mg bioclasts. The dissolution of these and aragonite bioclasts (especially ammonites) was probably associated with a drop in pH during sulphate reduction (Section 3.4.3c). Carbonate ions from the dissolved bioclasts would have caused a slow increase in $\delta^{13}\text{C}$ in the pore-waters whilst $\delta^{18}\text{O}$ was dropping because of rises in temperature and closed-system depletion (Hudson & Friedman 1974). An increase in $\delta^{13}\text{C}$ with a decrease in $\delta^{18}\text{O}$ is recorded by limestone nodules which were cemented during compaction (Section 3.4.3). Limestone nodule growth therefore occurred during the later stages of sulphate reduction and during compaction. Laminated limestone nodules also grew during compaction as their laminae are pinched towards the edges. The single pair of isotope ratios from a laminated limestone bed ($\delta^{18}\text{O}=-2.95$, $\delta^{13}\text{C}=+2.40$ - Campos & Hallam 1979) has such a high $\delta^{13}\text{C}$ value that either neomorphism post-dated that in other rock types or the initial cementation occurred during fermentation (Section 3.4.3).

The isotopes of the marls, the laminated shale and the limestone beds indicate that neomorphism occurred whilst $\delta^{18}\text{O}$ and $\delta^{13}\text{C}$ ratios were

more negative than normal marine ratios. The fact that the microspar is non-ferroan indicates that the main sink for iron was still pyrite rather than carbonate so neomorphism must have occurred during sulphate reduction. As the value of $\delta^{18}\text{O}$ in the marls and shale is more negative than in limestone nodules and $\delta^{13}\text{C}$ is more positive than that in limestone nodules, neomorphism probably occurred at the end of sulphate reduction. Isotopes from cavity-filling spar in an ammonite chamber ($\delta^{18}\text{O}=-4.59$, $\delta^{13}\text{C}=-4.49$ - Campos & Hallam 1979) indicate that bioclast cavities were being infilled towards the end of sulphate reduction and ferroan-calcite inside some specimens (Section 2.2.2a) shows that this continued during fermentation. Beef calcite includes ferroan and non-ferroan species so beef formation probably straddled the end of sulphate reduction and the start of fermentation (perhaps during over-pressuring - Marshall 1982). Beef horizons are compacted round limestone nodules (Fig 2.1B) so compaction continued during fermentation. Sub-vertical calcite veins which cut the limestones might have formed during decarboxylation and fault movements according to Campos and Hallam (1979, $\delta^{18}\text{O}=-10.8$ and -12.2 , $\delta^{13}\text{C}=+0.29$ and $+1.14$).

A summary of the history of diagenesis at Lyme Regis follows and incorporates information from Section 5.2:

1) Deposition: $\delta^{18}\text{O}\approx-0.85$ per mil, $\delta^{13}\text{C}\approx+1.43$ per mil.

Three interbedded sediment types were deposited: light marl (well oxygenated bottom-water); dark marl (poorly oxygenated bottom-water); dark, laminated shale (anoxic and very poorly oxygenated bottom-water).

2) Direct and Bacterial Oxidation: pH rising, $\delta^{18}\text{O} \sim 0$, $\delta^{13}\text{C} \sim 0$.

The organic matter was partially oxidized (this was extremely limited in dark, laminated shale).

3a) Early Sulphate Reduction: pH falling, $\delta^{18}\text{O} \sim 0$, $\delta^{13}\text{C}$ falling rapidly.

The pyrite (iron-limited) formation started. Limestone beds formed within some light marl beds almost immediately (by pore-space infilling and coccolith aggradation to form micrite). Laminated limestone beds formed within laminated shale beds (some room for doubt - alternatively they formed during early fermentation). Primary carbonate contents probably determined the sites of cementation. Compaction started (which caused a decrease in carbonate contents towards the edges of limestone beds).

3b) Mid-Late Sulphate Reduction: pH falling, $\delta^{18}\text{O}$ falling, $\delta^{13}\text{C}$ rising.

The pyrite formation continued. High-Mg and aragonite bioclasts dissolved causing the rise in pore-water $\delta^{13}\text{C}$ ratios. The $\delta^{18}\text{O}$ ratio in the pore-water fell due to ultra-filtration, closed-system depletion and temperature increases (Hudson & Friedman 1974). Micro-dolomite formed in the marls and laminated shale (Mg was supplied from dissolution of bioclasts and possibly clays). The limestone nodules grew in the light marl during compaction (which caused decrease in carbonate contents towards edges). Laminated limestone nodules grew in the laminated shales during compaction (the laminae were pinched towards edges).

3c) Latest Sulphate Reduction: pH falling, $\delta^{18}\text{O}$ falling, $\delta^{13}\text{C}$ rising.

The pyrite formation finished. Neomorphism of the coccoliths and micrite in the limestone, light marl, dark marl and laminated shale

produced non-ferroan microspar. Bioclast cavities filled with non-ferroan calcite spar. Over-pressuring allowed precipitation of non-ferroan calcite beef especially at the base of laminated shale beds.

4) Fermentation: pH rising, $\delta^{18}\text{O}$ falling, $\delta^{13}\text{C}$ rising rapidly.

The centres of bioclast cavities filled with ferroan calcite spar. Over-pressuring continued with precipitation of ferroan calcite beef. Compaction of light marl, dark marl, laminated shale beds and calcite beef horizons occurred around the limestone nodules.

5) Calcite Veins:

Possibly formed during decarboxylation and faulting.

5.2 Environmental Changes recorded in the basal Lias.

5.2.1 Changes in sediment composition.

It has been shown earlier (Section 2.7.3) that three sediment types were deposited over wide areas of South Britain during the earliest Jurassic: light marl, dark marl and dark, laminated shale. The main components of these sediments were: clay minerals probably derived from runoff or perhaps from winds blowing from land (Section 2.3, Loughman 1982); carbonate mud supplied as coccoliths in zooplankton faecal pellets (Section 2.6); carbonate bioclasts from marine planktonic, nektonic and benthonic organisms; and organic matter from land (wood and pollen grains - Wall 1965) and of marine origin (acritachs, dinoflagellates and amorphous matter) (Sections 2.1.1 and 2.2.2). Trace components included quartz silt, derived from rivers or blown out from land and phosphatic fish scales and marine reptile bones.

The three sediment types had characteristic petrographies even on the sea-floor (Sections 2.2.2 and 2.7.3). The light marl consisted of a homogeneous mixture of coccolithic carbonate mud, bioclasts and clay probably caused by bioturbation. The dark marl preserved a lamination of alternating clay and organic laminae with dispersed bioclasts and zooplankton faecal pellets. The dark, laminated shale was mainly composed of laminae of clay and organic matter with scattered bioclasts dominated by ostracods although thin laminae of concentrated bioclasts are sometimes preserved (Fig 2.2P).

As well as differences in petrography there were differences in average sediment composition (Section 3.2). On a carbonate-free as well as a whole-rock basis, the amount of organic matter preserved depended on the sediment type being deposited. On average, light marl now contains 2.5%, dark marl 3.7% and laminated shale 8.1% TOCcarb. free (Table 3K). Whether or not organic matter was lost by oxidation on the sea-floor (Section 5.2.2), some organic matter was undoubtedly destroyed by bacterial decomposition during diagenesis. Light marl now contains predominantly more-refractory lignite and palynomorphs whereas laminated shale mainly contains less-refractory amorphous, sapropelic matter (Ebukanson & Kinghorn 1985). Independent evidence concerning bottom-water oxygenation (Section 5.2.2) suggests that the most likely explanation is that the amount and type of organic matter now found in these rock types was determined by the amount of oxidation on and just below the sea-floor rather than by later diagenetic processes. Therefore, the present variation in values of TOC was probably mainly caused by primary or extremely early diagenetic processes (oxidation). The range of values of TOC might have been determined by variations in the rate of organic matter deposition or changes in bottom-water

oxygenation or a combination of the two (Section 5.4). The total amount of iron in these sediments is related to the amount of organic matter present, perhaps indicative of an association of colloids and organics. Because pyrite formation was iron-limited and iron contents are related to organic-carbon contents (Section 3.4.2b), the present amount of pyrite in the marls and shales is related to the amount of organic matter.

Average values for %CaCO₃ fall from 42% in light marls and 36% in dark marls to 33% in laminated shales (Table 3K). It is not immediately apparent that these represent primary differences because all these rock types contain microspar and therefore a certain proportion of calcite cement. However, the isotopic ratios for limestone beds, the marls and laminated shales lie on what has been interpreted as a mixing-line between original marine values and pore-water values during neomorphism (Fig 3.4F, Section 3.4.3d). On average, the laminated shale ratios are the most negative (Table 3K) suggesting that the laminated shales contain the most cement even though this rock has the lowest carbonate content. Thus the sequence: light marl; dark marl; laminated shale involved a primary decrease in carbonate content which has been partially masked by diagenetic cement formation.

5.2.2 Changes in bottom-water oxygenation.

As well as changes in sediment composition related to sediment type, there are a variety of lines of evidence which suggest that bottom-waters were variably oxygenated. The sediment was not anoxic just below the sediment/water interface during the deposition of light marl because the homogeneity of this rock type implies complete mixing by infauna. Conversely, the presence of undisrupted lamination and faecal

pellets (now coccolith aggregates and microspar blebs) in dark marls implies that this sediment was anoxic and was therefore not burrowed. This is confirmed by the common occurrence of Chondrites burrow-mottles at the contacts with light marls; Chondrites is characteristically associated with the development of anoxic sediment (Bromley & Ekdale 1984). The shale preserves lamination and almost always lacks burrow-mottled contacts, so it may be concluded that the sediment was entirely anoxic during shale deposition. Yet although this evidence indicates fluctuating pore-water oxygenation levels related to sediment type, this fluctuation might have arisen from variations in the rate of supply of organic matter. The development of associated anoxic bottom-water is not necessarily implied.

The most useful monitor for bottom-water oxygenation levels is the composition of the benthonic fossils. The light marl benthonic assemblage was both diverse and abundant, including echinoids, crinoids and brachiopods (Section 2.1.1b). The dark marl assemblage appears to be virtually identical (Section 2.1.1c), but crinoids were absent perhaps because of reduced bottom-water oxygen levels.

The dark, laminated shale benthos was dominated by ostracods (a large proportion appear to be united and therefore probably not transported - Fig 2.2P, Field 1965) with benthonic foraminifera and occasional dwarfed bivalves (Section 2.1.1c, Hallam 1960a). Brachiopods, echinoids, crinoids and Gryphaea are absent. This indicates that oxygen levels were very low and, if the results from offshore present-day California can be applied to this setting, the lack of echinoids indicates less than 0.3ml/l O₂, and the presence of well preserved lamination less than 0.1ml/l O₂ (Thompson et al. 1985). The fact that some benthonic organisms were present indicates that the bottom-waters

were not always anoxic. Thus the ostracods in the laminated shales, which were shown by Field (1965) to be identical in diversity and abundance to those of the marls, might have tolerated very low oxygen levels, but certainly not anoxia (Benson 1961). Therefore, oxygen levels were never above 0.3ml/l O₂ (to exclude echinoids) and although sometimes enough oxygen was present for ostracods, benthonic foraminifera and dwarfed bivalves to survive, the lamination indicates less than 0.1ml/l O₂. Burrowers were established rarely during the transition to dark marl or light marl deposition (Section 2.1.1d).

The palaeotemperature of the bottom-water averaged 15°C according to isotope ratios in Gryphaea (Section 3.4.3a). At this temperature, in normally oxygenated water, the organic membranes or pellicles which enclose and protect zooplankton faecal pellets are destroyed by biodegradation within a few days (Honjo 1976). So the preservation of discrete, coherent zooplankton faecal pellets in the dark marl and laminated shale probably indicates that bottom-waters were so deficient in oxygen that biodegradation was inhibited.

Carbon-isotope results for Gryphaea became slightly lower during dark marl deposition (Fig 3.4A, Section 3.4.3a). This could result from surface productivity variations or from the diffusion of pore-water carbonate ions into the bottom-waters. Organic matter has very negative carbon isotope ratios so phases of increasing productivity would correspond to increasing organic-matter oxidation and decreasing bottom-water carbon isotope composition providing the bottom-water remained oxidizing (McKenzie 1982). Alternatively, during times when the bottom-waters became anoxic or nearly so, it is possible that carbonate produced during sulphate reduction could have diffused upwards and caused a decrease in bottom-water carbon-isotope values. Therefore, the

Gryphaea isotopic results cannot be used to comment on levels of bottom-water oxygenation.

In Section 3.4.2b it was shown that pyrite formation in all rock types was iron-limited and that the degree of pyritization (DOP) is relatively high and constant (≈ 0.73). These data suggest that bottom-water oxygen levels were low (Raiswell & Berner 1985). It cannot be decided from this information whether the bottom-water ever became anoxic, but it does emerge that even during the deposition of light marl, oxygen levels were below normal (which also explains the fairly high organic-carbon contents despite thorough bioturbation) (Section 3.4.2b).

The organic geochemistry of the basal Lias can also be used to infer the degree of bottom-water oxygenation. Laminated shale and dark marl yield H/C ratios near 1.30 and O/C ratios around 0.11 indicating Type II kerogen (Loughman 1982, Ebukanson & Kinghorn 1985). The organic matter comprises abundant relatively low-density sapropelic amorphous matter, with very common 'cuticles' ^{and} minor humic fragments (wood and coal) (Ebukanson & Kinghorn 1985). Kerogen Type II and relatively low-density amorphous organics indicates deposition in a reducing (and presumably therefore anoxic) environment (Ebukanson & Kinghorn 1985). One sample of limestone reveals an H/C ratio of 1.01 and an O/C ratio of 0.14 or mixed Type II/III kerogen. This sample contains dominant relatively high-density fine-grained amorphous matter with minor palynomorphs and humic fragments; the density and kerogen type apparently indicate biodegradation and deposition in oxidizing conditions. In the lower Lias generally, it has been shown that higher values of TOC are associated with Type II kerogen and lower values of TOC with mixed Type II/III

kerogen; explained in terms of bottom-water oxygenation and preservation (Ebukanson & Kinghorn 1985).

Heavy metals can be enriched in sediments deposited in anoxic bottom waters because the reducing conditions allow precipitation (Brumsack 1980, Myers & Wignall in press). LeRiche (1959) analysed heavy metal concentrations in the planorbis to semicostatum zones. The results for samples with over 1% TOCcarb. free are compared with results for a normal marine shale (Wedepohl 1971) below:

<u>Element</u>	<u>Concentration in ppm (carb. free)</u>	
	Basal Lias (mean in brackets) (Le Riche 1959)	Normal Marine Shale (Wedepohl 1971)
Mo	6-320 (99)	3
V	120-460 (265)	130
Cu	19-95 (61)	45
Ni	93-260 (154)	68
Co	16-41 (29)	19

It is clear that dark marl and laminated shale are enriched in all these elements - especially in Molybdenum - so the bottom-waters were frequently anoxic during their accumulation. The lower values in the range are similar to normal marine shales and are probably derived from light marl samples. These conclusions are supported by recent results for the Blue Lias Member at Lyme Regis where up to 6ppm authigenic Uranium has been detected by γ -ray spectroscopy of laminated shale (Myers pers. comm. 1986). This also indicates that anoxic bottom-water was present for extended periods of time (Myers & Wignall in press).

In summary, there is good evidence for considerable oxygen in the bottom waters and oxygenated sediment during deposition of light marl. But the amount of organic matter (average 2.5% TOCcarb. free - Table 3K)

and the mode of pyrite formation (Section 3.4.2b) show that less oxygen was present than normal for the open sea. The deposition of dark marl was associated with anoxia just below the sediment/water interface and a reduction of oxygen concentration in bottom-waters which excluded crinoids and inhibited degradation of pellicles around zooplankton faecal pellets. Deposition of laminated shale involved the accumulation of sediment under water that was mainly anoxic so that lamination is very well preserved and heavy metals were concentrated. It is not known whether H_2S was actually present in the water column and caused syngenetic pyrite formation on the sea-floor, but it seems likely. Occasionally minor oxygenation (probably less than $0.3\text{ml/l } O_2$) allowed the establishment of ostracods, benthonic foraminifera and dwarfed bivalves, but not infauna.

5.3 Controls of sedimentation.

5.3.1 Climate.

In Section 4.3 Walsh power spectra were generated for several different logs in the basal Lias of South Britain. Although dating proved to be difficult because of poorly constrained chronostratigraphy, and hiatuses, it was demonstrated that regular sedimentary cycles that represent tens of thousands of years were produced throughout the basal Lias (several million years). Regular variations in precession (21kyr period) and obliquity (41kyr period) (Section 1.2) which caused climatic cycles appear to be the most likely explanation for this cyclicity. Orbital changes which affected sedimentation via climate changes currently appear to be the only viable mechanism which could have produced regular sedimentary cycles that represent tens of thousands of years and that persisted for millions of years (Schwarzacher 1975,

Crowley 1983, Schwarzacher 1985, Section 4.2.6e). Future work might reveal, for instance, regular tectonic (eg. Cisne 1986) or biological processes that operate on the right time-scale and are independent of climate, but for the moment it is suggested that the climatic explanation is most acceptable for the basal Lias (see Sections 6.8.2 and 6.9 for a discussion of conclusions which can be reached from spectral analysis of stratigraphic sequences). The climatic interpretation is supported by the ^{bed by bed} correlation _^ over large areas (8000km²) and distances (200km, Section 2.8.2).

At present there is no evidence for substantial or indeed any ice on the globe during the Jurassic; on the contrary there is good evidence for a world-wide equable climate that resembled the Cretaceous (Frakes 1979). So it seems to be very unlikely that the regular sedimentary cycles can be associated with glacio-eustatic changes in sea-level. Other likely causes of sea-level fluctuations probably occurred too slowly to account for cycles representing just a few thousand years (Donovan & Jones 1979, Weedon 1986). Therefore it appears to be most likely that regional, rather than global, climatic changes affected sedimentation in South Britain.

The spectral results mainly depend upon the broad classification of rock types (ie light marl/limestone, dark marl and laminated shale/laminated limestone) rather than the details (such as the position of limestone and laminated limestone beds) (Section 4.3.1). This means that the regular sedimentary cycles can be considered to represent alternations of light marl with laminated shale. These alternations arose from the unspecified forcing of the regional climate by independent variations in obliquity and precession. Dark marl deposition apparently represents an intermediate environment between that of the

light marl and laminated shale (Section 5.2). When climatic changes associated with precession and obliquity reinforced each other, either light marl or laminated shale was deposited. On the other hand, when climatic changes associated with the precession cycle offset those produced by the obliquity cycle, dark marl was deposited.

Not all of the light marl, dark marl and laminated shale beds analysed spectrally can be considered to form part of regular cycles; rather they represent the background 'noise' of the spectra. Such noise can have arisen from a variety of causes, the most obvious being: regular cycles truncated by hiatuses, harmonics caused by variations in sedimentation rate and/or compaction related to sediment type, irregular and very long term (trend) changes in sedimentation rate and/or compaction, damping produced by bioturbation, and errors in section measuring (Sections 4.2.5 and 4.2.6). Irregular variations in climate and in the sedimentary environment might also have produced noise on the spectra.

5.3.2 Water-depth.

Once the relative sea-level changes of the Lower Lias have been discussed, the effect of water-depth upon the deposition of the basal Lias can be assessed. Changes in relative sea-level in Britain were deduced from the onlap of sediments onto the London Platform which seems to broadly agree with onlap on the Radstock Shelf (Donovan et al. 1979, Donovan & Kellaway 1984). Overall water-depths probably remained more-or-less constant throughout the Lower Lias so the thick succession which accumulated did so on progressively subsiding crust (Donovan et al. 1979). Fig 5.3A illustrates this record of onlap. It appears there were relative sea-level rises during the deposition of the Pre-planorbis

Beds and during the planorbis, liasicus, semicostatum, turneri and raricostatum zones. Regression, interpreted as relative sea-level fall, occurred just after deposition of the Langport Member (or White Lias) and during the obtusum and oxynotum zones. This later relative sea-level fall is substantiated by hiatuses along the Dorset coast at the level of the coinstone and at the top of the Black Ven Marls (Fig 5.3A) (Hallam 1969, Cope et al. 1980). More evidence for a regression is provided from palaeontological studies in the Black Ven Marls. Thus Whalley (1985) showed that insect assemblages, which imply very little transport from an area of land and fresh water, are restricted to the top of the turneri and lower part of the obtusum zones. This he suggested is most easily explained by the formation of a temporary delta derived from the Cornubian land mass perhaps just a few miles from Lyme Regis and Charmouth. Palynological evidence from Dorset suggests that the coastline was relatively close throughout the early Jurassic (Wall 1965). However, the palynomorphs from the top of the Black Ven Marls (upper raricostatum zone) are dominated by exceptionally abundant Calamnospora (horsetail spores) indicating the nearby development of 'swampy' conditions (Wall 1965).

Hallam (1981) used a variety of lines of evidence from around the globe, including a consideration of continental flooding and facies, to develop a curve of 'eustatic' changes in sea-level (Fig 5.3A). Fine details such as small sea-level falls are confirmed by evidence for small gaps in Dorset in the conybeari subzone and at the top of the reynesi subzone (bucklandi and semicostatum zones respectively) (Section 2.5). The conybeari subzone sea-level drop is also recorded in Avon by the condensed surface of the Calcaria bed and on the Radstock Shelf by a major hiatus (Donovan & Kellaway 1984). There is good agreement between

the 'eustatic' curve and the onlap curve which were developed independently (Hallam 1981). Thus whether Hallam's curve relates to eustatic or the tectonic processes favoured by Donovan et al. (1979), it appears safe to adopt it in order to estimate relative water depths in South Britain using the assumption of near-constant subsidence rates (Fig 5.3A).

Hallam (1960a) and Palmer (1972) used the relative proportion of limestones per unit thickness to correlate different sequences in the basal Lias. Thus it was shown that different ammonite zones are characterised by different relative proportions of limestone, implying that facies exerted a control on the frequency of formation of these diagenetic limestones. In Section 5.1.1 and on Fig 2.8C it was shown that the proportion of limestone in unit thickness of rock was determined by the proportion of light marl during early diagenesis. Donovan et al. (1979) and Hallam (1981) considered that zones with a low proportion of limestone correlate with sediment deposited in relatively deep water and vice versa. This can now be explained in terms of the proportion of different sediment types; when the water was relatively deep, more dark marl and laminated shale was deposited than average so few limestones formed during diagenesis; when the water was relatively shallow, more light marl was deposited so the density of limestones formed during diagenesis was high. Figs 2.8A, 2.8B and 2.8C show the correlation between the density of limestone and the proportion of light marl. The lower planorbis and mid liasicus zones were times of increased deposition of dark marl and laminated shale, which correspond to times of rapid sea-level rise and relatively deep water (Fig 5.3A).

It is emphasized that the decimetre-metre scale regular sedimentary cycles attributed to climatic variations occur throughout the sections

studied in detail (Lyme Regis, Watchet, Lavernock Point and Long Itchington). The average composition of these cycles is what seems to have been affected by changes in water depth over hundreds of thousands of years. Although the changes in the relative proportions of different rock types occurred more or less simultaneously in Watchet and Lyme Regis, the absolute proportion of the different rock types depends on the locality.

The Pre-planorbis Beds to conybeari subzone interval at Lyme Regis consists, on average, of 56% light marl/limestone, 20% dark marl and 24% laminated shale/laminated limestone and is about 18m thick. However, the corresponding interval at Watchet consists of 40% light marl/limestone, 28% dark marl, and 32% laminated shale/laminated limestone and occupies about 89m. In addition, in the angulata zone and conybeari subzone there are many more laminated shale beds at Watchet than at Lyme Regis and Long Itchington which upset the correlation^{observed} in lower zones (Fig 2.8E, Sections 2.8.2, 5.5). Clearly areas of high net sedimentation rate had a greater tendency to accumulate dark marl and laminated shale than areas of low net sedimentation rate. Hallam & Bradshaw (1979), discussing bituminous shales in general, showed that in the Toarcian, bituminous shale associated with the falciferum zone anoxic event (Jenkyns & Clayton 1986) accumulated for longer in areas of higher sedimentation rate. They assumed that areas of expanded sequences corresponded to topographic lows and that topographic lows would have encouraged the development of anoxia. Using their model it can be suggested that local areas of deeper water were associated with relatively high sedimentation rates and relatively high proportions of dark marl and laminated shale. Thus, the unexpectedly large number of uncorrelatable laminated shale beds in the angulata zone and conybeari subzone at Watchet, might

indicate the development of a local topographic depression at the start of the angulata zone (Sections 2.8.2 and 4.3.3b). Hallam & Bradshaw (1979) thought that the topography must have encouraged anoxia via a relationship between stagnation and water depth; an alternative to this explanation is explored below (Section 5.4).

5.4 Models explaining the interbedding of light marl, dark marl and laminated shale.

Any models which link changes in the environment to changes in deposition must account for three aspects of the sedimentation.

1) The progression from light marl to dark marl to laminated shale deposition involved a decrease in bottom-water oxygen levels. This progression was also linked to an increase in the rate of deposition of clay relative to carbonate (Sections 5.2.1 and 5.2.2).

2) The interbedding of the three sediment types can be accounted for by regular orbitally driven climatic cycles. The model must therefore link climatic changes to changes in deposition (Section 5.3.1).

3) Over hundreds of thousands of years there were variations in relative water depth everywhere which affected the average proportions of light marl compared to dark marl and laminated shale within the regular sedimentary cycles. Times of increased water-depth were associated with a greater tendency towards the deposition of dark marl and laminated shale. Additionally, at any particular time, local areas of deep water were associated with greater sedimentation rates and a greater proportion of dark marl and laminated shale than surrounding, shallower areas (Section 5.3.2).

5.4.1 Productivity Model.

The palaeogeographic and palaeoclimatic work of Parrish & Curtis (1982) established that during the Early Jurassic there is no reason to believe that dynamic upwelling would have supplied abundant nutrients and caused very high productivity in Britain. Indeed, there is no evidence at all for very high productivity in the basal Lias; there are no cherts or phosphorites (Jenkyns 1986). This, however, does not exclude the possibility that productivity variations could explain the deposition of the basal Lias.

As dynamic upwelling can be neglected, the two principal sources of nutrients for surface production of organic matter in the sea would have been rivers and currents which stirred up bottom-water and so recycled nutrients from decaying organisms. Therefore, alternations of wet and dry climates caused by orbital-forcing would have induced variation in runoff and thus nutrient supply. Wet phases would have led to high productivity with attendant increases in the supply of organic matter to the sea-floor and the development of anoxia. The high runoff would imply above normal clay supply as well so that organic-rich, laminated and clay-rich sediment (laminated shale) would have accumulated. Dry climates would have involved relatively low rates of clay and nutrient supply so that carbonate contents would have risen by default, anoxia would never have developed and the sediment (light marl) would have been organic-poor, bioturbated and clay-poor.

As it stands this model cannot explain the link between greater water-depths and the tendency towards the deposition of dark marl and laminated shale. To accommodate this omission it is necessary to postulate that nutrients were also supplied by mixing in the water column and that overturn or circulation was greatest in the

deepest water. During times of relatively high sea-level, enhanced circulation would have supplied additional nutrients to the surface from the sea-bed or from mid-water. But it is also necessary to suggest that at any particular time, local areas of deeper water involved greater circulation and, therefore, locally relatively high surface productivity. This extension of the model is unable to satisfy the link between anoxic bottom-waters and increased clay deposition locally. This can be resolved if it is accepted that areas and times of relatively high productivity were associated with a change in the surface eco-systems. Thus during times and in areas of high productivity the plankton might have been dominated by organic-walled organisms such as dinoflagellates; during times and in areas of low productivity the plankton might have been dominated by coccolithophores (Jenkyns pers. comm. 1985). High productivity, locally or across the basin, would then be linked with lower rates of carbonate deposition and vice versa. This model is illustrated in Fig 5.4A.

There is no evidence to support the hypothesis that deeper water was associated with greater circulation and overturn. The only suggestion that bottom-water currents were present comes from the presence of winnowed horizons (Section 2.5) which are far too rare to imply sustained overturning of the bottom-water. It is difficult to reconcile an increase or indeed any clay deposition in local areas with relatively strong bottom currents. And the sub-millimetre clay/organic laminae in the laminated shale are very unlikely to have been preserved where even slight currents were common near the sea-floor. Therefore, if currents did supply nutrients to the surface by vertical mixing, they cannot have affected the sea-floor (except during unusually violent storms and hurricanes); instead nutrients must have been recycled from mid-water.

The laminated shales were mainly deposited under anoxic water, but frequently there was enough oxygen present for a restricted fauna to develop (Section 5.3.1). It is possible therefore, that during the deposition of laminated shales, complete overturn might have occurred in one season only (eg winter). This would have allowed partial oxygenation of the bottom-water and the transportation of nutrients to the surface. During the rest of the year overturn would have been restricted to the middle and upper part of the water-column and high productivity, partially based on the winters supply of nutrients, would have quickly re-established bottom-water anoxicity (McKenzie 1982).

The explanation for carbonate contents decreasing in deeper-water areas implies that clay contents increased in the sediment by default (ie less carbonate was deposited rather than more clay). Yet deeper-water areas were not only associated with more clay-rich sediment than normal, they were also areas of high net sedimentation rate. The power spectral results (Section 4.3.4) show that the wavelengths of the regular sedimentary cycles are greater in expanded sections (ie light marl, dark marl and laminated shale beds have a greater average thickness). So it cannot only be argued that deep-water, expanded sections had less gaps than shallow-water 'condensed' sections; it must also be accepted that the deeper water areas were associated with higher sedimentation rates rather than the lower rates implied by the productivity model.

This objection to the model does not rule out a rôle for productivity variations during the deposition of the basal Lias, but it does show that an alternative explanation is needed to explain some aspects of the depositional regime.

5.4.2 Stagnation Model.

An alternative explanation for the development of anoxic bottom-waters during laminated shale deposition might be that the water column was almost permanently density stratified. One way in which stratification might have developed in an epeiric sea is through the formation of a low-salinity surface wedge during phases of high runoff. Climate and runoff related stratification was proposed for the East Mediterranean in the Pleistocene and sapropel deposition and for epeiric sea black shales deposited in North America in the Cretaceous and Devonian-Carboniferous (Rossignol-Strick et al. 1982, Rossignol-Strick 1983, Barron et al. 1985, Ettensohn & Elam 1985).

Thus when the climate was relatively wet, high runoff would have supplied abundant clay and have caused the formation of a low-salinity surface wedge of water (separated from the water below by a halocline). This density stratification would have led to the development of anoxic bottom-water because the water column would have been prevented from overturning - so laminated shales would have been deposited. Conversely, during dry periods less clay would have been supplied whilst the comparative lack of fresh-water would allow permanent mixing of the whole water column by wind and waves leading to oxygenated bottom-waters and burrowing and hence to the accumulation of light marl.

This model must be refined in order to explain the association of dark marls and laminated marls with deeper water. The development of more anoxia in deeper water would be accounted for if mixing by wind and waves during dry phases was limited to a certain water depth (say 50-100m). Water below the mixed layer would have been still and, if enough organic matter was being supplied, anoxic. This is essentially the Hallam & Bradshaw (1979) explanation for bituminous shale deposition

in general. As it stands, this model does not explain why local deeper water areas had the highest sedimentation rates nor why the local anoxia was linked to local increases in the proportion of clay.

The deposition of clay was not allied to the deposition of zooplankton faecal pellets. Both Honjo (1976) and Porter & Robbins (1981) observed the inclusion of clay minerals and silt in zooplankton pellets as well as organic matter and coccoliths. However, during this study, SEM work (Figs 2.4E and 2.4H, Sections 2.4.3 and 2.4.4) showed that the pellets are almost devoid of entrained clay. As these faecal pellets are much larger than clay mineral particles, even when in colloidal form, it is to be expected that in agitated water the pellets would be deposited more quickly than clay. This is supported by settling rates in still water; zooplankton pellets settle at the rate of 560-2500 $\mu\text{m}/\text{sec}$ and clay settles at 5-50 $\mu\text{m}/\text{sec}$ (Honjo 1976, McCave pers. comm. 1986). Therefore, it is proposed that clay was mainly deposited where bottom-waters were stagnant and therefore anoxic, in agitated water it was mainly kept suspended. This explains the link between organic-matter concentrations and clay concentrations (or the inverse correlation between organic-matter contents and percentage carbonate). In addition it is clear that in pockets of relatively deep water, where bottom-waters were more likely to be stagnant, clay would have accumulated preferentially, so explaining the locally high sedimentation rates. At present there is no reason to suppose that the rate of zooplankton faecal pellet production was related to water depth. As discussed in Section 5.4.1 the restricted benthos in the laminated shales in spite of nearly permanent anoxia (Section 5.3.1), might indicate occasional mixing and overturn of bottom waters during the winter (McKenzie 1982).

There is little direct evidence for the direct involvement of fresh water in the depositional environment in the earliest Jurassic. Field (1965) found three specimens of what were probably fresh-water ostracods at Lyme Regis and the clay itself was probably transported by fresh-water. If it were possible to separate coccoliths from microspar the oxygen isotopes of the surface waters could be investigated, but unfortunately the coccoliths in the light marl and limestone were almost entirely destroyed during diagenesis (Section 2.4). Hallam (1960a) showed that the ammonites were probably stunted during laminated-shale deposition perhaps because of low surface-water salinities. Nevertheless, in spite of the meagre evidence for brackish surface-water, this model satisfactorily explains most aspects of the deposition of the basal Lias sediments.

5.4.3 Stagnation model with productivity changes.

Another possibility is that the stratification model accounts for most aspects of the deposition of the basal Lias. However, during wet phases, productivity might have increased, due to increased runoff, right across the basin causing laminated shale deposition. But as shown earlier, productivity changes cannot explain why deeper water areas were associated with the highest rates of clay deposition. In this model, clay deposition is controlled by bottom-water turbulence and deeper water areas are assumed to have had a greater tendency to become stagnant. There is no evidence for or against this hybrid model at present - but it is emphasized that even in this compromise, stratification related to low-salinity surface wedges and greater water depth is by far the most significant aspect.

5.5 Synthesis: a general environmental model for the deposition of the basal Lias.

It is assumed here that the interbedding of the three main sediment types was controlled by stratification related to runoff and water depths combined with higher productivity during times of increased runoff. Before a general environmental model can be presented, additional factors must be taken into account.

Evidence for hiatuses shows that occasionally bottom-water speeds were great enough to cause winnowing and erosion, perhaps during exceptional winter storms and hurricanes (Section 2.5). Hiatuses seem to be concentrated in the Pre-planorbis Beds and the conybeari subzone and higher in the Lower Lias (Fig 5.3A) when water depths were less than usual and major storms could influence bottom-water circulation more easily (Sections 2.5 and 5.3.2).

The nature of the rocks exposed on land seems to have influenced deposition to some extent. Where carbonate rocks were exposed, limestones formed offshore and, adjacent to exposures of siliceous rocks clay-rich sediments were deposited. Thus round the Carboniferous Limestone islands of Glamorgan and Avon, limestone lithoclasts and 'marginal facies' limestones (the Sutton Stone, Southerndown Beds and Brockley Down Stone) were deposited (Trueman 1922, Donovan & Kellaway 1984). Adjacent to the marginal facies light marl, dark marl and laminated shale accumulated, but because the water was shallow near land, deposition was within the photic zone so algal borers gastropods (partly algal grazers) could survive (Sections 2.2.1 and 2.5). The agitated water was also sufficiently free of clay for solitary corals and bryozoa (Hallam 1960a). Abundant, small bioclastic fragments were supplied by the areas of marginal facies deposition to the nearby

offshore facies (eg at Nash Point and Saltford - Section 2.1.2d, 2.1.2g and 2.2.2).

In most areas the offshore facies was deposited below the photic zone although the presence of clay in the water column may have meant that the photic zone was much less than 200m thick. These sediments were dominated by settled clay, pelagic fossils and coccolith mud thus warranting the description 'hemipelagic' despite accumulation in an epeiric sea (Sellwood pers. comm. 1984, Weedon 1986). Next to large land areas where siliceous rocks were exposed, deltas probably formed. The best evidence for the nature of pro-deltaic deposition might come from the Black Ven Marls in Dorset (Section 5.3.2). Hiatuses and palaeontology point to shallow water and the temporarily close proximity of land, perhaps a delta building out from Cornubia, whilst organic-rich marls and shales accumulated (Whalley 1985). There is no sand in this rock so presumably if a delta was present nearby, it was dominated by clay. Both the Black Ven Marls and the underlying Blue Lias Member on the Dorset coast produced iron-limited pyrite (Raiswell & Berner 1985 - Section 3.4.2b). Iron deposition in the Blue Lias was allied to organic matter contents, perhaps explicable by colloidal iron bound to organic matter. However, in the Black Ven Marls iron was probably associated with the deposition of clay and it certainly was not allied to the deposition of organic matter (Raiswell & Berner 1985). This might be explained by the hemipelagic deposition of the Blue Lias Member as opposed to the pro-deltaic deposition of the Black Ven Marls.

The Black Ven Marls and Shales-with-Beef show little evidence in the field for interbedding and cyclicity (although it is possible that an analysis of TOC throughout the section would reveal compositional variations - Jenkyns pers. comm. 1986). This might partly be explained

by the poor exposure of these rocks. Overlying the Black Ven Marls are the Belemnite Marls which show a very similar interbedding of marls and shales to the Blue Lias Member underneath the Shales-with-Beef. But carbonate contents are higher in the Belemnite Marls and diagenesis is less important (Sellwood 1970a, 1970b - Section 6.5.1). Spectral analysis of the Belemnite Marls (Section 6.5.2) reveals that precession and obliquity variations produced regular sedimentary cycles with very similar wavelengths to the obliquity and precession cycles in the Blue Lias (Sections 4.3.3a and 4.3.4). So the absence of pronounced cyclicity in the intervening rocks must probably be attributed to palaeogeographic rather than palaeoclimatic factors.

The Shales-with-Beef correspond to a phase of rapid sea-level rise and relatively deep water and are associated with a facies change correlated across Europe (Hallam 1981 - Section 5.3.2). Using the stagnation model of Hallam & Bradshaw (1979) and the last Section, it is likely that the deep water led to frequent stagnation and the deposition of dark marls and laminated shales with little light marl. This fits the description of rock types (Lang et al. 1923), but 'conchoidal' marl (? light marl) and a few limestone beds are present so the lack of cyclicity in the field might be more apparent than real. Conversely, as shown earlier, the Black Ven Marls might have been deposited at least partly as pro-delta muds during a regression. At several levels in the Black Ven Marls there are homogeneous limestone beds and nodules as well as laminated limestone nodules such as the Stonebarrow Flatstones. The limestones are separated by interbedded metre-scale beds of laminated shale and dark marl. Sedimentation rates were probably a lot higher than for the Blue Lias Member and Belemnite Marls and the high clay content might account for the apparent lack of cyclicity. Clearly

the development of typical interbedded offshore facies in the early Lias required deposition that was: 1) away from deltas, 2) below fair weather wave-base so that clay and coccolith-rich faecal pellets could be deposited, and 3) in water that was could be entirely overturned during dry periods so that light marls could accumulate.

A summary of the general environmental model developed here for South Britain is presented in Fig 5.5A. Localized areas of relatively deep water were not filled-in in spite of a tendency to accumulate clay in the more frequently stagnant water. This indicates some mechanism was able to maintain the bottom topography and following Sellwood & Jenkyns (1975) and Hallam & Sellwood (1976) this might have been movement on buried faults. At Watchet, large numbers of laminated shale beds, which are not correlated with those elsewhere, occur in the angulata and bucklandi zone only, suggesting local deepening at the end of the liasicus zone (Sections 2.8.2 and 4.3.3b). But as sea-levels were falling or static (Hallam 1981), the amount of laminated shale would be expected to have fallen - therefore Watchet probably subsided relative to the rest of Britain at the beginning of the angulata zone. This interpretation helps explain why the angulata zone and conybeari subzones at Watchet seem to be unusually thick compared to lower zones (Fig 2.5A).

The broad palaeogeographic setting is illustrated in Fig 5.5B (mainly based on Loughman 1982, Smith et al. 1981 and Ziegler 1982). The areas where the offshore facies accumulated (ie Britain, the Low Countries and Germany - Bloos 1982) lay to the North of the Tethys Ocean separated by an area of carbonate platform limestone deposition. To the East and North, coarse clastics (sand and gravel) were supplied by

rivers. To the West lay an area of land (Greenland and North America) separated by little-known sediments now off Portugal and Newfoundland.

The proposal that regional climatic changes account for the cyclicity of the basal Lias involving large variations in runoff can be tested by examination of clastic areas of deposition peripheral to South Britain. Significantly interbedded sandstones and shales or sandstones and limestones in Poland (Pienkowski 1985), Scandinavia (Troedsson 1951) and Scotland (Hallam 1959) are consistent with rapid and considerable variations in runoff. In the Hartford Basin, New England, semi-arid facies reveal expansions and contractions of Early Jurassic playa lakes connected to wet and dry phases (Domicco & Kordesch 1986). And in the Newark Basin nearby, spectral analysis of latest Triassic cyclic lake facies reveals variations in the lake levels related to the precession, obliquity and eccentricity cycles (Olsen 1986).

As yet it is not possible to develop a detailed model for the nature of climatic variations in Britain. Wet and dry periods seem to have alternated in an area that overall probably received moderate rainfall (Parrish et al. 1982). It is possible that the north margin of Tethys had a monsoonal climate as developed in central North America during the Cretaceous (Barron et al. 1985). This requires a large area of land developing low pressure to the north of a large area of sea with high pressure in mid to low latitudes (Barry & Chorley 1982). In such a case precession and variations in obliquity, which affect the distribution of insolation in a latitudinal sense, might have caused variations in the intensity of monsoonal rainfall (eg Rossignol-Strick 1983, Barron et al. 1985). This is no more than a tentative explanation for the hypothesized climatic variation; only the use of realistic General Circulation Models

will provide a firm basis for reconstructing climatic changes (Barron et al. 1985).

5.6 Conclusions.

1) Burrow mottling, petrography, organic-carbon contents (carbonate-free) and palaeontology all indicate that three distinct sediment types of the offshore facies were interbedded on the sea-floor during the Early Jurassic in South Britain. The progression from deposition of light marl to dark marl to laminated shale represented the development of anoxia in the bottom-water. This affected the benthos, infauna, petrography and organic-carbon contents. The percentage of clay was linked to the amount of organic matter accumulated. SEM observations indicate that substantial numbers of tightly packed coccolith aggregates are present in the dark marl and laminated shale. The aggregates probably represent zooplankton faecal pellets and their neomorphism seems to have produced the microspar blebs of the laminated shale and dark marl. Microspar dominates the carbonate of the 'offshore facies' and is believed to have been mainly formed from coccoliths by aggrading neomorphism. The dominance of coccoliths, pelagic macrofauna and clay in the sediments, shows that deposition can be considered to be hemipelagic, albeit in an epeiric sea. Deposition was mainly under the photic zone (there is a lack of evidence for algae and their borings) and under the average storm-wave base (as clay and faecal pellets were able to accumulate). Oxygen isotopes in Gryphaea arcuata indicate an average palaeotemperature of 15°C ($\delta^{18}\text{O} = -0.85$ per mil).

2) Limestone beds and nodules were formed by early diagenetic cementation of light marl horizons. Likewise, laminated limestone beds

and nodules were formed by early diagenetic cementation of laminated shale beds. The most important aspects of diagenesis^{are} as follows (more details in Section 5.1.3). Early diagenetic cementation started immediately after the start of sulphate reduction and pyrite formation. Pyrite formation was iron-limited with iron^{contents} linked to organic-carbon contents. Limestone and laminated limestone beds were created by carbonate cementation of pore-space. The main control of cementation within limestone and laminated limestone beds was probably primary carbonate content. During the latter phases of sulphate reduction, compaction accompanied the formation of limestone and laminated limestone nodules. This was followed by aggrading neomorphism of micrite and coccoliths in all rock types, forming microspar. At the end of sulphate reduction and the beginning of fermentation, beef calcite was formed at the base of laminated shale beds - perhaps as a response to over-pressuring. Compaction continued after the formation of the beef.

3) Hiatuses seem to have been formed at many levels and at all locations in the offshore facies. Some may have resulted from winter storms of exceptional strength and/or hurricanes. Power spectral results (see below) indicate that the sections studied are probably all about 20-40% complete at best - implying similar water depths across the whole basin. The limestone bed called the Calcaria Bed in Avon, can probably be traced over at least 2750km². As it is correlated over such a large area, the evidence of erosion it contains is more easily explained through a eustatic fall in sea-level in the conybeari subzone (Hallam 1981) than through some form of storm process.

4) Walsh power-spectral analysis of the basal Lias at a number of localities indicates that the interbedding of the marls and shale involves regular cycles. Wavelengths of the regular cycles are larger in expanded sections (representing areas of higher net sedimentation rate). The stability and duration of the regular cycles is explicable in terms of climatic variations induced by changes in orbital precession (21kyr period) and obliquity (41kyr period) (Section 6.9 for more spectral conclusions). Ice appears to have been absent from the globe during the Jurassic (Frakes 1979) so glacio-eustatic sea-level variations cannot explain the regular cycles; therefore a regional rather than global explanation is required. Individual laminated shale beds can be correlated for a distance of at least 200km which supports regional climatic changes rather than a tectonic explanation. Early Jurassic, interbedded sandstones and shales, and sandstones and limestones in Poland, Sweden and Scotland demonstrate frequent and very widespread changes in runoff. And recent results from lake-level cycles in New England (Domicco & Forbes 1986) and Newark (Olsen 1986), support the suggestion that in the Early Jurassic humidity varied in relation to orbital-forcing in other areas than Britain.

5) Two main factors controlled the interbedding of light marl, dark marl and laminated shale: regional climate and water-depth.

Orbitally-controlled regional changes in runoff affected density stratification across the whole basin (cf. Barron et al. 1985). Dry phases were associated with light marl deposition as the water column remained mixed, the turbulence tending to keep clay suspended and the bottom-water oxygenated. During wet periods, a brackish wedge caused widespread density stratification. The stagnant bottom-water enabled

increased clay settling and anoxia to develop so laminated shale was deposited. It is possible that the increased runoff during wet periods promoted surface productivity and therefore encouraged bottom-water anoxicity.

Above average water-depths encouraged bottom-water stagnation and anoxia (cf. Hallam & Bradshaw 1979). Pockets of deep water were associated with above average subsidence and sedimentation rates. These deep water pockets developed stagnant bottom-water so that even during dry periods laminated shale accumulated locally. At Watchet for instance, all the zones are relatively thick, but unusually thick developments of the angulata and bucklandi zones are associated with abnormally large numbers of uncorrelatable laminated shale beds. So Watchet probably represented an area of relatively rapid subsidence which deepened significantly at the beginning of the angulata zone, perhaps as a result of faulting.

Times of relative sea-level rise caused the development of relatively deep water across the whole basin and increased average proportions of dark marl and laminated shale. So when sea-levels were high, stagnation and anoxia developed earlier than normal during the transition from a dry to a wet climate.

CHAPTER 6

WALSH POWER SPECTRA FOR VARIOUS OPEN-MARINE SEQUENCES

AND POWER SPECTRAL CONCLUSIONS.

6.1 Introduction.

This chapter is devoted to the Walsh power-spectral analysis of a variety of 'cyclic' open-marine formations from several Systems. In all cases the sections involved were studied in the field by the author, but the stratigraphic log for the Boom Clay Formation was provided by Prof. N.Vandenberghe of the Catholic University of Leuven, Belgium. All the measurements used are compiled in the Appendix for this chapter.

The sedimentology of these formations was not investigated in detail as in most cases much has already been published. Each formation is treated in reverse stratigraphic order with an introduction to the sedimentology and stratigraphy followed by spectral analysis. The methods used in spectral analysis are set out in Chapter 4 where a 'significant' peak was defined as one distinguishable from white and/or red noise and which can be detected in both halves of the time series. The end of this chapter is given over to a discussion of the spectral results in general and to conclusions.

6.2 Boom Clay Formation (Lower Oligocene), Belgium.

6.2.1 Introduction.

The sedimentology, diagenesis, and geochemistry of the Boom Clay was first studied in depth by Vandenberghe (1978). The formation is Rupelian in age and is exposed in a large number of brick pits and on some river banks (eg. the River Rupel) (Fig 6.2A). Vandenberghe split the formation into three members and was able to correlate individual beds over an area of 500km² (now extended into the Netherlands and the lower Rhine in Germany) (Vandenberghe 1978, Gullentops & Vandenberghe 1985).

The most important rock types are the ubiquitous silt and clay which form beds centimetres to decimetres thick with plane but gradational

contacts (Fig 6.2A). Certain horizons within the clay beds are black with detrital woody organic matter. Because these organic-rich horizons are frequently found where clay beds are succeeded by silt beds, the deposition of organic matter as well as the clay and silt, might be related to turbulence in the bottom-water (see below) (Vandenberghe 1978). At irregular intervals, in both silt and clay beds, calcareous horizons occur without relation to grain size or organic matter. The calcareous horizons contain septarian limestone nodules (named S1-S11). Coccoliths and foraminifera preserved in the calcareous horizons allow dating. The fossils are dominated by bivalves (preserved in situ in the limestone nodules) and occasional burrow-mottles of Chondrites can be seen within some silt beds and on the surface of some nodules in the field, but X-rays have revealed many more (Vandenberghe 1978). These rocks have suffered little diagenesis as total overburden never exceeded 100m (Vandenberghe & Laga 1986). The grain-size analysis and burrow mottling indicate a primary alternation of clay and silt. The current calcareous horizons appear to represent primary carbonate-rich horizons where precipitation formed limestone nodules during diagenesis (Vandenberghe & Laga 1986). Conversely the intervening rock has suffered a certain amount of carbonate dissolution.

The range of grain-sizes is the same in clay and silt beds, but the modal grain-size depends on the rock type (Vandenberghe 1978). As coarser grains were available from the source area and the grain-size range is constant, the clay/silt alternations cannot have arisen from variations in the strength of currents supplying the sediment or in the source of sediment (Vandenberghe 1978). Instead the alternations probably indicate variations in the turbulence of the bottom-water. It has been suggested that water-depths were controlled by tectonism or

glacio-eustatic sea-level changes which determined bottom-water turbulence and hence the sediment composition (Gullentops & Vandenberghe 1985).

6.2.2 Spectral Analysis.

The stratigraphic log supplied by Prof. Vandenberghe is actually a composite from four pits and one bore-hole (Fig 6.2B) with beds measured to the nearest centimetre. Because the origin of the calcareous and organic-rich horizons is not clear, two sets of codes have been employed. These are: clay=-1.0, calcareous clay=-0.5, black clay=0.0, calcareous silt=+0.5 and silt=+1.0 and alternatively: clay=-1.0, calcareous clay=-1.0, black clay=-1.0, calcareous silt=+1.0 and silt=+1.0. The coccoliths indicate biozones NP22-23 and the lower part of NP24, whilst the foraminifera indicate zones P18-20 and perhaps P21 (Gullentops & Vandenberghe 1985). Using the most recent time-scale for the Palaeogene (Berggren et al. 1986) this indicates a duration of 5.8Myr (35.0-29.2Ma) and as the composite log is 58.91m thick, the sedimentation rate ^{was} 1.016 cmkyr^{-1} . The very close correspondence of stratigraphy in widely spaced pits and the uniformity of bed thickness suggests that the formation is virtually free of hiatuses (Vandenberghe pers. comm. 1986).

Comparison of the spectra of Fig 6.2C and 6.2D reveals remarkable consistency despite the different codes used. A similar result was found for the basal Lias at Long Itchington reported elsewhere (Weedon 1986 Section 4.3.1). The similarity of the spectral shapes shows that the broad classification of rock types (or zero-crossing by code values) is much more important than the details. For the basal Lias the broad classification was based on the texture (homogeneous or laminated)

whereas for the Boom Clay it was based on the grain-size of the rocks (silt or clay).

Regardless of the choice of code values, three peaks are considered to be significant with wavelengths of 141, 111 and 93cm (Figs 6.2C & 6.2D). With two codes (Fig 6.2D) an extra peak of 205cm is significant, it is fairly well developed on the five code spectrum, but it is unstable according to the corresponding subspectra. At present it is assumed that only the peaks common to spectra generated with both sets of code values can be considered significant.

The sedimentation rate and lack of hiatuses suggests that the regular cycles have periods of about 137, 109 and 92kyr. These periods are simply explained as components of the modern variation in eccentricity (136, 109, 95kyr - Berger 1977). Peaks of 49cm (~48kyr) and 19cm (~19kyr) are strongly developed. Using their estimated periods, these peaks may correspond to obliquity and precession cycles. Yet the subspectra show that they are only significant in the lower part of the time series. Shorter time series could be used to trace the changing spectral contributions of these components.

The spectral analysis provides strong evidence for eccentricity variations forcing sedimentation. Such a scenario would be expected for a glaciated globe as Pleistocene records also reveal much greater importance for the 100kyr peak than that predicted by the Milankovitch Theory (Hays et al. 1976). Shackleton (1986) recently reviewed the isotopic evidence for a phase or phases of limited glaciation during the Early Oligocene. Glacio-eustatic changes apparently had a range of less than 40m. The depth of the shelf during deposition of the Boom Clay was probably 50m or more (Vandenbergh 1978). Therefore the variation in bottom-water turbulence which seems to have caused the silt/clay

alternations may well have been controlled by glacio-eustatic sea-level changes. If the precession and obliquity components of orbital variation did contribute to the cyclicity, then the subspectra suggest that their relative contributions changed significantly between the bottom and the top of the Boom Clay. Such changes in the importance of spectral peaks have also been reported for the Pleistocene (eg Ruddiman et al. 1986).

6.3 Upper Kimmeridge Clay Formation (Upper Jurassic), Dorset, England.

6.3.1 Introduction.

A very extensive literature exists for the Kimmeridge Clay partly because it represents the principal source-rock for North Sea oil. The formation has been correlated bed by bed from Norfolk to Dorset; similar facies are recognised everywhere in South Britain, but the overall thickness changes substantially from place to place (Gallois 1976, Cox & Gallois 1980).

The main rock types are calcareous mudstone (sometimes called 'clay'), bituminous shale, oil shale, coccolith limestones and dolomitic limestone beds and nodules (Fig 6.3A). The dolomitic limestones formed during early diagenesis and mostly represent calcareous mudstone in which case they are homogeneous and weather into 'dicey' fracture surfaces. In two cases internal lamination reveals an origin by cementation of bituminous shale (Cox & Gallois 1980). Irwin (1980) discussed the diagenesis of the dolomitic limestones and Irwin et al. (1977) investigated the isotopic evolution of the pore-waters generally.

The calcareous mudstone is homogeneous and contains a fairly abundant, low diversity benthos; organic contents range up to 4% TOC, with up to 42% CaCO₃ (Tyson et al. 1979, Cox & Gallois 1980, Farrimond

et al. 1984). ^{The} Bituminous shales' (<30% TOC, <25% CaCO₃) macrofauna is rarer than in the calcareous mudstone, and lamination is preserved. The oil shales, in common with the closely associated coccolith limestones, have lamination preserved and very rare benthos; they also have very high organic-carbon contents (<57% TOC, <30% CaCO₃) (Tyson et al. 1979, Farrimond et al. 1984). Bed contacts are usually sharp and planar but the contact between calcareous mudstone and bituminous mudstone can be gradational over about 4cm stratigraphic thickness. This has probably introduced measurement errors (Section 4.2.5e), but compared to the thickness of most beds this is unlikely to have affected spectral peaks corresponding to wavelengths of more than 50cm. Excluding the dolomitic limestones, the different rock types are likely to represent sediments with distinct primary compositions considering the occasional burrow mottling between oil shale and coccolith limestone beds and the homogeneity of the calcareous mudstone. The oil shales and bituminous shales have overlapping values for %TOC, but they weather very differently with oil shales lacking the fissility of bituminous shales and standing proud of them on weathered sections.

There has been some controversy over the environmental significance of the different rock types. Gallois (1976) suggested that mainly oxygenated bottom-waters prevailed with occasional algal blooms lowering oxygen contents somewhat and allowing enhanced preservation of organic matter ^{so} forming oil shales. Occasional coccolithophore blooms were thought to have generated the coccolith limestones. Tyson et al. 1979 preferred a stagnant basin model analogous to the Black Sea. Thus the sequence: calcareous mudstone - bituminous shale - oil shale - coccolith limestone, was thought to indicate the development of anoxic bottom-waters during stagnation and the rise of anoxic water in the

water column. The coccolith limestones were believed to indicate coccolithophore blooms formed when nutrient-rich bottom-water was stirred to the surface causing enhanced productivity.

Irwin accepted most of the Tyson et al. model, but suggested that coccolith limestones formed under oxygenated bottom-water whilst previously anoxic water was stirred to the surface. Farrimond et al. 1984 showed through an organic geochemical study that the organic matter supply was dominantly algal regardless of sediment type. The preservation of certain types of molecules was taken to indicate that the calcareous mudstone was deposited in oxygenated bottom-water whereas the bituminous shale, oil shale and coccolith limestones accumulated in anoxic bottom-water. This supported all aspects of the model of Tyson et al.. Tyson and colleagues suggested that thermoclines rather than haloclines were responsible for stagnation and that these combined with local subsidence, productivity or climatic variations to generate the interbedded sequence. Dunn (1974) used Fourier power-spectral analysis of a 20m section centred on the Blackstone Band (Fig 6.3B) and showed that cycles of 10m, 4m and perhaps 1.43 and 1.05m were related to orbital-forcing of sedimentation. Hallam & Bradshaw (1979) and House (1985) also suggested that Milankovitch-cycles were involved.

The section measuring undertaken for this study is based on the detailed log provided by Cox & Gallois (1980). This log was compared in the field with the rocks and was found to correspond very closely in most cases. In some beds recorded as undifferentiated mudstone, thin bituminous shales were recognised and incorporated into the amended log. Every bed was remeasured (Appendix Section 6.2) to the nearest centimetre although gradational contacts were a problem in some cases. It proved impossible to remeasure the thickness of the calcareous

mudstone bed underneath the Basalt Stone Band so the thickness indicated on the published log was used. The type section for the Upper Kimmeridge Clay Formation was measured between Kimmeridge Bay and just east of Freshwater Steps (Grid Ref.s: SY908791-SY955771) (Cox & Gallois 1980). The following allows a comparison of the zonal thicknesses measured here with those of Cox & Gallois (1980):

Ammonite Zone	Thickness: Cox & Gallois 1980	Thickness: This Study	%Difference
<u>P.pectinatus</u>	4530cm	4100cm	-9.5%
<u>P.hudlestoni</u>	4915cm	4903cm	-0.2%
<u>P.wheatleyensis</u>	2785cm	2630cm	-5.6%
<u>P.scitulus</u>	1945cm	2137cm	+9.9%
<u>P.elegans</u>	2100cm	2206cm	+5.1%

6.3.2 Spectral Analysis.

The environmental model of Tyson et al. (1979) was adopted here and using their environmental extremes leads to the following coding: calcareous marl=+1.0, bituminous shale=-1.0, oil shale=-1.25, coccolith limestone=-1.5. The dolomitic limestone beds form only a small part of the succession and were coded according to their origin as cemented calcareous mudstone (most examples) or cemented bituminous shale (the Yellow Ledge Stone Band and Blake's bed 42). Section 6.2.2 showed that spectral results are largely independent of the details of rock type classification so the dolomitic limestones have not been given separate codes and their thicknesses are left unadjusted (Section 4.3.4). Cox & Gallois (1979) distinguished undifferentiated and calcareous mudstone; except where thin bituminous shale beds were recognised, the undifferentiated mudstone was classified as calcareous mudstone.

It is apparent from Fig 6.2B and the thicknesses quoted above, that the lower three ammonite zones are much thinner than the upper two and that, more importantly, the mean thickness of beds in the upper two zones is much larger (ie. the section cannot be considered to be 'stationary'). This suggests that the sedimentation rate changed from the lower to the upper part of the Upper Kimmeridge Clay. There is no clear evidence for hiatuses in the section to date so the change in sedimentation rate might be related to subsidence rates or a change in the rate of supply of sediment. Because the section is clearly not stationary, the spectral analysis was conducted on two halves of the section. The mean thickness of the lowest three ammonite zones combined with the assumption that each zone represents 1Myr (Section 4.2.6e), yields an average sedimentation rate of 2.32 cmkyr^{-1} . Similarly for the top two zones the mean sedimentation rate is 4.72 cmkyr^{-1} .

The top part of the section contains two significant peaks with wavelengths of 910 and 122 cm (Fig 6.3C). The bottom part of the section also contains two significant peaks of 546 and 158 cm (Fig 6.3D). These two peaks cannot be immediately related to the peaks in the higher part of the stratigraphy. Thus although the mean sedimentation rate increased two-fold, the 910 cm cycle in the upper data is only 1.7 times larger than the 546 cm cycle in the lower data. Further the 122 cm cycle detected higher-up is actually shorter than the 158 cm cycle found lower-down.

There is good agreement between Dunn's (1974) results and the results for the lower part of the section derived in this study. This is in spite of the fact that Dunn used a Fourier instead of the Walsh transform and his section only spanned 20m (compared to about 82m used here). His 4 m peak is represented by the 546cm peak of this analysis here and his 1.43 and 1.05m peaks correspond to the 158 cm peak detected here.

Dunn's 10m cycle may correlate with a fairly well developed peak of about 10m recorded on Fig 6.3D although this seems to be unstable when the subspectra are compared. Dunn also suggested that either a 20m cycle or a trend was present; the lack of a 20m peak here and the presence of very strong low-frequency power supports his latter interpretation. He used a sedimentation rate of 10 cmkyr^{-1} , but the number of ammonite zones has since been increased in the Kimmeridgian Stage (Cox & Gallois 1980).

The 910cm and 122cm cycles have a wavelength ratio of about 7.46 which is closest to that of the 410 and 41kyr orbital cycles (10.0). Yet the resolution of the spectra is so high that it must be admitted that the expected and observed ratios are very poorly matched. Likewise the 546cm and 158cm cycles have a wavelength ratio of 3.46 which cannot easily be reconciled with the main orbital cycles. Although the dating from the sedimentation rates may well be inaccurate, the regular cycles detected occupy the range of cycle periods (500-10kyr) which suggests that orbital forcing can be invoked. Assuming that these regular cycles do not arise from some regular tectonic or unknown process (Section 6.8.2), and that they are related to one of the main orbital cycles described from the Pleistocene (410, ~100, 41, 21kyr), some process seems to have altered the wavelength ratios. One possibility is that as yet undetected minor hiatuses have been able to change the relative position of peaks on the power spectra by acting as a kind of filter applied to the originally complete time series (Coe pers. comm. 1986) (Fig 4.2B and Section 4.3.4).

The regular cycles detected here have been dated by assuming that the present wavelength ratios are closest to particular orbital-cycle wavelength ratios and by accepting the dating constraints. Thus for the

bottom

spectrum the 546cm peak has an implied period of 100kyr and the 158cm regular cycle represents 41kyr. The upper part of the section seems to involve regular cycles with durations of 410kyr (910cm) and 41kyr (122cm).

It is not clear why the top and bottom of the section should record obliquity in both cases, but different eccentricity components. This might indicate some sort of change in the nature of climatic variation, or in the nature of sedimentation, or both. House (1985) suggested that obliquity was dominant in the cyclicity of the Kimmeridge Clay although he alluded to eccentricity components as well. This agrees with the present results in that obliquity is more consistently developed than eccentricity, but the variance (power) associated with eccentricity cycles is greater though overall the trend component contains the bulk of the variance.

6.4 Middle Pliensbachian-Toarcian of Breggia Gorge, Ticino, Switzerland.

6.4a Introduction.

In Breggia Gorge near Morbio Superiore, Canton Ticino, in the Southern Alps, is a well exposed section through a pelagic facies of the Lias. The stratigraphy and biostratigraphy are summarized by Bernoulli (1964) and Wiedenmayer (1980). Overall the sequence is dominated by various expressions of limestone/marl alternations with an independent and long-term variation in the oxidation state of the iron oxides present (as revealed by the colour of the rocks). The position of the different parts of the sequence that were measured in this study are indicated in Fig 6.4A and each part is treated separately below. The

possibility of orbitally forced sedimentation does not seem to have been considered previously.

6.4.2 Toarcian Section: Introduction.

Limestone and marl beds are interbedded in beds centimetres thick with sharp, planar contacts. Two slumps punctuate the sequence and suggest some form of palaeoslope (Fig 6.4A). Towards the top of the section the limestones are grey with occasional burrow-mottling. The limestones contain occasional chert nodules whilst the shales have infrequent limestone nodules. Below the lower slump most limestones are pink and the marls red/purple with green reduction spots (Fig 6.4B). Certain parts of the Rosso Ammonitico Lombardo, as it is called, are particularly clay-rich (eg Bernoulli's bed 3, Fig 6.4C) and below the limestone/marl alternations are red and white mottled marls.

In the lowest part of the Toarcian section bed contacts are gradational because of intense burrowing. The mottled marl at the base of the section might represent limestone/marl alternations which have been largely homogenised by burrowers. It is difficult to explain why limestone beds only 1cm thick should have survived burrowing and are now preserved higher in the section. Burrowing was not inhibited by anoxia as there is no lamination preserved and organic matter is preserved in negligible quantities judging from the the colour of these rocks. The mottled marl represents the falciferum zone which is usually developed as black shales elsewhere; isotopic evidence, even from Breggia Gorge, suggests that this was an ocean-wide event (Jenkyns & Clayton 1986). Therefore it is suggested here that normally in the Toarcian productivity was so low, and oxygen-levels so elevated, that too little organic-matter was present in the sediment to sustain an active infauna.

However, during the falciferum zone productivity increased substantially and enough benthos was present to thoroughly mix what would have been limestone/marl alternations and leave a mottled marl.

6.4.3 Toarcian Section: Spectral Analysis.

The section was measured to the nearest centimetre and the rocks given the codes: marl=-1.0, limestone=+1.0. The slumps were subtracted from the section before analysis. Bernoulli (1964) indicated that beds 2-9 represent 1378cm whereas here they represent 1600cm (+16.1% difference). This part of the sequence contains four ammonite zones which span 2034cm as measured in this study (Fig 6.4A & 6.4C). Assuming that each ammonite zone represents 1Myr (Sections 4.2.6e), this yields a sedimentation rate of 0.509 cmkyr^{-1} .

Three peaks seem to be significant on Fig 6.4D. The 57cm peak has been accepted as significant because although it is indistinguishable from white noise at the 95% level, it can be distinguished from red noise and it is stable according to the subspectra (Section 4.2.4). The dating suggests that regular cycles with periods of less than 112kyr are involved. The wavelength ratio of the 57 and 14cm peaks is 4.07 which is fairly close to that expected for orbital cycles of 100 and 21kyr. On the other hand the 57 and 18cm peaks (wavelength ratio=3.17) are not easily explained by orbital cycles of 100 and 21 or 100 and 41kyr. One possibility is that the 57cm and 14cm regular sedimentary cycles represent orbital cycles of 100 and 21kyr and that the 18cm peak is a difference tone produced by the other peaks (ie $1/18 \approx 1/14 - 1/57$) (Section 4.2.5c). Alternatively, the wavelength ratios observed would fit with the 57, 18 and 14cm cycles representing periods of 100, 30 and 21kyr. This would agree with results from the basal Lias of Britain

(Section 4.3.4) and for the Middle Pliensbachian section results for Breggia Gorge (Sections 6.4.7 and 6.8.2).

6.4.4 Upper Pliensbachian Section: Introduction.

The section represents the top part of the Morbio Formation and although it is often described as 'Ammonitico Rosso facies' the rocks are quite different from the Rosso Ammonitico Lombardo. The limestone beds (decimetre-scale) are much thicker than the intervening marls (centimetre to millimetre-scale) (Figs 6.4E and 6.4F). The contacts are exceedingly sharp and planar. There are no cherts, limestone nodules or stylolites, but ammonites are comparatively common. Occasional Chondrites' burrow-mottling provide evidence against a purely diagenetic origin for these alternations. The top part of the section contains yellow-weathering limestones and green marls whereas the rest consists of pink limestones and red marls.

6.4.5 Upper Pliensbachian Section: Spectral Analysis.

The section was measured to the nearest millimetre because many marl beds are only a few millimetres thick. The codes used were: marl=-1.0, limestone=+1.0. Wiedenmayer's beds 1000-1115 were measured by him as spanning 1386.4cm, in this study they occupied a total of 1353.3cm (-2.4% difference). The gibbosus - hawskerense subzones from which the main time series was derived (Fig 6.4F), represent a combined thickness of 871.4cm as measured here. These subzones span 1.333Myr if the gibbosus subzone (one of three subzones in the margaritatus zone) occupies 333kyr. This implies a sedimentation rate of 0.654 cmkyr^{-1} .

In Fig 6.4G no peaks to the left of the <20kyr limit appear to be stable. The most likely reason for this is that, using the thickness of

the margaritatus, spinatum and tenuicostatum zones (Fig 6.4A), the sedimentation rate was decreasing rapidly during the Upper Pliensbachian. This means that if any regular process (in time) was controlling the limestone/marl alternations, the beds would become progressively thinner and regular cycles could not be preserved as such (Section 4.2.6b). Support for this idea comes from an inspection of the time series (Fig 6.4F) which shows some decrease in average bed thickness towards the top of the section. The very strong asymmetry in the thickness of limestone compared to marl beds may have introduced a large number of harmonics as well (Section 4.2.5b) - adding to the 'noisy' appearance of the spectrum.

6.4.6 Middle Pliensbachian Section: Introduction.

This part of the sequence in Breggia Gorge is characterised by what appear to be fairly regular alternations of decimetre-scale white limestone beds and centimetre-scale green 'shale' but, occasionally, white 'marl' beds split limestone beds (Figs 6.4H and 6.4I). The limestones often contain chert nodules or bands. Rarely the limestone beds are discontinuous with rounded, perhaps nodular, terminations separated by white marl (Fig 6.4H). There is no good evidence for a primary distinction of the various rock types. However, the occurrence of cherts limited to the centre of limestones may indicate primary chert beds or the migration of silica to more calcareous horizons prior to limestone cementation. This and the presence of undoubtedly primary alternations in the overlying rocks is taken as support for the primary distinction of the present rock types.

6.4.7 Middle Pliensbachian Section: Spectral Analysis.

The section was measured to the nearest centimetre and the beds were coded: shale=-1.0, marl=0.0, limestone=+1.0. Beds 931-980 of Wiedenmayer were recorded as spanning 1627cm by him and 1583cm here (-2.7% difference). The davoei zone is 1113cm thick and suggests that the sedimentation rate was 1.11 cmkyr^{-1} .

Two regular sedimentary cycles of 256 and 49cm wavelength appear to be stable and are distinguishable from red and white noise. There is a peak at 85cm which appears to be stable and is distinguishable from white noise, but not from red noise (at the 95% level of confidence). Considering the wavelength ratio and dating constraints, the 256 and 49cm cycles probably correspond to orbital cycles of 100 and 21kyr respectively. The same 2 orbital cycles were apparently recorded in the Toarcian Section and even their relative power seems have remained more or less the same. The wavelength ratio of the 85cm cycle with the 256 and 49cm cycles is consistent with a period of about 30kyr. A 30kyr period has been suggested for the 18cm cycle in the Toarcian Section of Breggia Gorge and for the basal Lias of South Britain (Sections 4.3.4 and 6.8.2).

6.5 Belemnite Marls (Lower Jurassic), Charmouth, Dorset, England.

6.5.1 Introduction.

The Belemnite Marls (Lower Pliensbachian) are exposed near Charmouth and have recently been referred to as the Stonebarrow Marl Formation (Phelps 1982). The lithostratigraphy and biostratigraphy have been discussed by Lang (1928) and Sellwood (1970a & b). Argillaceous calcilutite (50-80% CaCO_3), calcareous clay (30-60% CaCO_3) and bituminous calcareous shale form the three rock types (Sellwood 1970a &

b). Despite the difference in percentage carbonate, the calcilutite and clay bear a remarkable similarity to the light and dark marl of the Blue Lias Member at Lyme Regis (a few kilometres along the coast) which led Sellwood to suggest that the Belemnite marls underwent less diagenetic modification than the basal Lias (Fig 6.5A). However, the lack of early cementation has meant that aragonitic fossils are not usually preserved; leaving few body fossils except belemnites and crinoid debris which are concentrated in storm scours at the top of calcilutite beds (Sellwood 1970a). Bioclasts are more common in the calcilutites and Schizosphaerella-like structures (Section 2.4) embedded in microspar and clay have been observed with the SEM by Sellwood (1970a). Contacts between the beds are usually sharp, burrow-mottling between the calcilutite and clay is very common and the bituminous shales are laminated, indicating that the three rock types represent three original sediment types (Fig 6.5A) (Sellwood 1970b).

Two explanations have been advanced for the transition from bituminous shale to clay to calcilutite (Sellwood 1970a & b). Either turbulence increased progressively so that the bituminous shale accumulated in stagnant water whilst the bioclast-rich ('coarser') calcilutite accumulated in agitated water with scouring and a trace-fossil assemblage different from the clay, or facies belts of clay-rich (near-shore, shallower) and carbonate-rich (off-shore, deeper) sediments migrated back and forth across the area. Thus the interbedding was attributed to water-depth variations with an assumed tectonic origin (Sellwood 1970b). However, a climatic explanation for the interbedding of the rock types is also possible (Sellwood pers. comm. 1986). Thus, the turbulence of the bottom-water might have been related to orbitally-controlled variation in the strength and frequency of storms.

Or alternatively, if the analogy with the basal Lias is used, a density stratification and/or productivity model might be suggested (Sections 5.4 and 5.5).

6.5.2 Spectral Analysis.

The section was measured to the nearest centimetre. The codes were chosen to be analogous to the basal Lias so that: bituminous shale=-1.0, calcareous clay=0.0, and argillaceous calcilutite=+1.0. Lang's beds 110b-117 (Fig 6.5B) are 995cm thick according to Sellwood (1970a; Fig 3) and 981cm thick in this analysis (-1.4% difference). The brevispina and jamesoni subzones (Sellwood 1970a; Table III) are 690cm combined and dividing by 0.5Myr ^{as} (there are four subzones in the jamesoni zone) leads to a sedimentation rate of 1.380 cmkyr⁻¹.

Two peaks are considered to be significant on Fig 6.5C, representing regular cycles 114 and 49cm long. A well developed peak corresponding to a 341cm cycle is present, but it cannot be decided from the subspectra whether this peak is stable. The wavelength ratio of the 114 and 49cm cycles is closer to that expected for the 100 and 41kyr orbital cycles, but although admittedly crude, the dating suggests that the 114cm cycle represents less than 83kyr. So instead it is suggested that these peaks correspond to the 41 and 21kyr cycles. If this interpretation is correct the 100kyr orbital component would be expected to produce a cycle of around 256cm which, considering the bandwidth, is close to the peak with a wavelength of 341cm. Section 6.8.3 discusses the similarity between this spectrum and that for the basal Lias at Lyme Regis.

6.6 'Siliceous Shales' (Lower Jurassic), Robin Hood's Bay, Yorkshire, England.

6.6.1 Introduction.

The 'Siliceous Shales' (Upper Sinemurian) at present form an informal division of the Redcar Mudstone Formation (Powell 1984). This sequence of rocks from the oxynotum - raricostatum zones (Table 1B) accumulated at the same time as the Black Ven Marls of the Dorset Coast (Section 5.5). The rock types are divided into argillaceous sandstone, silty sandstone, silty shales and mudstones and the sedimentology was considered in detail by Sellwood (1970a & b).

The argillaceous sandstones have sharp, planar or undulose (burrowed) upper contacts, occasional pyrite nodules and ferroan carbonate cement (Section 3.4.3c, Fig 6.6A). The sand grains are fine or very fine in grade and well-sorted, but they have been mixed with silt and clay. The lower contact is gradational over a few centimetres at most. The burrow-mottling of the sands includes vertically retrusive Rhizocorallium (Sellwood 1970b). The silty sands and mudstones have siderite nodules and gradational or sharp contacts where they overlie each other. Sandstone-filled scours, (Fig 6.6A) which occur in all lithologies, are approximately circular in plan, 50-120cm wide and up to 24cm deep, and have symmetrically rippled tops and basal lags. They probably indicate storms, and as they sometimes occur at particular levels, they might indicate gaps in the succession (Sellwood 1970a).

Two models proposed by Sellwood (1970b) involve explanations for the 'coarsening upwards cycles' which suggest changing water-depths. Firstly it was suggested that gradual shallowing during the transition from mud to sand accumulation led to increased turbulence and a particular trace-fossil assemblage. Rapid deposition of sand produced vertically-retrusive Rhizocorallium and Pholadomyids. Fines were removed by the increased turbulence, although to some extent burrowers mixed the

silt and clay with the sand. Alternatively, it was suggested that the mudstone accumulated rapidly in a fairly near-shore setting until increasing water depth led to greater current speeds and therefore turbulence. It was implied that sand deposition occurred intermittently from rip currents from coastal areas before being mixed with the silt and clay by burrowers. The irregular distribution of storm scours suggests that storms occurred at any stage of deposition (Fig 6.6B).

6.6.2 Spectral Analysis.

The section was measured in the northern part of Robin Hood's Bay (Sellwood 1970a; Fig 2) and the beds were measured to the nearest centimetre although the gradational contacts have probably caused errors. The codes used were: mudstone=-1.0, silty shale=0.0, argillaceous sandstone=+1.0. Beds 2-8 (Sellwood 1970a) were previously measured as 941cm whereas in this study they totalled 961cm (+2.1% difference). It is assumed that the top of the oxynotum zone occurs at the top of bed 6 (Sellwood 1970; Appendix 1), in which case the measured section begins in the upper simpsoni subzone and ends in the lower raricostatoides subzone according to the thicknesses published by Cope et al. (1980) (Fig 6.6B). Each ammonite zone is assumed to last one million years (Sections 4.2.6e) so dividing each zone by the number of subzones, the oxynotum and densinodulum subzones, which occupy 530 + 140cm (Cope et al. 1980), represent 500 + 250kyr. Therefore the average sedimentation rate was about 0.89 cmkyr^{-1} .

Fig 6.6C shows that no peaks are significant to the left of the <20kyr limit. Thus it cannot be inferred that clastic sediment supply or water-depth changes responded to orbital forcing. However, it is not possible to decide what the lack of regular cyclicity actually indicates

(Section 6.8.2). It may be that in the clastic environment represented by these rocks, the input of coarse sediment from the coast was entirely random. On the other hand the prevalence of storm scours might imply frequent and widespread phases of erosion related to storm induced turbulence. This hypothesized erosion might have produced enough hiatuses to have caused significant damping of any regular signals. Another possibility is that measurement errors connected to the gradational contacts have caused flattening of any spectral peaks.

6.7 Upper Birkhill Shales (Lower Silurian), Dob's Linn, Dumfries & Galloway, Scotland.

6.7.1 Introduction.

The Upper Birkhill Shales (Llandovery) consist of black mudstone (usually called shale), grey mudstone and pyroclastic claystone in beds millimetres to a few decimetres thick with sharp, planar contacts (Fig 6.7A). The stratigraphy and graptolite biostratigraphy has been summarized by Williams (1980). The Birkhill shales were deposited in very low palaeolatitudes perhaps over oceanic crust and a nearby continental margin shed turbidites which now directly overlie the Birkhill Shales (the Gala Greywackes) (Leggett 1978a). The claystones which represent altered tuffs and indicate volcanic activity (presumably on the continent) probably accumulated almost instantaneously (Leggett 1978a).

Fossils include predominant graptolites, with a blind trilobite, displaced inarticulate brachiopods, conodonts, scolecodonts, bivalves and nautiloids (Williams & Rickards 1984). Currents are suggested by aligned graptolites and the sequence contains gaps now marked by winnowed graptolite horizons, pyroclastic claystone seams of variable

thickness and possible black mudstone rip-up clasts (Williams & Rickards 1984). Rare micro-faulting, micro-imbrication and the overlying turbidites suggest some form of slope (Williams & Rickards 1984). The micro-faulting and black mudstone clasts inside grey mudstone support the idea that two sediment types were deposited on the sea-floor and refutes the claim by Stephens et al. 1975 that the lithological properties of these rocks were only determined by diagenetic and metamorphic processes (although such may be the case for geochemical parameters).

The laminated shales are considered to represent anoxic and the grey mudstones dysaerobic bottom-waters (Leggett 1978a, Williams & Rickards 1984). Leggett ruled-out a restricted basin model in view of the width of the Iapetus Ocean in the Llandovery. He considered 'black-shale' deposition to result from relatively high eustatic sea-level and consequent high productivity (Leggett 1978a). The sea-level rise in the Llandovery corresponds to the melting of the Ashgill (Late Ordovician) glaciers (Leggett 1978b) when the 'Barren mudstones' or Upper Hartfell Shales accumulated. These grey mudstones were assumed to indicate good oxygenation related to glaciation and oceanic circulation whilst the rare black mudstone levels were thought to correlate with interglacials, stagnation and anoxia (Leggett 1978a & b). This model accords well with Pleistocene results of Duplessy & Shackleton (1985). Leggett et al. (1981) suggested that the black/grey alternations correspond to Milankovitch cycles; the spectral analysis conducted here can test this idea.

6.7.2 Spectral Analysis.

Because many beds are only a few millimetres thick, the whole section was measured to the nearest millimetre. The small-scale faulting in the Dob's Linn section limited correlation from one side of the stream to the other so a section of only about 7.3m long could be measured. The section consisting of alternating grey and black mudstone is succeeded (the beds are overturned) by 7.68m of grey mudstone with claystone seams before the Gala Greywackes are reached. The measurements included the claystone seams, but as these accumulated very quickly and bear no relation to the black/grey alternation, they were subtracted out before spectral analysis (Fig 6.7B). The code values used were black mudstone=-1.0, grey mudstone=+1.0.

The sedimentation rate estimate is crude for a number of reasons. It was not possible to locate zonal boundaries in the field so the thicknesses indicated by Leggett (1978a; Fig 21) were used to locate the position of the sedgwickii zone (Fig 6.7B). The thickness of the zone excluding claystone seams is 5591mm. According to McKerrow et al. (1986), the Llandovery represents about 10Myr with 11 graptolite zones. The sedgwickii zone is assumed to have lasted about 1Myr (it seems to be about average thickness). This yields a sedimentation rate of 0.559 cmkyr^{-1} . Although this is inaccurate, the nature of the radiometric time-scale and the presence of gaps in the section makes 'better' estimates of the sedimentation rate impracticable at present.

Fig 6.7C shows that one regular cycle with a wavelength of 31.5cm and a period of less than 56kyr is present. It is not possible to decide whether this regular cycle corresponds to 21kyr or 41kyr. Ruddiman & McIntyre (1984) showed that variations in sea surface temperature in the Pleistocene North Atlantic, are dominated by precession and eccentricity

frequencies below 55° and by obliquity and eccentricity frequencies above this latitude. On this basis the 31.5cm cycle is most likely to be related to precession (21kyr) considering the low palaeolatitude of the time. Orbital forcing of sedimentation as suggested by Leggett *et al.* (1981) seems to be borne out by these results, but no comment can be made about the climatic processes involved (ie. regional or glacio-eustatic control).

6.8 Discussion of Power Spectral Results.

6.8.1 Walsh Power Spectra.

Digitizing measured sections is an extremely efficient way of producing time series. Experimentation with different codes (Section 6.2.2, Weedon 1986) shows that the details of rock type classification (eg. calcareous silt distinguished from silt) do not affect spectral results significantly whereas the more fundamental classification does (eg. silt distinguished from clay). Large time series can be generated for stratigraphic sections much more quickly by digitization of rock types than by making geochemical determinations of some parameter. It cannot be over-emphasized how important it is to demonstrate a primary distinction of rock types so that the spectral analysis can be regarded as meaningful in terms of sedimentology. Walsh power spectra produce similar results to Fourier spectra for real data (Section 6.3.2) as suggested by Schwarzacher (1985).

6.8.2 Interpreting Power Spectra.

The most serious problems with the interpretation of the power spectra generated in this thesis, concern dating and wavelength ratios. It is admitted that the dating used here is crude (Section 4.2.6e), but

no better constraint is available at present. Sadler (1981) showed that sedimentation rate estimates decrease for a particular set of rocks when longer and longer intervals of time are considered. Therefore when using sedimentation rates to date orbital cycle peaks, intervals of tens of thousands of years should be employed. If instead intervals of millions of years are employed, the required sedimentation rate is likely to be underestimated and the periods of the peaks overestimated (Weedon 1986). Unfortunately, this point does not appear to be widely accepted as yet (eg. Herbert & Fischer 1986).

The suggestion by House (1985) that orbitally forced sedimentary cycles be used to refine the chronology of the Jurassic is exciting. Something similar has already been achieved, using stable isotopes, for the last 780kyr of the Pleistocene (the SPECMAP time-scale: Imbrie et al. 1984). But in the Jurassic no system comparable to global correlation via stable isotopes is available as yet. Some form of filtering of time series, applied in view of spectral results, might be able to replace the crude 'cycle' counting used by House and thus separate superimposed orbital cycles. Yet the inherent incompleteness of the stratigraphic record and the difficulty of recognizing small-scale stratigraphic gaps, may well mean that the suggestion is premature.

Many of the spectra generated here contain regular cycles with approximately the expected durations of orbital cycles, but with wavelength ratios which do not fit the Milankovitch Theory. Three possible explanations for this can be advanced:

- 1) Some process other than orbital forcing such as tectonic controls might be involved (Cisne 1986, Section 5.3.1). However, in this thesis it is assumed that orbital forcing is the most likely explanation for the spectral results because sufficiently regular and stable

alternative processes have yet to be demonstrated (Schwarzacher 1985, 1986).

2) Orbital components other than those dominant in the Pleistocene (410, 100, 41 & 21) may have been operative. One candidate for an alternative orbital period is the 30kyr obliquity component, which has been discovered in Pleistocene data (Berger 1977, 1984, Ruddiman et al. 1986). This orbital cycle would explain the wavelength ratios found for spectra from the Hettangian to Lower Sinemurian of South Britain (Section 4.3.4), and from the mid Pliensbachian and Toarcian of South Switzerland (Sections 6.4.3 and 6.4.7). There is also independent evidence for a 30kyr cycle in the uppermost Triassic rocks of North America (Olsen 1986).

3) Hiatuses (or some other sedimentary process), may have altered the expected wavelength ratios of the main orbital cycles by acting as a kind of filter (Section 4.3.4). This last possibility certainly merits investigation before some of these spectral interpretations can be accepted unequivocally.

In three cases spectra were produced which showed no evidence for regular cyclicity. In the Upper Pliensbachian of Breggia Gorge (Section 6.4.5) it seems likely that rapidly changing sedimentation rates obscured the orbital cycles demonstrated higher (Section 6.4.3) and lower (Section 6.4.7) in the sequence. At Nash Point in the Early Sinemurian (Section 4.3.3d) the input of bioclastic fragments from the shore or the extreme nodularity of the sequence (which caused measurement errors), seem to have prevented detection of the regular cycles found elsewhere in the basal Lias of Britain. The 'Siliceous Shales' at Robin Hood's Bay in the Upper Sinemurian are developed in clastic facies (Section 6.6.2). Irregular input of clastics from the

shore, or hiatuses related to storms or measurement errors might be responsible for the lack of regular cyclicity.

This case introduces a major problem with the digitization of sections. Many beds at Robin Hood's Bay are only a few centimetres thick so it appeared sensible to measure the section to the nearest centimetre in order to avoid aliasing (Section 4.2.2). However, the contacts are often gradational over several centimetres which suggests that a longer sample interval is needed. It was thus decided that it was best to avoid aliasing and merely accept that 'large' measurement errors might obscure any regular cyclicity which might be present. If the possibility that regular cycles are present is to be pursued in the future, the next course of action might be to use some other property than rock type (eg. grain size) to construct a new time series and to proceed with Fourier analysis instead.

The preceding paragraphs show that it is usually impossible to interpret a negative result. The most likely reasons for the lack of significant spectral peaks in any given section peaks are: the absence of regular cyclic sedimentation; random changes in sedimentation rates or compaction; unidirectional changes in sedimentation rates; hiatuses in the section; time series too short to resolve orbital cycles; and measurement errors.

However, regular cycles were detected in ten out of thirteen spectra generated for this thesis. In these ten cases, the regularity, combined with the estimated duration and/or the wavelength ratios, strongly favour orbital forcing of sedimentation. When regular cycles are consistent with the Milankovitch Theory, some attempt can be made to produce a model that links climatic change and sedimentation. Yet it is not possible to choose between specific climatic and depositional

mechanisms without taking into account sedimentology, palaeontology and geochemistry.

6.8.3 Spectral Evolution.

The results documented in this thesis support the notion that orbital forcing of sedimentation has occurred at least since the Early Silurian whether there was ice on the globe (Early Oligocene, Early Silurian) or not (Jurassic). The spectra for the basal Lias (Section 4.3.3) show that it is possible to correlate regular cycles in different locations within a particular time slice. But it is difficult to compare wavelength ratios and relative power in detail given the variation in frequency resolution. It would be interesting to try to trace the evolution of spectral peaks through time with these data. But to compare similar climatic regimes, results from one location should be used.

Three spectra have been generated for the Dorset coast and relate to the Hettangian-Early Sinemurian (Blue Lias Member; Section 4.3.3a), Early Pliensbachian (Belemnite Marls; Section 6.5) and Kimmeridgian (Kimmeridge Clay; Section 6.3). The Dorset Coast sections remained close to a palaeolatitude of 35°N throughout the Jurassic (Smith et al. 1981). The obliquity cycle (41kyr) seems to have remained an important element of cyclic sequences throughout the Jurassic whereas the precession cycle does not appear to have affected sedimentation in the Kimmeridgian. The long eccentricity cycle (410kyr) might be involved in part of the Kimmeridgian, whereas the short eccentricity cycle (100kyr) has only been detected in part of the Kimmeridgian and perhaps in the the Belemnite Marls. The persistence of the obliquity cycle was suggested by House (1985, 1986) and would be expected to be more prominent than the precession cycle at 35°N (Ruddiman & McIntyre 1984). Presumably the

change from dominant obliquity to dominant eccentricity power and the waning of precessional-forcing, is related to the long-term change towards a semi-arid climate at the end of the Jurassic (Hallam 1984).

Sellwood's suggestion that the Belemnite Marl and Blue Lias deposition might be analogous is strengthened by the spectral results for these rocks which used the same code values. The regular cycles at Lyme Regis (Blue Lias) and Charmouth (Belemnite Marls) seem to have similar wavelengths. This suggests that, if the cycles involved had periods of 41 and 21kyr, accumulation rates measured over tens of thousands of years were almost identical. But measured over hundreds of thousands or millions of years, the accumulation rate was much slower at Lyme Regis. This might indicate that the section at Lyme Regis is less complete on the scale of ammonite zones even though the regular cycles have similar wavelengths (cf. McCave 1979). The wavelength ratio of the regular cycles at Lyme differs from that of the regular cycles in the Belemnite Marls. If periods of 41 and 21kyr are involved in both sections, this might be related to the greater section loss suggested for the basal Lias (Section 4.3.4). Alternatively the longer regular sedimentary cycle at Lyme Regis might actually represent 30kyr and not 41Kyr (Section 6.8.2). The sedimentology of the Shales-with-Beef and the Black Ven Marls are considered in Section 5.5 because these rocks record deposition in Dorset after the basal Lias (Blue Lias) and prior to the Belemnite Marls.

The sections in the Toarcian and Middle Pliensbachian of Breggia Gorge in the Southern Alps (Sections 6.4.3 & 6.4.7) suggest that the 100kyr eccentricity and 21kyr precession cycles controlled sedimentation for about 9 million years. An obliquity cycle with a period of 30kyr might also have influenced sedimentation (Section 6.8.2). During this

time precession seems to have been^a more important control of sedimentation than eccentricity. During the Late Pliensbachian sedimentation rates slowed down considerably so that the orbital cycles have not been detected spectrally. In the falciferum zone limestone/marl alternations appear to have been destroyed by burrowing (Section 6.4.2).

The section through the Boom Clay (Early Oligocene) spans about 6Myr and contains evidence for a variety of strongly developed eccentricity cycles (Section 6.2). There is some evidence that obliquity and precessional forcing was involved in the lower half of the section, but this requires further investigation.

Eight of the Lower Jurassic spectra have what have been interpreted as significant peaks (Sections 4.3.3, 6.5.2, 6.4.3 and 6.4.7). If the dating of these peaks is correct then all of these spectra show much greater power associated with the obliquity (41kyr and/or 30kyr) and/or precession (21kyr) cycles than with the eccentricity cycles (100kyr, 410 kyr). This contrasts with the opposite scenario in the Upper Jurassic (Section 6.3), the Cretaceous (eg. Schwarzacher & Fischer 1982, Herbert & Fischer 1986), the Early Oligocene (Section 6.2) and the Pleistocene (eg. Imbrie et al. 1984). The reason for this change in the relative importance of eccentricity is not known at present.

6.9 Power Spectral Conclusions.

1. Digitization of rock types provides a fast and simple way to produce long time series from stratigraphic sections. Contacts between beds must be sharp and a primary distinction of rock types must have been demonstrated first.

2. The discontinuous (stepped) time series produced by digitization is best analysed spectrally using the Walsh transform. Walsh spectral analysis apparently produces good agreement with Fourier spectral analysis.

3. Spectral analysis provides an objective way to demonstrate regularity in a time series. Lack of regular cyclicity in open-marine sequences possessing interbedded rock types, cannot be attributed to a particular cause in most cases. Many geological processes can produce distortion of regular (climatic) signals (eg. hiatuses and irregular or unidirectional changes in sedimentation rate and compaction). Others processes appear to be able to introduce harmonic components into time series (eg. differential sedimentation rates and differential compaction).

4. Regular sedimentary cycles, denoted by significant peaks on power spectra, which represent durations between 500 and 10kyr and which are stable for hundreds of thousands to millions of years, suggest orbitally forced sedimentation. In such cases sedimentary models explaining the cyclicity can include climatic elements. The exact climatic mechanism involved can only be selected by using sedimentological, palaeontological and geochemical data. It is, of course, possible that previously undocumented processes (eg. tectonics) might mimic the regularity, periods and stability of Milankovitch cycles.

5. Wavelength ratios of regular sedimentary cycles can often be used to identify specific orbital cycles. When the observed ratios do not

match those of the main orbital periods, it is suggested that hiatuses might be responsible for changing the relative positions of spectral peaks. Another possibility is that orbital components other than those dominating the Pleistocene are involved. One such orbital component might be an obliquity cycle with a period of 30kyr. This cycle would explain wavelength ratios in spectra produced in this study from Hettangian-Lower Sinemurian rocks in South Britain (ie. the basal Lias). It would also account for the structure of spectra obtained here from mid Pliensbachian-Toarcian rocks in South Switzerland (ie. the Morbio Formation and the Ammonitico Rosso Lombardo).

6. Thirteen Walsh power spectra for nine different 'cyclic' formations have been generated. Three spectra produced no evidence for regular cyclicity. Ten spectra contain peaks which are considered to indicate regular sedimentary cyclicity. All the regular cycles can be explained in terms of the Milankovitch Theory. Therefore, at present it appears that in the order of 80% of 'cyclic' open-marine sequences can be explained in terms of the Milankovitch Theory.

7. Milankovitch cycles have been documented from sequences representing the Early Silurian, the Jurassic and the Early Oligocene. The Jurassic examples prove that such cyclicity is common-place despite the absence of ice-related processes such as glacio-eustatic sea-level fluctuations. The changing response of particular palaeoclimatic regimes to orbital forcing, even over several tens of millions of years, has been demonstrated (Section 6.8.3). The spectra for the Early Jurassic suggest that the variations in precession and obliquity of the Earth's orbit exerted a greater influence on sedimentation (and presumably

climate) than variations in eccentricity. For unknown reasons this represents the reverse of the scenario in the later Mesozoic, the Oligocene and in the Pleistocene.

REFERENCES

AGER D. 1986

A reinterpretation of the basal 'Littoral Lias' of the Vale of Glamorgan. Proc. Geol. Assoc. 97 pp29-35.

ANDERSON R.Y. 1982

A long geoclimatic record from the Permian. J. Geophys. Res. 87C pp7285-7294.

ANDERSON R.Y. 1984

Orbital forcing of evaporite sedimentation. In: Milankovitch and Climate. Ed.: Berger et al. pp147-162.

ANDERSON R.Y. & KOOPMANS L.H. 1963

Harmonic analysis of varve time series. J. Geophys. Res. 68 pp877-893.

AMIRI-GARROUSSI K. 1978

Sedimentological and palaeoecological studies in the Broadford Beds (Hettangian-Sinemurian) of North West Scotland. D.Phil. Thesis U. of Oxford.

ARMSTRONG R.L. 1978

Pre-Cenozoic, Phanerozoic time scale: computer file of critical dates and consequences of new and in-progress decay constant revisions. In: The Geologic time scale Am. Assoc. Pet. Geol. Studies in Geology No.6 pp73-91.

ARMSTRONG R.L. 1982

Late Triassic-Early Jurassic time scale calibration in British Columbia, Canada. In: Numerical dating in stratigraphy, Ed.: G.S. Odin, Wiley pp504-514.

ARTHUR M.A., DEAN W.E., BOTTJER D. & SCHOLLE P.A. 1984

Rhythmic bedding in Mesozoic-Cenozoic pelagic carbonate sequences: the primary and diagenetic origin of Milankovitch-like cycles. In: Milankovitch and Climate. Ed.: Berger et al. pp191-122.

BAKER P.A. & KASTNER M. 1981

Constraints on the formation of sedimentary dolomite. Science 213 pp214-215.

BARRON E.J., ARTHUR M.A. & KAUFFMAN E.G. 1984

Cretaceous rhythmic bedding sequences: a plausible link between orbital variations and climate. Earth Planet. Sci. Lett. 72 pp327-340.

BARRY R.G. & CHORLEY R.J. 1982

Atmosphere, Weather and Climate. 407pp Fourth Edition, Methuen.

BATHURST R.G. 1975

Carbonate sediments and their diagenesis. Developments in Sedimentology No.12 Elsevier.

BATTEN D.J., TREWIN N.H. & TUDHOPE A.W. 1986

The Triassic-Jurassic junction at Golspie, Inner Moray Firth Basin.
Scott. J. Geol. 22 pp85-98.

BEAUCHAMP K.G. 1975

Walsh Functions and their applications Techniques of Physics No.3
236pp Academic Press.

BENSON R.H. et al. 1961

Treatise on Invertebrate Palaeontology Part Q, Arthropoda 3,
Crustacea, Ostracoda. 442p.

BERGER A.L. 1977

Support for the astronomical theory of climatic change. Nature 269
pp44-45.

BERGER A.L. 1980

The Milankovitch astronomical Theory of palaeoclimatic change: a
modern review. Vistas in Astron 24 pp103-122.

BERGER A.L. 1984

Accuracy and frequency stability of the Earth's orbital elements
during the Quaternary. In: Milankovitch and Climate Ed.: Berger et
al. pp3-39.

BERGER A., IMBRIE J., HAYS J., KUKLA G., & SALTZMAN B. 1984

Ed.s: Milankovitch and Climate NATO ASI C126 Reidel.

BERGER W.H. & CROWLEY J.C. 1982

Ed.s: Climate in Earth history. Papers from the Amer. Geophys. Union meeting Toronto 1980, 198p.

BERGGREN W.A., KENT D.V. & FLYNN J.J. 1986

Paleogene geochronology and chronostratigraphy. In: The Chronology of the Geological Record, Ed.: N.J. Snelling Geol. Soc. (Lond.) Mem. No.10 pp141-198.

BERNER R.A. 1970

Sedimentary pyrite formation. Am. J. Sci. 268 pp1-23.

BERNER R.A. & RAISWELL R. 1984

C/S method for distinguishing freshwater from marine sedimentary rocks. Geology 12 pp365-368.

BERNOULLI D. 1964

Sur geologie des Monte Generoso. Beitr. Geol. Karte Schweiz. 118 pp134.

BERNOULLI D. & JENKYNS H.C. 1974

Alpine, Mediterranean, and central Atlantic Mesozoic facies in relation to the early evolution of the Tethys. In: Modern and ancient geosynclinal sedimentation, Ed.: R.H. Dott & R.H. Shaver, Spec. Publ. Soc. Econ. Palaeon. Mineral. 19 pp129-160.

BRADLEY W.H. 1929

The varves and climate of the Green River Epoch. U.S. Geol. Surv.
Prof. Paper 158E pp87-110.

BROMLEY R.G. 1970

Borings as trace fossils and Entobia cretacea as an example. In:
Trace Fossils, Ed.: Crimes T.P. & Harper J.C., Geol. J. Spec. Issue
No.3 pp49-90.

BROMLEY R.G. 1972

On some ichnotaxa in hard substrates, with a redefinition of
Trypanites Magdefrau. Palaont. Zeitschrift 46 pp93-98.

BROMLEY R.G. & EKDALE A.A. 1984

Chondrites: a trace fossil indicator of anoxia in sediments. Science
224 pp872-874.

BRUMSACK H.J 1980

Geochemistry of Cretaceous black shales from the Atlantic ocean
(DSDP legs 11, 14, 36 & 41). Chem. Geol. 31 pp1-25.

BURKI P.M., GLASSER L.S.D. & SMITH D.N. 1982

Surface coatings on ancient coccoliths. Nature 297 pp145-147.

CARSS B.W. & NEIDELL N.S. 1966

A geological cyclicity detected by means of polarity coincidence
correlation Nature 212 pp136-137.

CAMPOS H.S. & HALLAM A. 1979

Diagenesis of English Lower Jurassic limestones as inferred from oxygen and carbon isotope analysis. Earth Planet. Sci. Lett. 45 pp23-31.

CHAO G.Y. 1969

20 (Cu) Table for common minerals. Geol. Paper 69-2 Dept. of Geology, Carleton U., Ottawa, Canada, 42p.

CISNE J.L. 1986

Earthquakes recorded stratigraphically on carbonate platforms. Nature 323 pp320-322.

CLEMENTS R.G. & Members of the field studies in local geology class 1975

The geology of the Long Itchington Quarry (Rugby Portland Cement Co. Ltd., Southam Works). Percival Guildhall, Rugby and Dept. of Geology, University of Leicester.

COPE J.C.W., GETTY T.A., HOWARTH M.K., MORTON N. & TORRENS H.S. 1980

A correlation of Jurassic rocks in the British Isles, Part one: introduction and Lower Jurassic. Geol. Soc. Lond. Spec. Rep. No.14 73pp Blackwell Scientific.

COPESTAKE P. & JOHNSON B. 1981

The Hettangian to Toarcian. In Chap.6 In: Stratigraphical Atlas of Fossil Foraminifera. Ed.: D.G. Jenkins & J.W. Murray Brit. Micropal. Soc.

COTILLON P. & RIO M. 1984

Cyclic sedimentation in the Cretaceous of DSDP sites 535 & 540 (Gulf of Mexico) 534 (Central Atlantic) and in the Vocontian Basin (France). Int. Rep. DSDP 77 pp339-376.

COX B.M. & GALLOIS R.W. 1980

The stratigraphy of the Kimmeridge Clay of the Dorset type area and it's correlation with some other sequences. Inst. Geol. Sci. Report 80/4 44p.

CRAIG H. 1957

Isotopic standards for carbon and oxygen, and correction factors for mass-spectrometric analysis of carbon dioxide. Geochim. Cosmochim. Acta 12 pp131-149.

CROWLEY T.J. 1983

The geological record of climatic change. Rev. Geophys. Space Phys. 21 pp828-877.

CUTTS J.A. & LEWIS B.H. 1982

Models of climate cycles recorded in Martian polar Layered Deposits. Icarus 50 (2/3) pp216-244.

DALFES H.N., SCHNEIDER S.H. & THOMPSON S.L. 1984

Effects of bioturbation on climatic spectra inferred from deep-sea cores. In: Milankovitch and Climate Ed.: Berger et al. pp481-492.

DEAN W.E., GARDNER J.V., JANSÁ L.F., CEPEK P. & SEIBOLD E. 1977

Cyclic sedimentation along the continental margin of NorthWest Africa. Int. Rep. DSDP 41 pp965-990.

DEAN W.T., DONOVAN D.T. & HOWARTH M.K. 1961

The Liassic ammonite zones and subzones of the NorthWest European Province. Bull. Brit. Mus. (Nat. Hist.) Geology 4 No.10 pp435-505.

DE BOER P.L. 1982

Cyclicity and the storage of organic matter in Middle Cretaceous pelagic sediments. In: Cyclic and Event Stratification Ed.: G.Einsele & A.Seilacher Springer-Verlag pp456-475.

DE BOER P.L. & WONDERS A.A.H. 1984

Astronomically induced rhythmic-bedding in Cretaceous pelagic sediments near Moria (Italy). In: Milankovitch and Climate Ed.: Berger et al. pp177-190.

DEINES P. 1970

Mass spectrometer correction factors for determination of small isotopic variation of carbon and oxygen. Int. J. Mass Spectrom. Ion Phys. 4 pp283-295.

DICKSON J.A.D. 1965

A modified staining technique for carbonates in thin section. Nature 205 p587.

DOMICCO R.V. & KORDESCH E.G. 1986

Facies sequences of a semi-arid closed basin: the Lower Jurassic Eat
Berlin Formation of the Hartford Basin, New England, USA.

Sedimentology 33 pp107-118.

DONOVAN D.T. 1953

Synoptic supplement to T.Wright's Monograph of the Lias ammonites of
the British Isles - 1878-1886. Pal. Soc. Monograph pp1-54.

DONOVAN D.T. 1956

The zonal stratigraphy of the Blue Lias around Keynsham, Somerset.

Proc. Geol. Assoc. 66 pp182-212.

DONOVAN D.T., HORTON A. IVEMEY-COOK H.C. 1979

The transgression of the Lower Lias over the northern flank of the
London Platform. J. Geol. Soc. (Lond.) 136 pp165-173.

DONOVAN D.T. & JONES E.J.W. 1979

Causes of world-wide changes in sea-level. J. Geol. Soc. (Lond.)
136 pp187-192.

DONOVAN D.T. & KELLAWAY G.A. 1984

Geology of the Bristol District: the Lower Jurassic rocks. Memoir
Brit. Geol. Surv. Special Sheet. HMSO

DUFF P.M.D., HALLAM A. & WALTON E.K. 1967

Cyclic Sedimentation. Developments in Sedimentology No.10 Elsevier.

DUNN C.E. 1974

Identification of sedimentary cycles through Fourier analysis of geochemical data. Chem. Geol. 13 pp217-232.

DUPLETTY J.-C. & SHACKLETON N.J. 1985

Response of global deep-water circulation to Earth's climatic change 135,000 - 107,000 years ago. Nature 316 pp500-507.

EBUKANSON E.J. & KINGHORN R.R.F. 1985

Kerogen facies in the major Jurassic mudrock formations of Southern England and the implication on the depositional environments of their precursors. J. Pet. Geol. 8 pp435-462.

EBUKANSON E.J. & KINGHORN R.R.F. 1986

Maturity of organic matter in the Jurassic of Southern England, and it's relation to the burial history of the sediments. J. Pet. Geol. 9 pp259-280.

EDER W. 1982

Diagenetic redistribution of carbonate, a process in forming limestone-marl alternations (Devonian and Carboniferous, Rheinisches Schiefergebirge, W.Germany. In: Cyclic and Event Stratification Ed.s G.Einsele & A.Seilacher Springer-Verlag pp98-112.

EINSELE G. 1982a

Limestone-marl cycles (periodites): diagnosis, significance, causes - a review. In: Cyclic and Event Stratification, Ed.: G.Einsele & A.Seilacher Springer-Verlag pp8-53.

EINSELE G. 1982b

General remarks about the nature, occurrence and recognition of cyclic sequences (periodites). In: Cyclic and Event Stratification Ed.: G.Einsele & A.Seilacher Springer-Verlag pp3-7.

ETTENSohn & ELAM 1985

Defining the nature and location of a late Devonian-Early Mississippian pycnocline in east Kentucky. Bull. Geol. Soc. Am. 96 pp1313-1321.

FARRIMOND P., COMET P., EGLINGTON G., EVERSLED R.P., HALL M.A., PARK D.W., & WARDROPER A.M.K. 1984

Organic Geochemical Study of the Upper Kimmeridge Clay of the Dorset type area. Mar. Pet. Geol. 1 pp340-354.

FIELD R.A. 1968

Lower Jurassic ostracoda from England and Normandy. Ph.D. Thesis U. of London (Univ. Coll.) 400pp.

FISCHER A.G. 1964

The Lower Cyclothem of the Alpine Triassic. In: Symposium on Cyclic Sedimentation. Ed.: D.F.Merriam Kansas Geol. Surv. Bull. 169 pp107-149.

FISCHER A.G. 1980

Bedding rhythms and geochronology. In: The Scientific Ideas of G.K. Gilbert. Geol. Soc. Am. Spec. Paper 183 pp93-104.

FISCHER A.G. 1986

Climatic rhythms recorded in strata. Ann. Rev. Earth Planet. Sci.
14 pp351-376.

FISCHER A.G. & SCHWARZACHER W. 1984

Cretaceous bedding rhythms under orbital control ? In: Milankovitch
and Climate. Ed.: Berger et al. pp163-175.

FLETCHER C.J.N., DAVIES J.R., WILSON D. & SMITH M. 1986

The depositional environment of the basal 'Littoral Lias' in the
Vale of Glamorgan - a discussion of the reinterpretation by Ager
(1986). Proc. Geol. Assoc. 97 pp383-384.

FOLK R.L. 1965

Some aspects of recrystallization in ancient limestones. In:
Dolomitization and limestone diagenesis - a symposium. SEPM Special
Pub. No.13 Ed.: L.C.Pray & R.C.Murray pp14-48.

FRAKES L.A. 1979

Climates throughout geologic time Elsevier 310pp.

GALLOIS R.W. 1976

Coccolith blooms in the Kimmeridge Clay and the origin of North Sea
Oil. Nature 259 pp473-475.

GILBERT G.K. 1895

Sedimentary measurement of Cretaceous time. J. Geol. 3 pp121-127.

GLUYAS J.G. 1983

The genesis and diagenesis of shale nodular limestone sequences.

Ph.D. Thesis unpubl. U. of Liverpool.

GLUYAS J.G. 1984

Early carbonate diagenesis within Phanerozoic shales and sandstones

of the N.W. European Shelf. Clay Min. 19 pp309-321.

GULLENTOPS F. & VANDENBERGHE N. 1985

Rhythmicity in the Boom Clay (Rupelian) sedimentation. Terra Cognita

5 p245.

HALLAM A. 1959

Stratigraphy of the Broadford Beds of Skye, Raasay and Applecross.

Proc. Yorks. Geol. Soc. 32 pp165-184.

HALLAM A. 1960a

A sedimentary and faunal study of the Blue Lias of Dorset. Phil.

Trans. Roy. Soc. Lond. B243 pp1-44.

HALLAM A. 1960b

Kulindrichnus langi, a new trace fossil from the Lias. Palaeontology

3 pp64-68.

HALLAM A. 1964

Origin of the limestone-shale rhythms in the Blue Lias of England:

a composite theory. J. Geol. 72 pp157-169.

HALLAM A. 1969

A pyritized hardground in the lower Jurassic of Dorset (England).
Sedimentology 12 pp231-240.

HALLAM A. 1975

Jurassic Environments. Cambridge Earth Sci Series., Cambridge U.
Press, 269p.

HALLAM A. 1981

A revised sea-level curve for the early Jurassic. J. Geol. Soc.
(Lond.) 138 pp735-743.

HALLAM A. 1984

Continental humid and arid zones during the Jurassic and Cretaceous.
Palaeogeog. Palaeoclim. Palaeoecol. 47 pp195-223.

HALLAM A. 1986

Origin of minor limestone-shale cycles: climatically induced or
diagenetic ? Geology 14 pp609-612.

HALLAM A. 1987

Reply to Comment by Weedon (1987) on Hallam (1986) Geology 15
pp93-94. (Appendix Section 5.3.)

HALLAM A. & BRADSHAW M.J. 1979

Bituminous shales and oolitic ironstones as indicators of
transgression and regression. J. Geol. Soc. (Lond.) 136 pp157-164.

HALLAM A., HANCOCK J.M., LA BREQUE J.L., LOWRIE W. & CHANNELL J.E.T.

1986

Jurassic to Palaeogene, Part 1: Jurassic and Cretaceous
geochronology and Jurassic to Palaeogene magnetostratigraphy. In:
The chronology of the geological record, Ed.: N.J. Snelling
pp118-140.

HALLAM A. & SELLWOOD B.W. 1976

Middle Mesozoic sedimentation in relation to tectonics in the
British area. J. Geol. 84 pp301-321.

HAMILTON G.B. 1982

Triassic and Jurassic calcareous nannofossils. Chap.3 In: A
Stratigraphic Index of Calcareous Nannofossils. Ed.: A.R. Lord Brit.
Micropal. Soc. Ser. pp17-39.

HARLAND W.B., COX A.V., LLEWELLYN P.G., PICKTON C.A.G., SMITH A.G. &

WALTERS R. 1982

A Geologic Timescale. Cambridge Earth Sci. Ser., Cambridge U.
Press.

HATTIN D.E. 1975

Petrology and origin of fecal pellets in Upper Cretaceous strata of
Kansas and Saskatchewan. J. Sed. Petrog. 45 pp686-696.

HAY W.H., BEHENSKY J.F., BARRON E.J. & SLOAN J.L. 1982

Late Triassic-Liassic palaeoclimatology of the Proto-central North Atlantic rift system. Palaeogeog. Palaeoclim. Palaeoecol. 40 pp13-30.

HAYS J.D., IMBRIE J. & SHACKLETON N.J. 1976

Variations in the Earth's orbit: pacemaker of the ice ages. Science 194 pp1121-1132.

HERBERT T.D. & FISCHER A.G. 1986

Milankovitch climatic origin of mid-Cretaceous black shale rhythms in central Italy. Nature 321 pp739-743.

HODGES P. 1986

The Lower Lias (Lower Jurassic) of the Bridgend Area, South Wales. Proc. Geol. Assoc. 97 pp237-242.

HONJO S. 1976

Coccoliths: production, transportation and sedimentation. Mar. Micropalaeon. 1 pp65-79.

HOUSE M.R. 1985

A new approach to an absolute timescale from measurements of orbital cycles and sedimentary microrhythms. Nature 315 pp721-725.

HOUSE M.R. 1986

Are Jurassic sedimentary microrhythms due to orbital forcing? Proc. Ussher Soc. 6 pp299-311.

HUDSON J.D. & FRIEDMAN I. 1974

Carbon and oxygen isotopes in concretions: relationship to pore-water changes during diagenesis. In: Proceeding of the international symposium on water-rock interaction. Ed.: J. Cadek & T. Paces. pp331-339.

IMBRIE J. 1985

A theoretical framework for the Pleistocene ice ages. J. Geol. Soc. (Lond.) 142 pp417-432.

IMBRIE J., HAYS J.D., MARTINSON D.G., MCINTYRE A., MIX A.C., MORLEY J.J.

PISIAS N.G., PRELL W.L. & SHACKLETON N.J. 1984

The orbital theory of Pleistocene climate: support from a revised chronology of the marine $\delta^{18}\text{O}$ record. In: Milankovitch and Climate Ed. Berger et al. pp269-305.

IMBRIE J. & IMBRIE K.P. 1979

Ice Ages: Solving the Mystery. Enslow 224pp.

IRWIN H. 1979

Comment on the environmental model for the type Kimmeridge Clay. Nature 277 pp377-380. (Nb. followed by reply by Tyson et al.)

IRWIN H. 1980

Early diagenetic carbonate precipitation and pore-fluid migration in the Kimmeridge Clay of Dorset, England. Sedimentology 27 pp577-591.

IRWIN H., CURTIS C. & COLEMAN M. 1977

Isotopic evidence for source of diagenetic carbonates formed during burial of organic-rich sediments. Nature 269 pp209-213.

JENKINS W.M. & WATTS D.G. 1968

Spectral Analysis and it's Applications. Holden-Day.

JENKYNS H.C. 1974

Origin of red nodular limestones (Ammonitico Rosso, Knollenkalke) in the Mediterranean Jurassic: a diagenetic model. In: Pelagic sediments on land and under the sea. Ed.: K.J. Hsü and H.C. Jenkyns, Int. Assoc. Sed. Spec. Publ. 1 pp249-271.

JENKYNS H.C. 1986

Pelagic environments. In: Sedimentary environments and facies, Ed.: H.G. Reading, pp343-398.

JENKYNS H.C. & CLAYTON C.J. 1986

Black shales and carbon isotopes in pelagic sediments from the Tethyan Lower Jurassic. Sedimentology 33 pp87-106.

JONES D.G. 1981

Regional studies in the sedimentology, mineralogy and geochemistry of the Penarth Group ('Rhaetic') of Britain. D.Phil. Thesis U. of Oxford.

JONES D.S., WILLIAMS D.F. & ROMANEK C.S. 1986

Life history of symbiont-bearing giant clams from stable isotope profiles. Science 231 pp46-48.

KALIN O. & BERNOULLI D. 1984

Schizosphaerella Deflandre & Dangeard, in deeper-water carbonate sediments, Mazagan continental margin (hole 547B) and Mesozoic Tethys. Int. Rep. DSDP 79 pp411-436.

KANASEWICH E.R. 1981

Time Sequence Analysis in Geophysics. Univ. of Alberta Press.

KENNEDY W.J. & GARRISON R.E. 1975

Morphology and genesis of nodular chalks and hardgrounds in the Upper Cretaceous of Southern England. Sedimentology 22 pp311-386.

KENNEDY W.J. & ODIN G.S. 1982

The Jurassic and Cretaceous timescale in 1981. In: Numerical dating in stratigraphy, Ed.: G.S.Odin, Wiley, pp557-592.

KENT P.E. 1936

The formation of hydraulic limestones of the Lower Lias. Geol. Mag. 73 pp476-478.

KENT P.E. 1937

The Lower Lias of South Nottinghamshire. Proc. Geol. Assoc. 48 pp163-174.

LANG W.D. 1924

The Blue Lias of the Devon and Dorset Coasts. Proc. Geol. Assoc. 35
pp169-185.

LANG W.D., SPATH L.F. & RICHARDSON W.A. 1923

'Shales with Beef' a sequence in the Lower Lias of the Dorset Coast.
Quat. J. Geol. Soc. (Lond.) 79 pp47-99.

LANG W.D., SPATH L.F. COX L.R. & MUIR-WOOD H.M. 1928

The Belemnite Marls of Charmouth, a series in the Lias of the Dorset
Coast. Quat. J. Geol. Soc. (Lond.) 84 pp179-257.

LE RICHE H.H. 1959

The distribution of certain trace elements in the Lower Lias of
Southern England. Geochim. Cosmochim. Acta 16 pp101-122

LEGGETT J.K. 1978a

Studies in the Ordovician rocks of the Southern Uplands, with
particular reference to the Northern Belt. D.Phil. Thesis U. of
Oxford.

LEGGETT J.K. 1978b

Eustacy and pelagic regimes in the Iapetus Ocean during the
Ordovician and Silurian. Earth Planet. Sci. Lett. 41 pp163-169.

LEGGETT J.K., MCKERROW W.S., COCKS L.R.M. & RICKARDS R.B. 1981

Periodicity in the early Palaeozoic marine realm. J. Geol. Soc.
(Lond.) 138 pp167-176.

LORD A.R. 1971

Revision of some Lower Lias ostracoda from Yorkshire. Palaeontology
14 pp642-665.

LORD A.R. 1978

Hettangian to Toarcian. In: A Stratigraphical Index of British
Ostracoda. Ed.: R.H.Bate & J.E.Robinson Spec. Publ. Brit. Micropal.
Soc., Geol. J. Spec. Issue 8, pp189-212.

LOUGHMAN D.L. 1982

A facies analysis of the Triassic/Jurassic boundary beds of the
world - with special reference to Northwest Europe and the Americas.
Ph.D Thesis, U. of Birmingham.

LOWENSTAM H.A. & EPSTEIN S. 1954

Palaeotemperatures of the post-Aptian Cretaceous as determined by
the oxygen isotope method. J. Geol. 62 pp207-248.

MARSAGLIA K.M. & KLEIN G. de V. 1983

The palaeogeography of Palaeozoic and Mesozoic storm depositional
systems. J. Geol. 91 pp117-142.

MARSHALL J.D. 1982

Isotopic composition of displacive fibrous calcite veins: reversals
in pore-water composition trends during burial diagenesis. J. Sed.
Petrog. 52 pp615-630.

MARTINI I.P., SAGRI M., & DOVETON J.H. 1978

Lithological transition and bed thickness periodicities in turbidite successions of the Antola Formation, Northern Apennines, Italy.

Sedimentology 25 pp605-623.

MCCAVE I.N. 1979

Depositional features of organic-carbon-rich black and green mudstone at DSDP Sites 386 & 387, Western North Atlantic. Int. Rep.

DSDP 43 pp411-416.

MCCREA J.M. 1950

On the isotopic chemistry of carbonates and a palaeo-temperature scale. J. Chem. Phys. 18 pp849-857.

MCKENZIE J.A. 1982

Carbon-13 cycle in Lake Greifen: a model for restricted ocean basins. In: Nature and origin of Cretaceous carbon-rich facies. Ed.: S.O.Schlanger & M.B.Cita, Academic Press, pp197-207

MCKERROW W.S., LAMBERT R. St. J. & COCKS L.R.M. 1986

The Ordovician and Silurian Periods. In: The Geochronology of the Geological Record, Ed.: N.J.Snelling, Geol. Soc. (Lond.) Mem. No.10 pp.73-80.

MERRIAM D.F. 1964

Ed.: Symposium on Cyclic Sedimentation. Kansas Geol. Surv. Bull. 169 636pp.

MIX A.C. & RUDDIMAN W.F. 1984

Oxygen-isotope analysis and Pleistocene ice volumes. Quat. Res. 21
_^
 pp1-20.

MYERS K.J. & WIGNALL P.B. in press

Understanding Jurassic organic-rich mudrocks: new concepts using
 γ -ray spectroscopy and palaeoecology: examples from the Kimmeridge
 Clay of Dorset and the Jet Rock of Yorkshire. In: Marine clastic
 sedimentology: new developments and concepts, Ed.: J.K.Leggett.

NEGI J.G. & TIWARI R.K. 1983

Matching long-term periodicities of geomagnetic reversals and
 galactic motions of the solar system. Geophys. Res. Lett. 10
 pp713-716.

NEGI J.G. & TIWARI R.K. 1984

Periodicities of palaeomagnetic intensity and variations: a
 Walsh spectral approach. Earth Planet. Sci. Lett. 70 pp139-147.

NOWROOZI A.A. 1967

Table for Fisher's test of significance in harmonic analysis
Geophys. J. Roy. Ast. Soc. 12 pp517-520.

OLSEN P.E. 1984

Periodicity of lake-level cycles in the Late Triassic Lockatong
 Formation of the Newark Basin (Newark Supergroup) New Jersey and
 Pennsylvania. In: Milankovitch and Climate. Ed.: Berger et al.
 pp129-146.

OLSEN P.E. 1986

A 40 million year lake record of Early Mesozoic orbital climatic forcing. Science 234 pp842-848.

OWEN C.B. 1861-1881

A monograph of the fossil Reptilia of the Liassic Formations. Pal. Soc. Monograph, Part 1 pp1-14, Part 2 pp1-26, Part 3 pp1-134. Nb. for a list of Fishes recorded at Lyme Regis see Wright 1878-1886 pp61-66.

PALMER C.P. 1972

The Lower Lias (Lower Jurassic) between Watchet and Lillstock in North Somerset (United Kingdom). Newsl. Strat. 2 pp1-30.

PARRISH J.T. & CURTIS R.L. 1982

Atmospheric circulation, upwelling, and organic-rich rocks in the Mesozoic and Cenozoic Eras. Palaeogeog. Palaeoclim. Palaeoecol. 40 pp31-66.

PARRISH J.T., ZIEGLER A.M. & SCOTese C.R. 1982

Rainfall patterns and the distribution of coals and evaporites in the Mesozoic and Cenozoic. Palaeogeog. Palaeoclim. Palaeoecol. 40 pp67-101.

PEDERSEN G.K. 1985

Thin fine-grained storm layers in a muddy shelf sequence: an example from the Lower Jurassic in the Stenlille 1 Well, Denmark. J. Geol. Soc. (Lond.) 142 pp357-373.

PERCH-NIELSEN K. 1985

Mesozoic calcareous nannofossils. In: Plankton Stratigraphy. Ed.:
H.M.Bolli, J.B.Saunders & K.Perch-Nielsen Cambridge U. Press
pp329-426.

PESTIAUX P. & BERGER A. 1984a

An optimal approach to the spectral characteristics of deep-sea
climatic records. In: Milankovitch and Climate Ed.: Berger et al.
pp417-445.

PESTIAUX P. & BERGER A. 1984b

Impacts of deep-sea processes on palaeoclimatic spectra. In:
Milankovitch and Climate Ed.: Berger et al. pp493-510.

PHELPS M.C. 1982

A facies and faunal analysis of the Carixian-Domarian boundary beds
in North-West Europe. Ph.D. Thesis U. of Birmingham.

PIENKOWSKI G. 1985

Early Liassic trace fossil assemblages from the Holy Cross
Mountains, Poland: their distribution in continental and marginal
marine environments. In: Biogenic structures: their use in
interpreting depositional environments, Ed.: H.A. Curren, Soc. Econ.
Palaeon. Mineral. Spec. Publ. 35 pp37-51.

PISIAS N.G. & LEINEN M. 1984

Milankovitch forcing of the oceanic system: evidence from the north-western Pacific. In: Milankovitch and Climate Ed.: Berger et al. pp307-330.

PORTER & ROBBINS 1981

Zooplankton fecal pellets link fossil fuel and phosphate deposits. Science 212 pp931-933.

POWELL J.H. 1984

Lithostratigraphical nomenclature of the Lias Group in the Yorkshire Basin. Proc. Yorks. Geol. Soc. 45 pp51-58.

RAISWELL R. 1971

Growth of Cambrian and Liassic concretions. Sedimentology 17 pp147-171.

RAISWELL R. & BERNER R.A. 1985

Pyrite formation in euxinic and semieuxinic sediments. Am. J. Sci. 285 pp710-724.

RICKEN W. 1985

Epicontinental marl-limestone alternations: event deposition and diagenetic bedding (Upper Jurassic, South-West Germany). In: Sedimentary and Evolutionary Cycles Ed.: U.Bayer & A.Seilacher Lecture Notes in Earth Sci. 1 pp127-162.

RICKEN W. 1986

Diagenetic bedding: a model for marl-limestone alternations. Lecture Notes in Earth Sci. 6 210p.

ROSSIGNOL-STRICK M. 1983

African monsoons, an immediate climate response to orbital insolation. Nature 304 pp46-49.

ROSSIGNOL-STRICK M., NESTEROFF W., OLIVE P. & VERGNAUD-GRAZZINI C. 1982

After the deluge: Mediterranean stagnation and sapropel formation. Nature 295 pp105-110.

RUDDIMAN W.F. & MCINTYRE 1984

Iceage thermal response and climatic role of the surface Atlantic Ocean 40° to 63°N. Geol. Soc. Am. Bull. 95 pp381-396.

RUDDIMAN W.F., SHACKLETON N.J. & MCINTYRE A. 1986

North Atlantic sea-surface temperatures for the last 1.2 million years. In: North Atlantic Palaeoceanography, Ed.: C.P. Summerhayes and N.J. Shackleton, Geol. Soc. (Lond.) Spec. Publ. No.21.

SADLER P.M. 1981

Sediment accumulation rates and the completeness of stratigraphic sections. J. Geol. 89 pp569-584.

SANDER B. 1936

Beiträge zur kentniss der Anlagerungsgefüge rhythmische Kalke und Dolomite aus der Trias. Mineralog. Petrog. Mitt. 48 pp27-209.

SCHIFFELBEIN P. 1984

Effect of benthic mixing on the information content of deep-sea stratigraphic signals. Nature 311 pp651-653.

SCHIFFELBEIN P. & DORMAN L. 1986

Spectral effects of time-depth nonlinearities in deep-sea sediment records: a demodulation technique for reanalysing time and depth scales. J. Geophys. Res. B91 pp3821-3835.

SCHWARZACHER W. 1964

An application of statistical time-series analysis to a limestone-shale sequence. J. Geol. 72 pp195-213.

SCHWARZACHER W. 1975

Sedimentation Models and Quantitative Stratigraphy. Developments in Sedimentology No.19 Elsevier.

SCHWARZACHER W. 1985

Principles of quantitative lithostratigraphy-the treatment of single sections. In: Quantitative Stratigraphy. Ed.: F.M.Gradstein, F.P.Agterberg, J.C.Brower, W.S.Schwarzacher, Reidel pp361-386.

SCHWARZACHER W. & FISCHER A.G. 1982

Limestone-shale bedding and perturbations of the Earth's orbit. In: Cyclic and Event Stratification Ed.s: G.Einsele & A.Seilacher Springer-Verlag pp72-95.

SELLWOOD B.W. 1970a

Sedimentological and faunal studies in the topmost Sinemurian (raricostatum zone) and lowest Pliensbachian (jamesoni zone) of Great Britain. D.Phil. Thesis, U. of Oxford.

SELLWOOD B.W. 1970b

The relation of trace fossils to small-scale sedimentary cycles in the British Lias. In: Trace Fossils, Ed.: T.R.Crimes & J.C.Harper, I.U.G.S. Conference Proceedings, pp489-504.

SELLWOOD B.W. & JENKYNS H.C. 1976

Basins and swells and the evolution of an epeiric sea. J. Geol. Soc. (Lond.) 131 pp373-388.

SHACKLETON N.J. 1986

Paleogene stable isotopic events. Palaeogeog. Palaeoclim. Palaeoecol. 57 pp91-101.

SHACKLETON N.J. & KENNETT 1975

Palaeotemperature history of the Cenozoic and the initiation of Antarctic glaciation. Int. Rep. D.S.D.P. 29 pp743-755

SHACKLETON N.J. & PISIAS N.G. 1985

Atmospheric carbon dioxide, orbital forcing and climate. In: The Carbon Cycle and Atmospheric Carbon Dioxide. Ed.: E.T.Sundquist & W.S.Broecker, Geophys. Monog. 32 pp303-317.

SHUKRI N.M. 1942

Rhythmic bedding in the Lower Lias of England. Fac. Sci. Fouad I Univ. Cairo Bull. 24 pp66-73.

SMITH A.G., HURLEY A.M. & BRIDEN J.C. 1981

Phanerozoic Paleontological World Maps. Cambridge Earth Sci. Ser.
102pp.

SPATH L.F. 1924

The ammonites of the Blue Lias. Proc. Geol. Assoc. 35 pp186-211.

STEPHENS W.E., WATSON S.W., PHILIP P.R. & WEIR J.A. 1975

Elemental associations and distribution through a Lower Palaeozoic graptolitic shale sequence in the Southern Uplands of Scotland.
Chem. Geol. 16 pp269-294.

THOMPSON J.B., MULLINS H.T., NEWTON C.R. & VERCOUTERE T.L. 1985

Alternative biofacies model for dysaerobic communities. Lethaia 18
pp167-179.

TROEDSSON G. 1951

On the Höganäs Series of Sweden (Rhaeto-Lias). Acta Universitatis Lundensis 47 pp1-268.

TRUEMAN A.E. 1920

The Liassic rocks of the Cardiff district. Proc. Geol. Assoc. 31
pp93-107.

TRUEMAN A.E. 1922

The Liassic rocks of Glamorgan. Proc. Geol. Assoc. 33 pp245-285.

TRUEMAN A.E. 1930

The Lower Lias (bucklandi zone) of Nash Point, Glamorgan. Proc. Geol. Assoc. 41 pp148-159.

TYSON R.V., WILSON R.C.L. & DOWNIE C. 1979

A stratified water column environmental model for the type Kimmeridge Clay. Nature 277 pp377-380.

VANDENBERGHE N. 1978

Sedimentology of the Boom Clay (Rupelian) in Belgium. Verhandel. Konink. Acad. Wetenschappen, Klasse der Wetenschappen 40 137p.

VANDENBERGHE N. & LAGA P. 1986

The septaria of the Boom Clay (Rupelian) in its type area in Belgium. Aardkundige Mededelingen 3 pp229-238.

VAN HINTE J.E. 1976

A Jurassic time scale. Am. Assoc. Pet. Geol. Bull. 60 pp489-497.

VAN HOUTEN F.B. 1964

Cyclic sedimentation, U.Triassic Lockatong Formation, Central New Jersey & adjacent Pennsylvania. In: Symposium on Cyclic Sedimentation. Ed.: D.F.Merriam, Kansas Geol. Surv. Bull. 169 pp497-531.

VOIGT E. 1972

Über Talpina ramosa v. Hagenow 1840, ein wahrscheinlich zu den
Phronidea gehoriger Bohrorganismus aus der oberen Kriede.

Nachrichten Akad. Wissinschaften Gottingen Maths-Phys. Nr.7

pp93-126.

WALL D. 1965

Microplankton, pollen and spores from the Lower Jurassic in Britain.

Micropal. 11 pp151-190.

WARRINGTON G., AUDLEY-CHARLES M.G., ELLIOTT R.E., EVANS W.B.,

IV. MEY-COOK H.C., KENT P., ROBINSON P.L., SHOTTON F.W. & TAYLOR F.M.

1980

A correlation of Triassic rocks in the British Isles. Geol. Soc.

Lond. Spec. Rep. No.13 78pp.

WEDEPOHL K.H. 1971

Environmental influences on the chemical composition of shales and

clays. In: Physics and chemistry of the Earth 8 Ed.: L.H.Ahrens,

F.Press, S.K.Runcorn & H.C.Urey, pp307-333.

WEEDON G.P. 1985

Palaeoclimatic information from ancient pelagic and hemipelagic

cyclic sediments. Terra Cognita 5 p110. (Appendix Section 5.1.)

WEEDON G.P. 1986

Hemipelagic shelf sedimentation and climatic cycles: the basal Jurassic (Blue Lias) of S.Britain. Earth Planet. Sci. Lett. 76 pp321-335. (Appendix Section 5.2.)

WEEDON G.P. 1987

Comment on 'Origin of minor limestone-shale cycles: climatically induced or diagenetic ?' (Hallam 1986) Geology 15 pp92-94. (Appendix Section 5.3.)

WHALLEY P.E.S. 1985

The systematics and palaeogeography of the Lower Jurassic insects of Dorset, England. Brit. Mus. (Nat. Hist.) Geol. Ser. 39 pp107-189.

WHITTAKER A. & GREEN G.W. 1983

Geology of the country around Weston-super-Mare. Geol. Surv. G.B. Memoir for sheet 279, 147p.

WIEDENMAYER F. 1980

Die ammoniten der mediterranen Provinz im Pliensbachian und untern Toarcian aufgrund neuer Untersuchungen im Generoso-Becken (Lombardische Alpen). Denschr. Schweiz. naturf. Ges. 93 261p.

WILLIAMS G.E. & SONNETT C.P. 1985

Solar signature in sedimentary cycles from the late Precambrian Elatina Formation, Australia. Nature 318 pp523-527.

WILLIAMS G.L. & BUJAK J.P. 1985

Mesozoic and Cenozoic dinoflagellates. In: Plankton Stratigraphy.
Ed.: Bolli H.M., Saunders J.B. & Perch-Neilsen K., Cambridge Earth
Sci. Ser. Cambridge University Press pp847-964.

WILLIAMS S.H. 1980

An excursion guide to Dob's Linn. Proc. Geol. Soc. Glasgow
Session 121-122 pp13-18.

WILLIAMS S.H. & RICKARDS R.B. 1984

Palaeoecology of graptolitic black shales. In.: Aspects of the
Ordovician System, Ed.: D.L Bruton, Palaeont. Contrib. from the U.
of Oslo No.295 pp159-166.

WOBBER F.J. 1965

Sedimentology of the Lias (Lower Jurassic) of South Wales. J. Sed.
Petrog. 35 pp683-703.

WOBBER F.J. 1966

A study of the depositional area of the Glamorgan Lias. Proc. Geol.
Assoc. 77 pp127-137.

WOBBER F.J. 1967

Post-depositional structures in the Lias in South Wales. J. Sed.
Petrog. 37 pp166-174.

WOBBER F.J. 1968a

Microsedimentary analysis of the Lias in South Wales. Sed. Geol. 2
pp13-49.

WOBBER F.J. 1968b

Faunal analysis of the Lias (Lower Jurassic) of South Wales (Great
Britain). Palaeogeog. Palaeoclim. Palaeoecol. 5 pp269-308.

WRIGHT T. 1878-1886

Monograph of the Lias ammonites of the British Isles. Pal. Soc.
Monograph Parts 1-4 pp1-264. Nb See also Donovan 1953.

WOOLLAM R. & RIDING J.B. 1983

Dinoflagellate cyst zonation of the English Jurassic. Inst. Geol.
Sci. Rep. No.83/2.

YANG C.-S. NIO S.-D. 1985

The estimation of palaeohydrodynamic processes from subtidal
deposits using time series analysis methods. Sedimentology 32
pp41-58.

ZEIGLER P.A. 1982

Geological atlas of western and central Europe. Shell Int. Pet.
Maatschappij B.V. 130p.